

Supplementary to “Robust Inference of Bi-Directional Causal Relationships in Presence of Correlated Pleiotropy with GWAS Summary Data”

Haoran Xue¹ and Wei Pan^{1, 2}

¹Division of Biostatistics, School of Public Health, University of Minnesota, Minneapolis, Minnesota 55455.

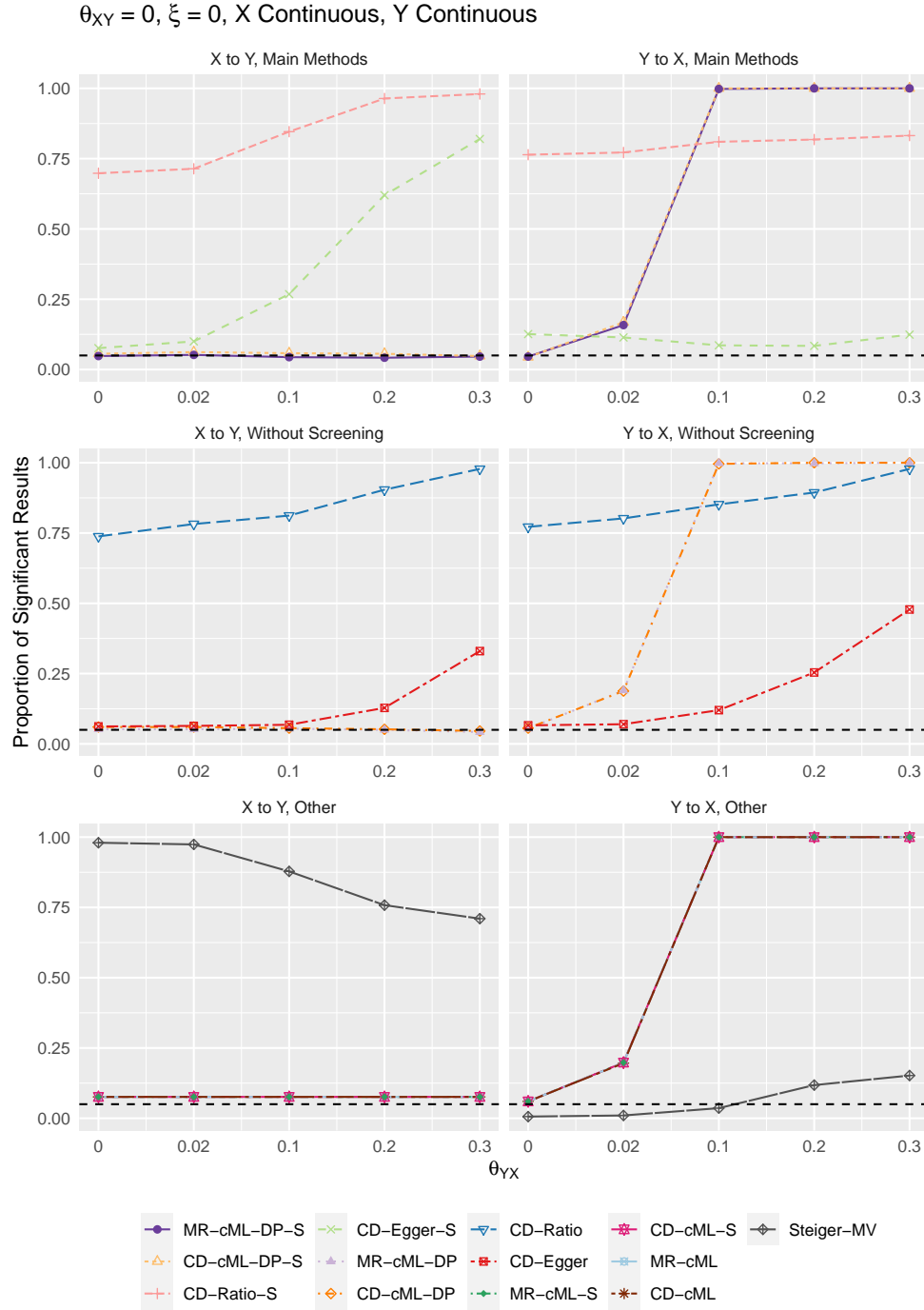
²Corresponding author. Email: panxx014@umn.edu. Phone: 612-624-4655. Fax: 612-626-0660.

Contents

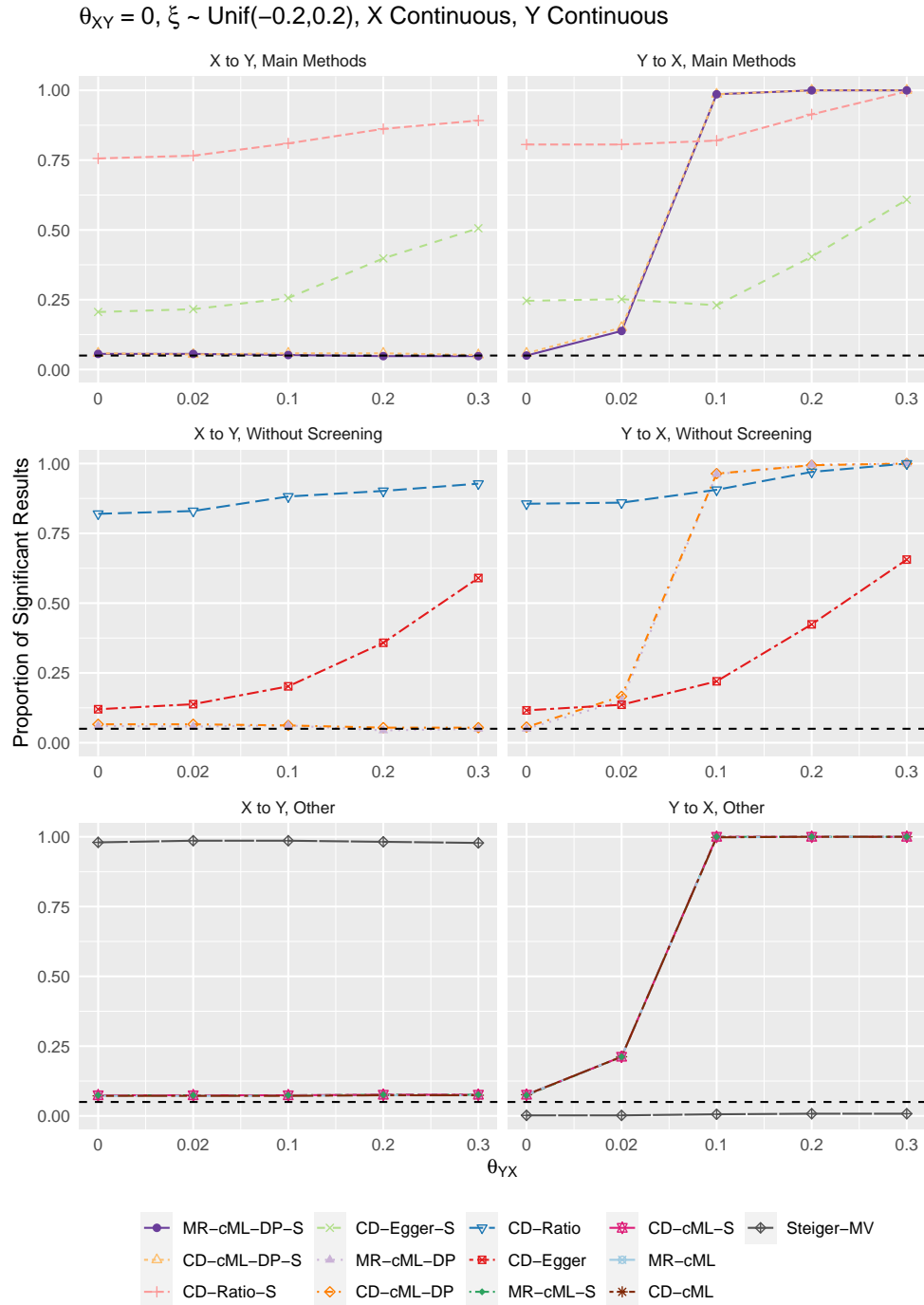
S1 Full Simulation Results	2
S2 Full Real Data Results	42
S2.1 48 Risk Factor-Disease Pairs	42
S2.2 Pairs of 4 Diseases	50
S2.3 Links to GWAS Summary Datasets	51
S3 Theoretical Results	52
S3.1 Proof of Theorem 1	52
S3.2 Proof of Theorem 2	55
S3.3 MR-cML with Data Perturbation	57

S1 Full Simulation Results

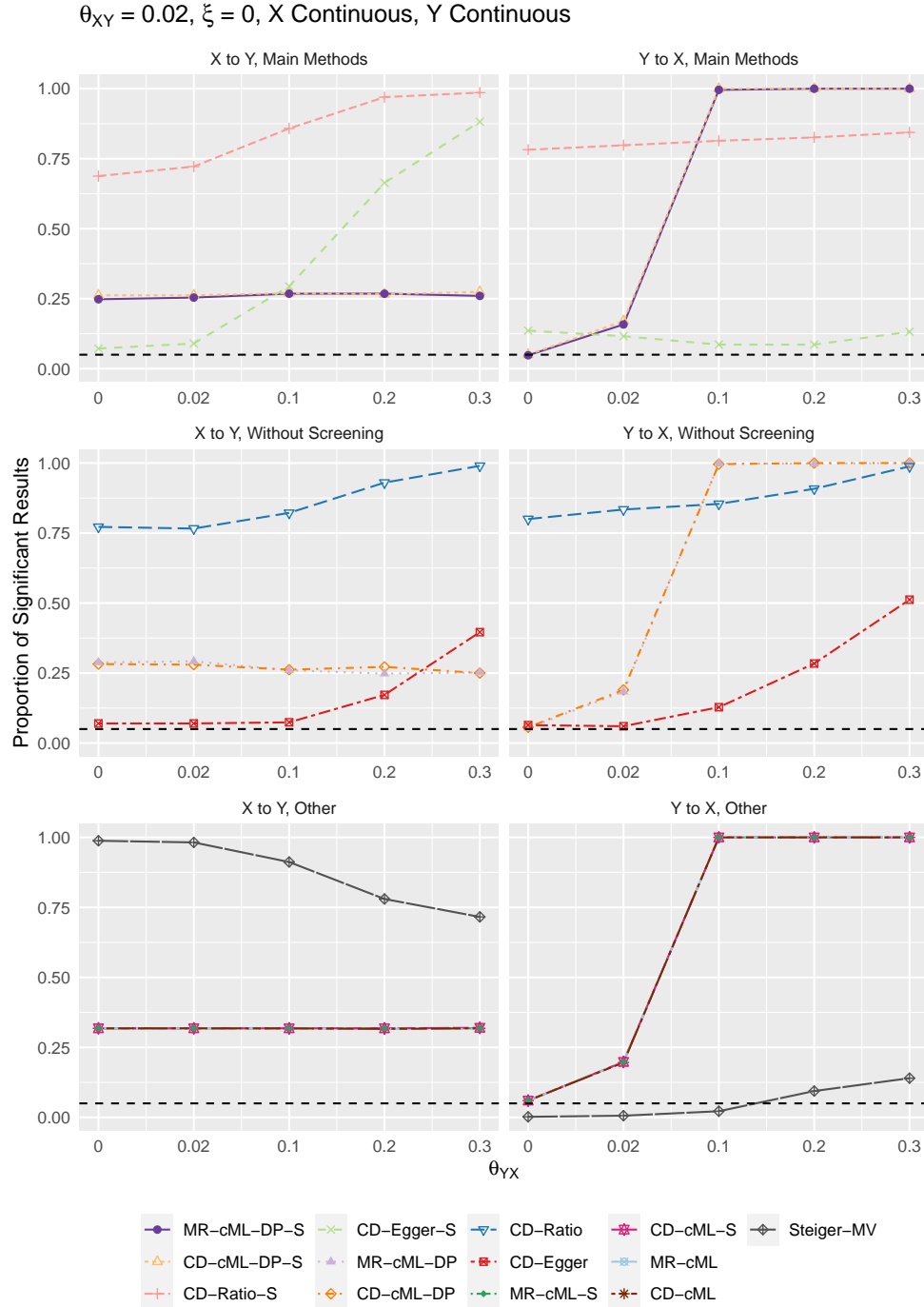
S1 Fig: When both X and Y are continuous, $\theta_{XY} = 0$ and $\xi = 0$, the proportions of significant simulation results obtained by the methods for direction $X \rightarrow Y$ (left column) and $Y \rightarrow X$ (right column). The first row shows results for four main methods: MR-cML-DP-S, CD-cML-DP-S, CD-Ratio-S, and CD-Egger-S; the second row shows results for four methods without screening: MR-cML-DP, CD-cML-DP, CD-Ratio, and CD-Egger; the third row shows results for other five methods.



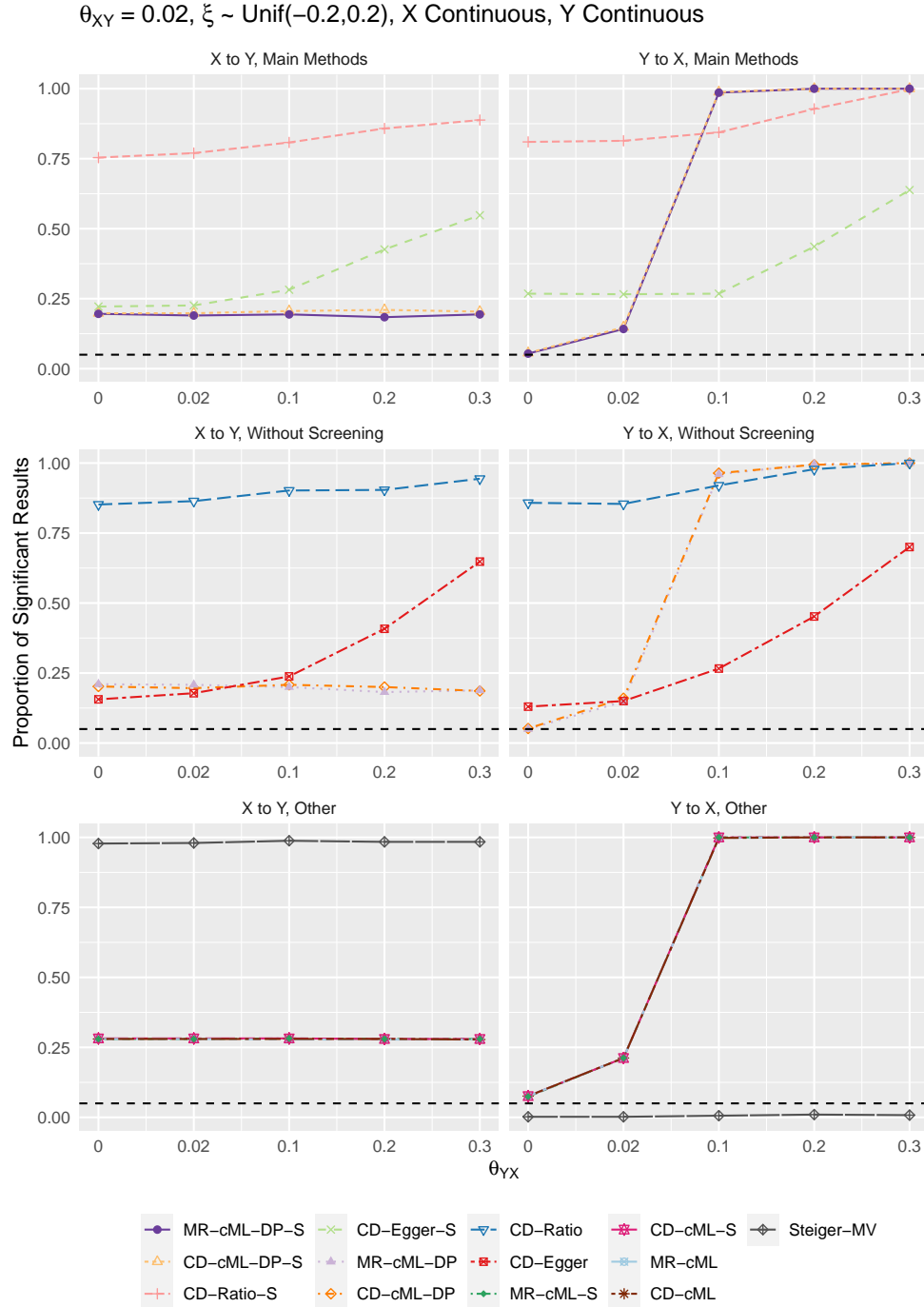
S2 Fig: When both X and Y are continuous, $\theta_{XY} = 0$ and $\xi \sim \text{Unif}(-0.2, 0.2)$, the proportions of significant simulation results obtained by the methods for direction $X \rightarrow Y$ (left column) and $Y \rightarrow X$ (right column). The first row shows results for four main methods: MR-cML-DP-S, CD-cML-DP-S, CD-Ratio-S, and CD-Egger-S; the second row shows results for four methods without screening: MR-cML-DP, CD-cML-DP, CD-Ratio, and CD-Egger; the third row shows results for other five methods.



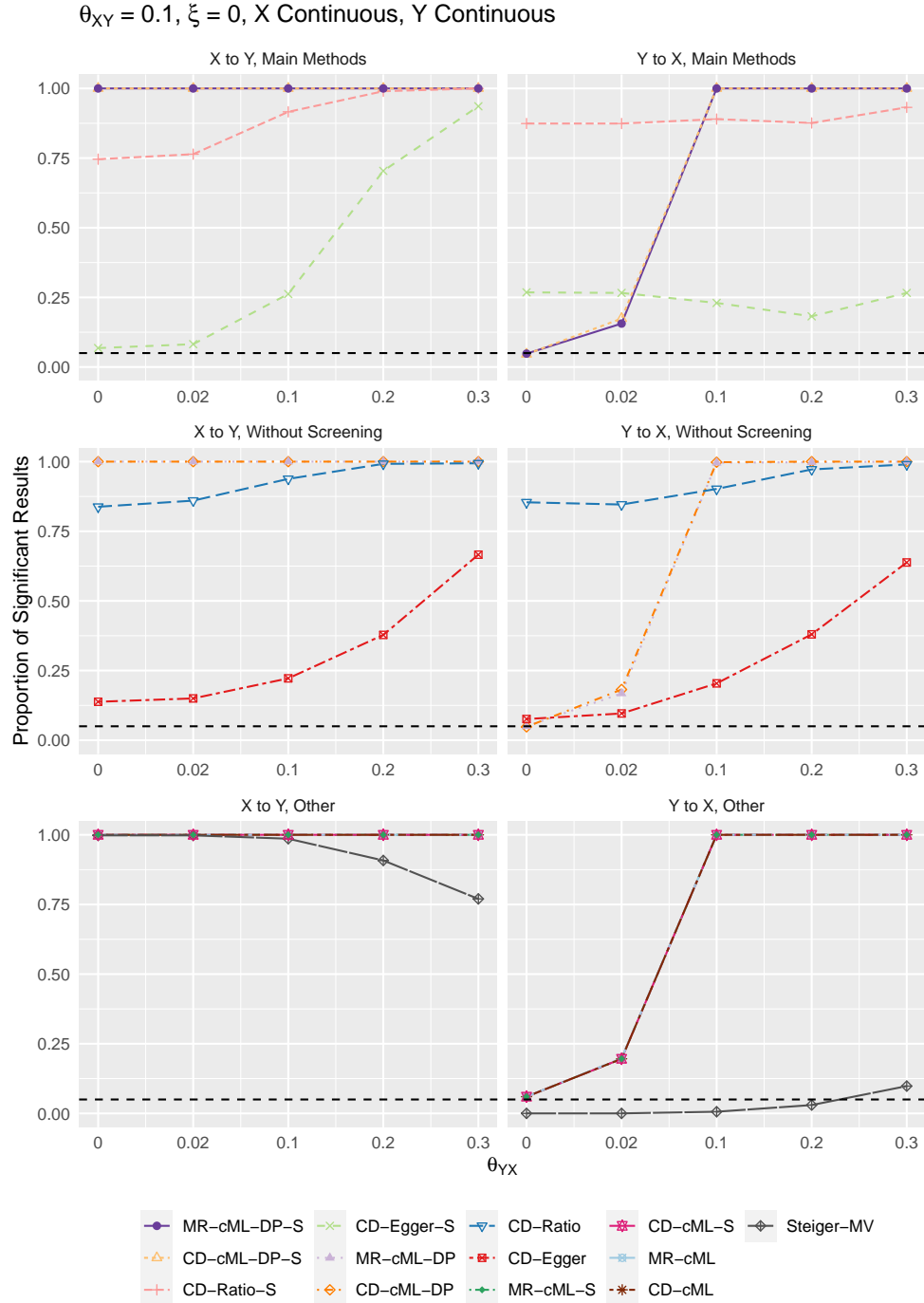
S3 Fig: When both X and Y are continuous, $\theta_{XY} = 0.02$ and $\xi = 0$, the proportions of significant simulation results obtained by the methods for direction $X \rightarrow Y$ (left column) and $Y \rightarrow X$ (right column). The first row shows results for four main methods: MR-cML-DP-S, CD-cML-DP-S, CD-Ratio-S, and CD-Egger-S; the second row shows results for four methods without screening: MR-cML-DP, CD-cML-DP, CD-Ratio, and CD-Egger; the third row shows results for other five methods.



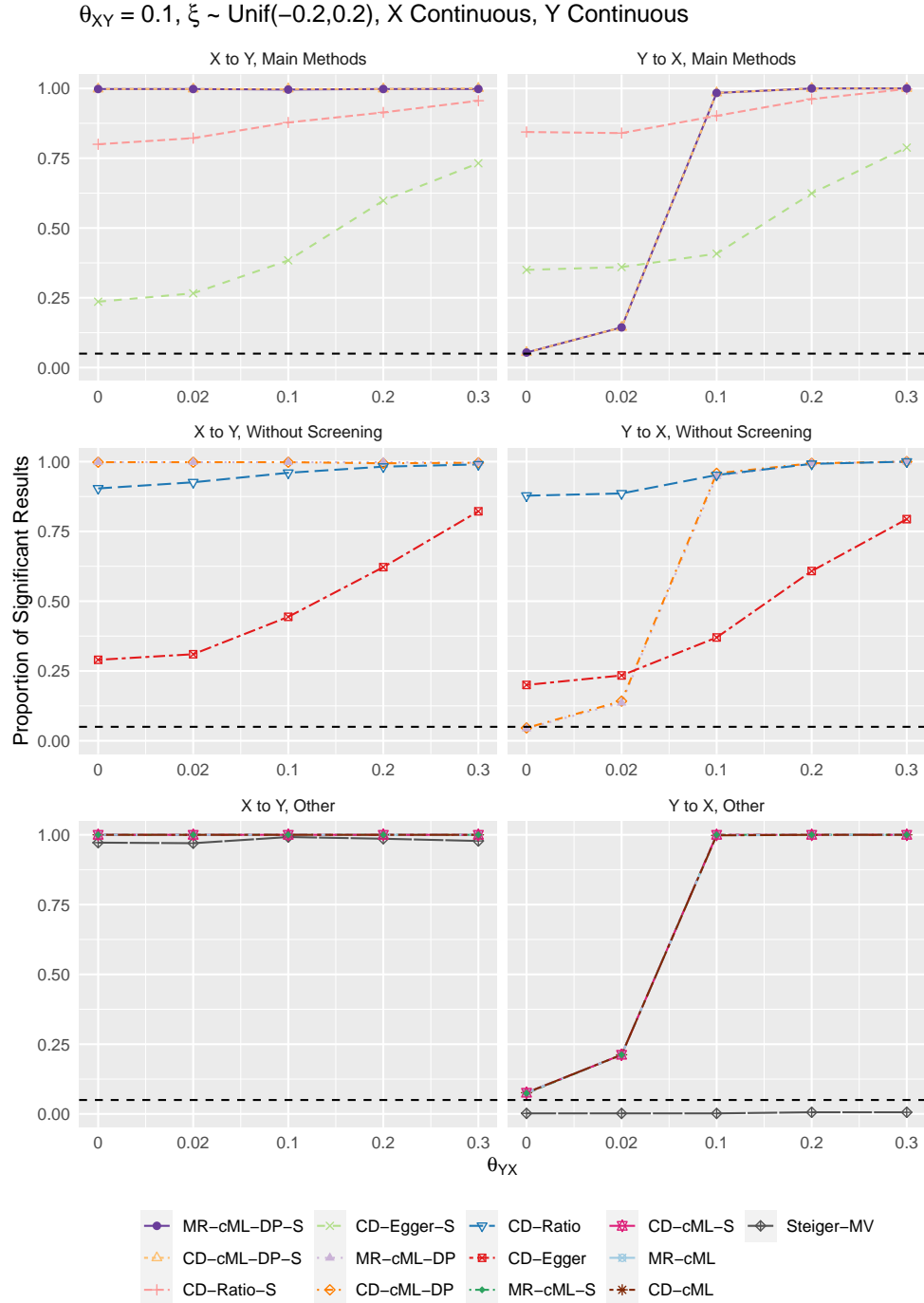
S4 Fig: When both X and Y are continuous, $\theta_{XY} = 0.02$ and $\xi \sim \text{Unif}(-0.2, 0.2)$, the proportions of significant simulation results obtained by the methods for direction $X \rightarrow Y$ (left column) and $Y \rightarrow X$ (right column). The first row shows results for four main methods: MR-cML-DP-S, CD-cML-DP-S, CD-Ratio-S, and CD-Egger-S; the second row shows results for four methods without screening: MR-cML-DP, CD-cML-DP, CD-Ratio, and CD-Egger; the third row shows results for other five methods.



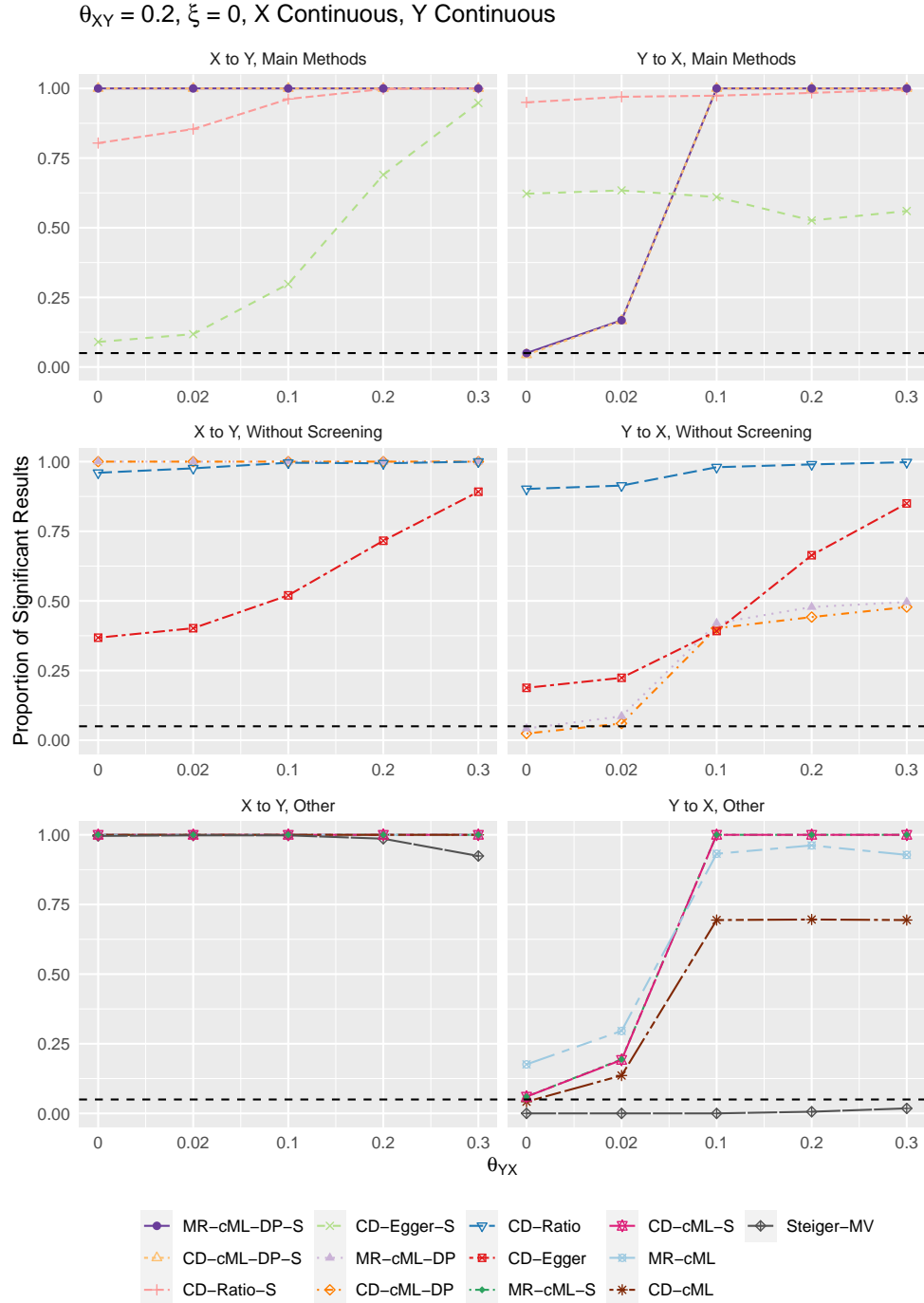
S5 Fig: When both X and Y are continuous, $\theta_{XY} = 0.1$ and $\xi = 0$, the proportions of significant simulation results obtained by the methods for direction $X \rightarrow Y$ (left column) and $Y \rightarrow X$ (right column). The first row shows results for four main methods: MR-cML-DP-S, CD-cML-DP-S, CD-Ratio-S, and CD-Egger-S; the second row shows results for four methods without screening: MR-cML-DP, CD-cML-DP, CD-Ratio, and CD-Egger; the third row shows results for other five methods.



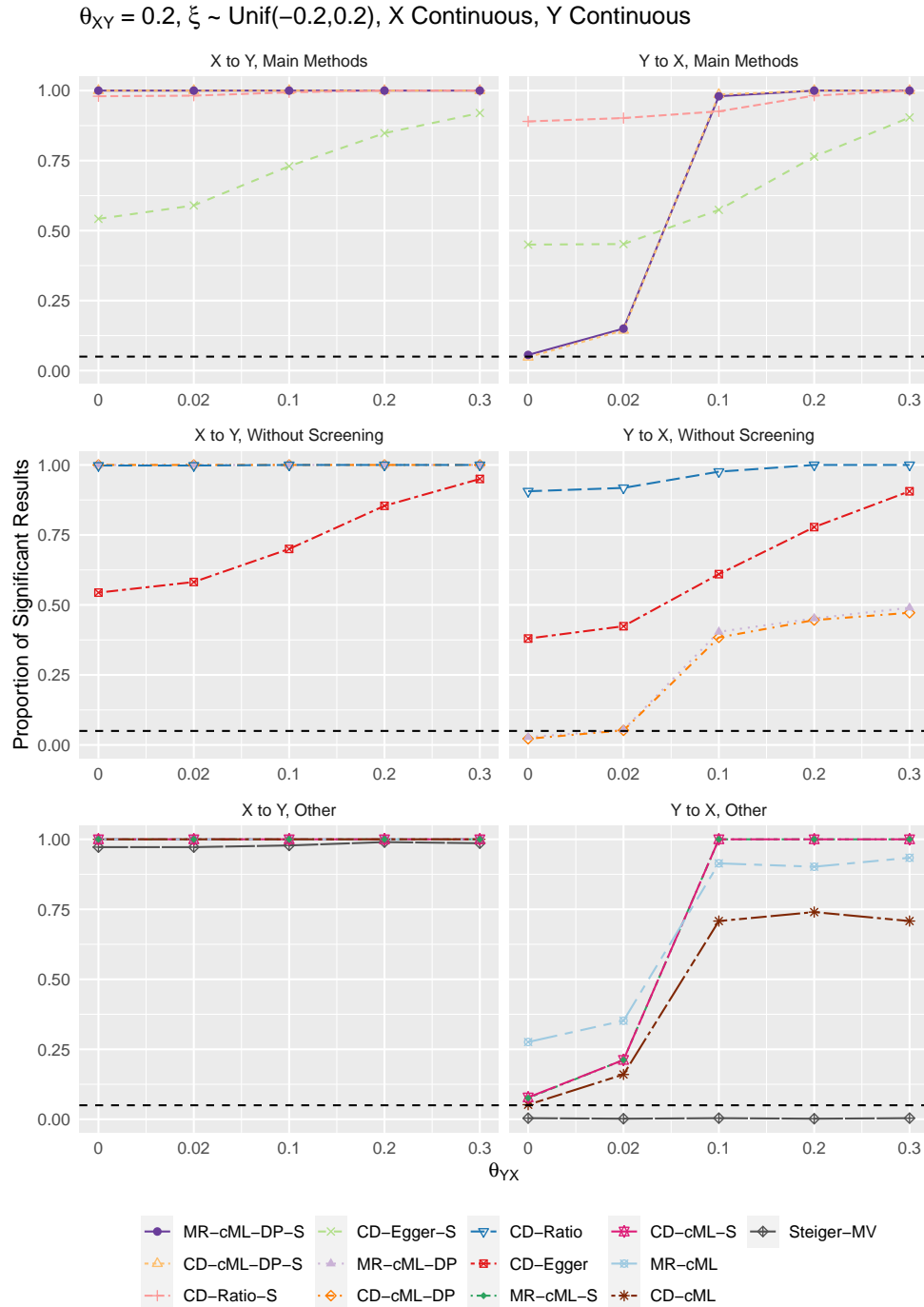
S6 Fig: When both X and Y are continuous, $\theta_{XY} = 0.1$ and $\xi \sim \text{Unif}(-0.2, 0.2)$, the proportions of significant simulation results obtained by the methods for direction $X \rightarrow Y$ (left column) and $Y \rightarrow X$ (right column). The first row shows results for four main methods: MR-cML-DP-S, CD-cML-DP-S, CD-Ratio-S, and CD-Egger-S; the second row shows results for four methods without screening: MR-cML-DP, CD-cML-DP, CD-Ratio, and CD-Egger; the third row shows results for other five methods.



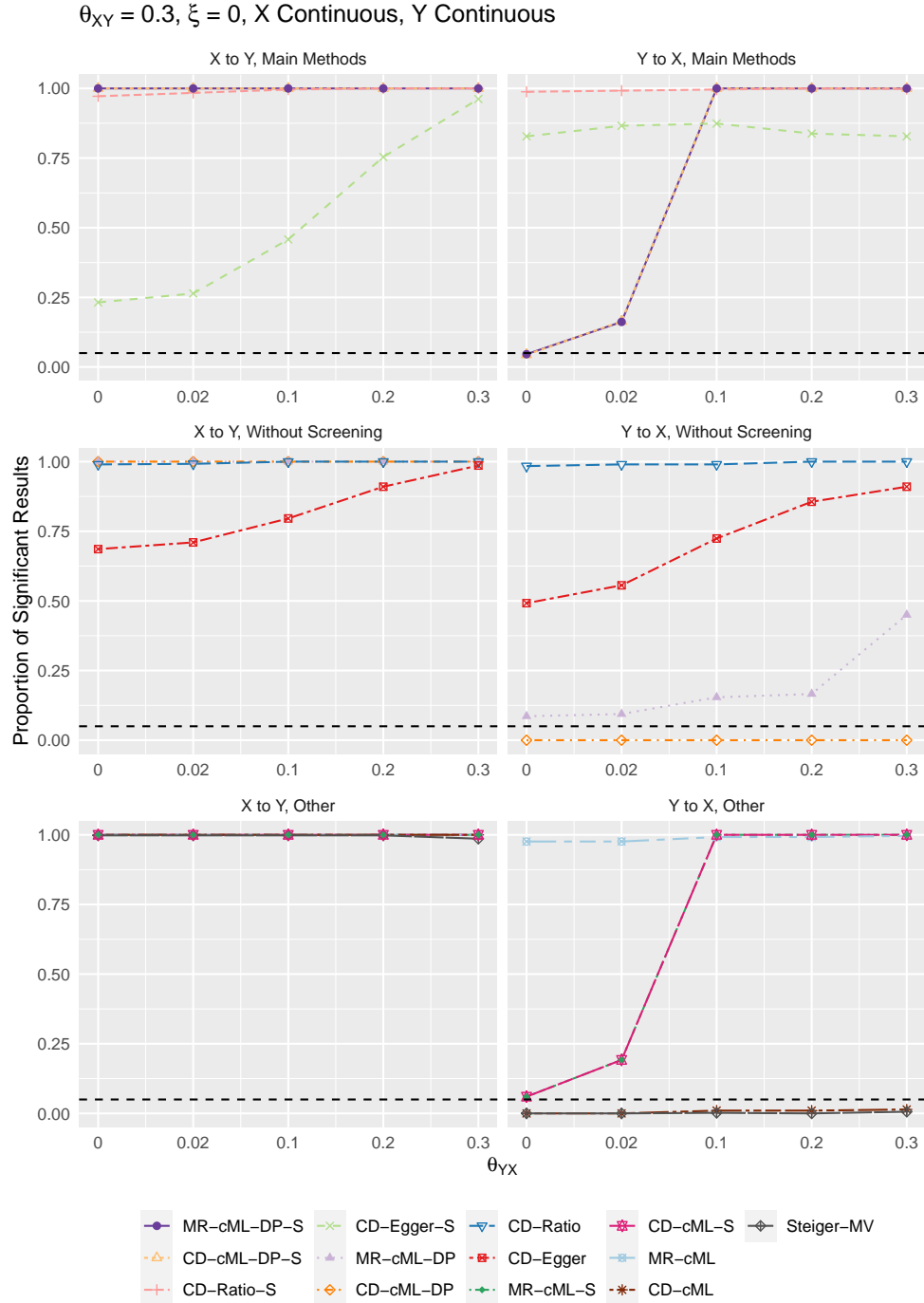
S7 Fig: When both X and Y are continuous, $\theta_{XY} = 0.2$ and $\xi = 0$, the proportions of significant simulation results obtained by the methods for direction $X \rightarrow Y$ (left column) and $Y \rightarrow X$ (right column). The first row shows results for four main methods: MR-cML-DP-S, CD-cML-DP-S, CD-Ratio-S, and CD-Egger-S; the second row shows results for four methods without screening: MR-cML-DP, CD-cML-DP, CD-Ratio, and CD-Egger; the third row shows results for other five methods.



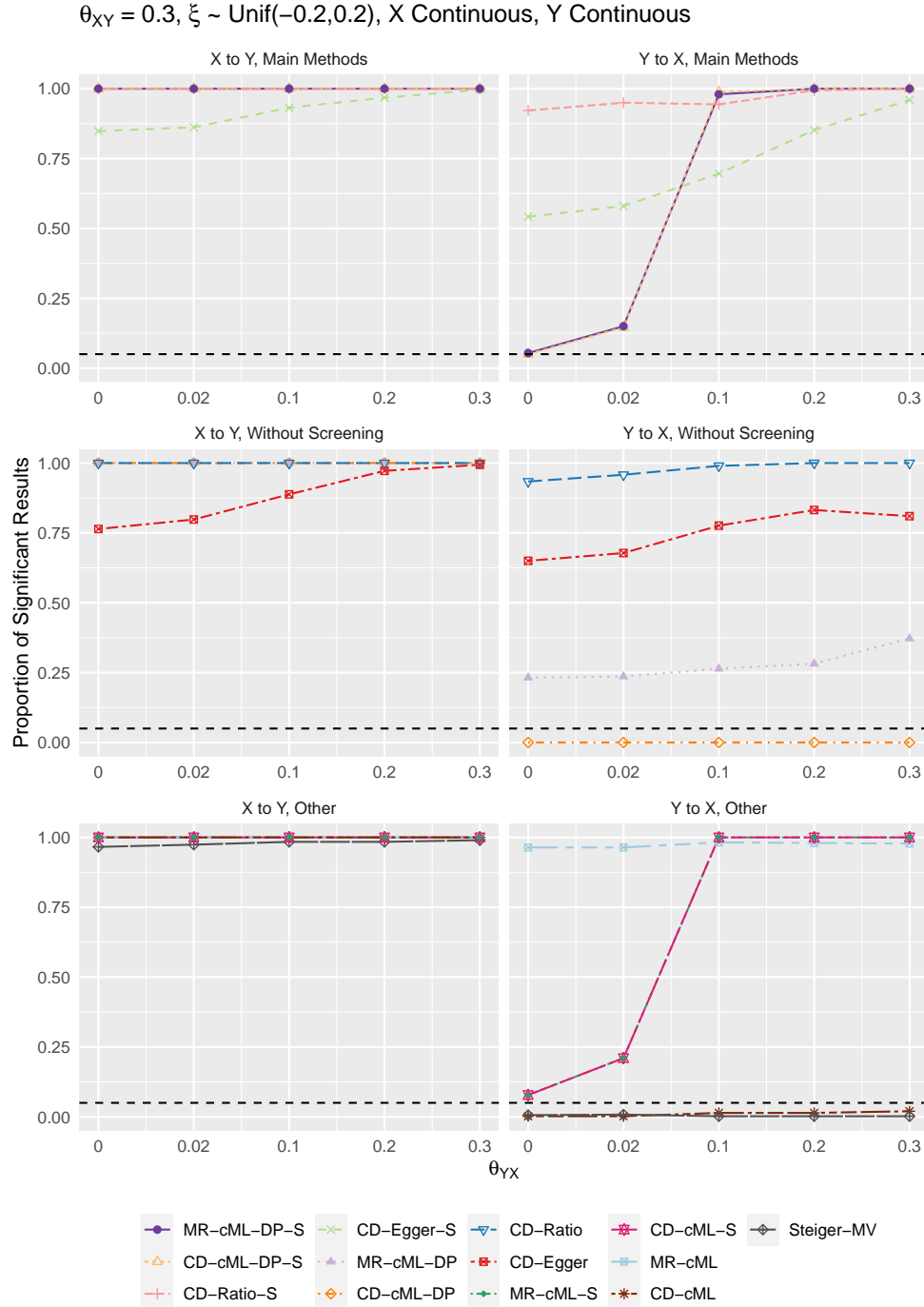
S8 Fig: When both X and Y are continuous, $\theta_{XY} = 0.2$ and $\xi \sim \text{Unif}(-0.2, 0.2)$, the proportions of significant simulation results obtained by the methods for direction $X \rightarrow Y$ (left column) and $Y \rightarrow X$ (right column). The first row shows results for four main methods: MR-cML-DP-S, CD-cML-DP-S, CD-Ratio-S, and CD-Egger-S; the second row shows results for four methods without screening: MR-cML-DP, CD-cML-DP, CD-Ratio, and CD-Egger; the third row shows results for other five methods.



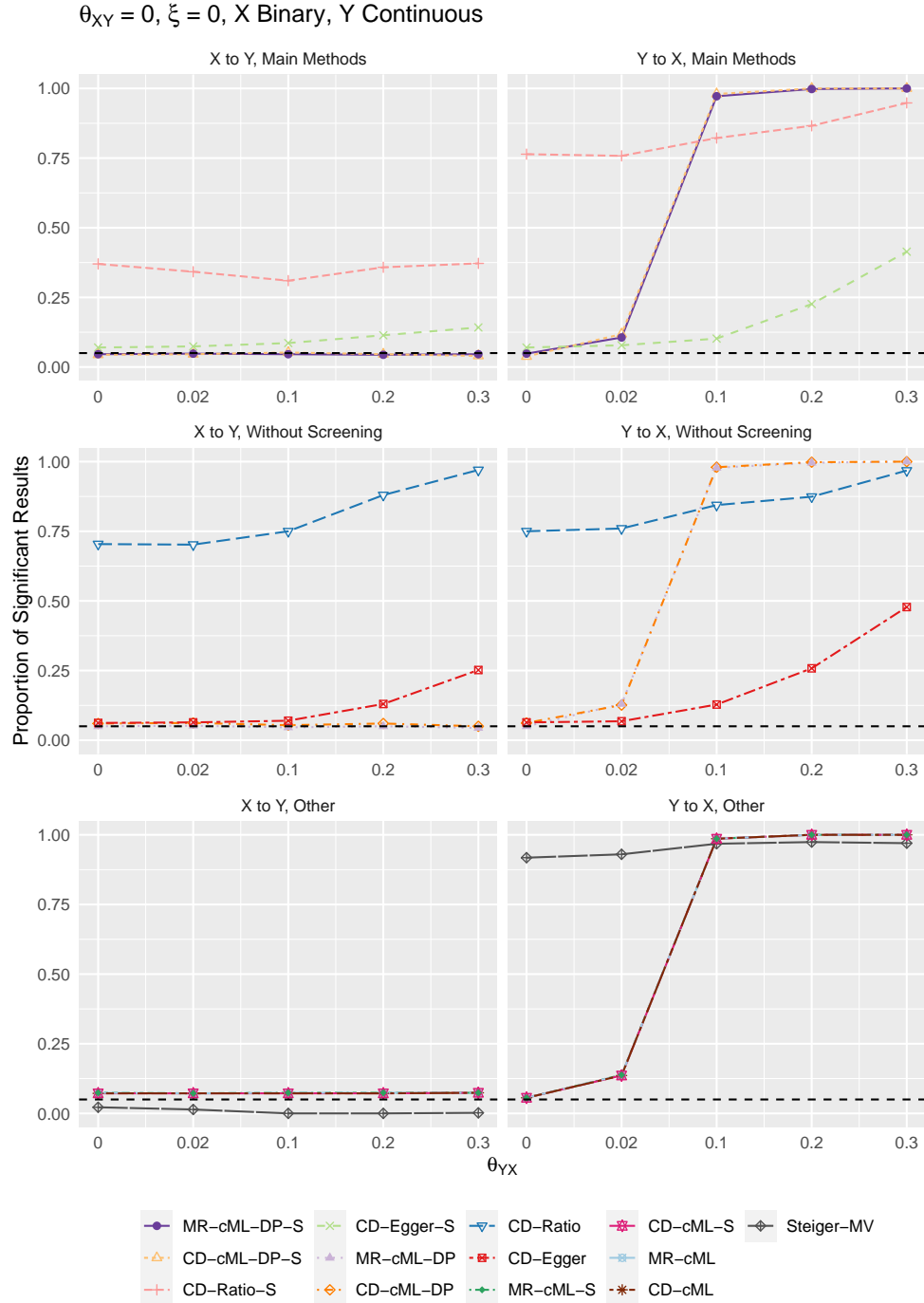
S9 Fig: When both X and Y are continuous, $\theta_{XY} = 0.3$ and $\xi = 0$, the proportions of significant simulation results obtained by the methods for direction $X \rightarrow Y$ (left column) and $Y \rightarrow X$ (right column). The first row shows results for four main methods: MR-cML-DP-S, CD-cML-DP-S, CD-Ratio-S, and CD-Egger-S; the second row shows results for four methods without screening: MR-cML-DP, CD-cML-DP, CD-Ratio, and CD-Egger; the third row shows results for other five methods.



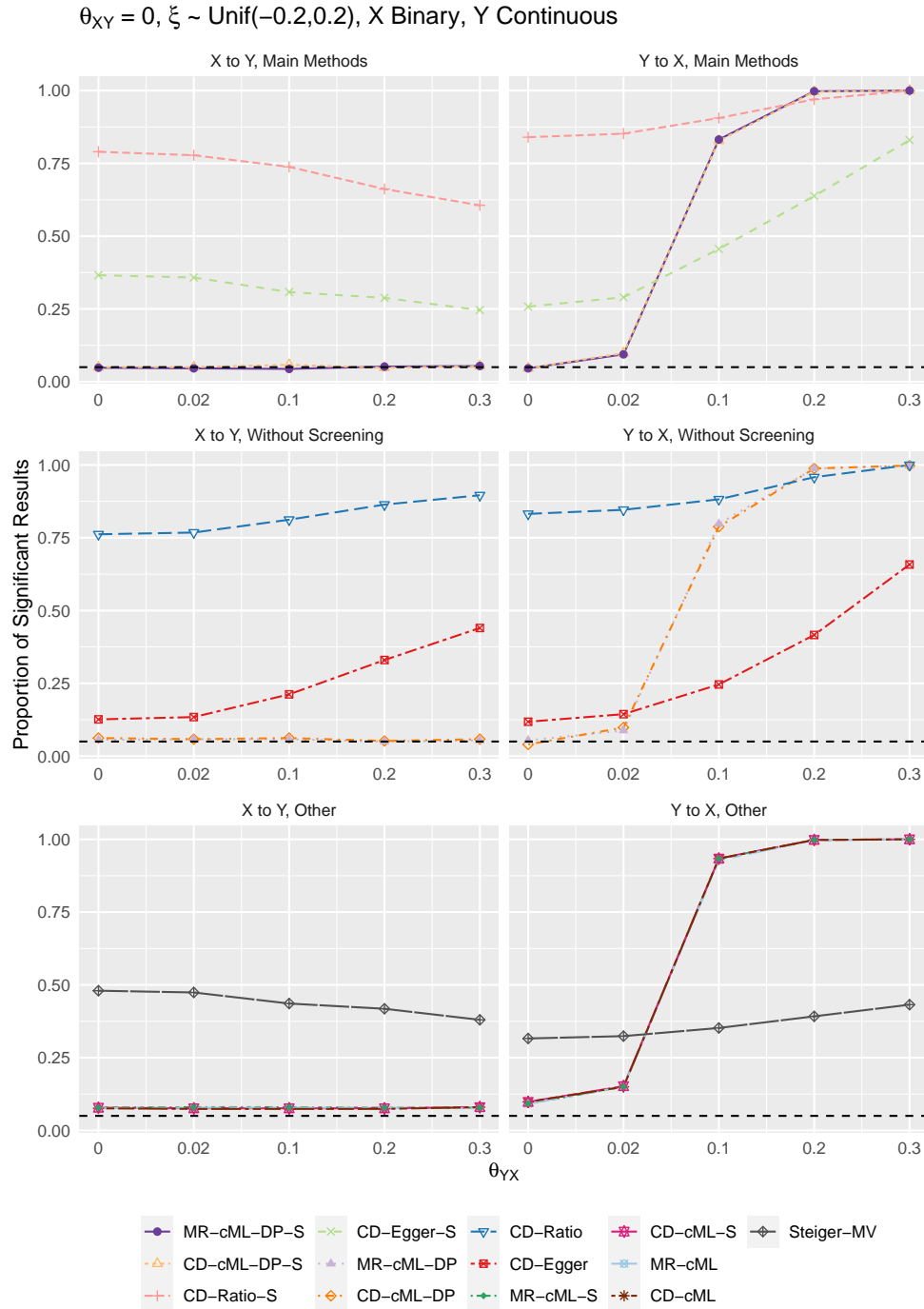
S10 Fig: When both X and Y are continuous, $\theta_{XY} = 0.3$ and $\xi \sim \text{Unif}(-0.2, 0.2)$, the proportions of significant simulation results obtained by the methods for direction $X \rightarrow Y$ (left column) and $Y \rightarrow X$ (right column). The first row shows results for four main methods: MR-cML-DP-S, CD-cML-DP-S, CD-Ratio-S, and CD-Egger-S; the second row shows results for four methods without screening: MR-cML-DP, CD-cML-DP, CD-Ratio, and CD-Egger; the third row shows results for other five methods.



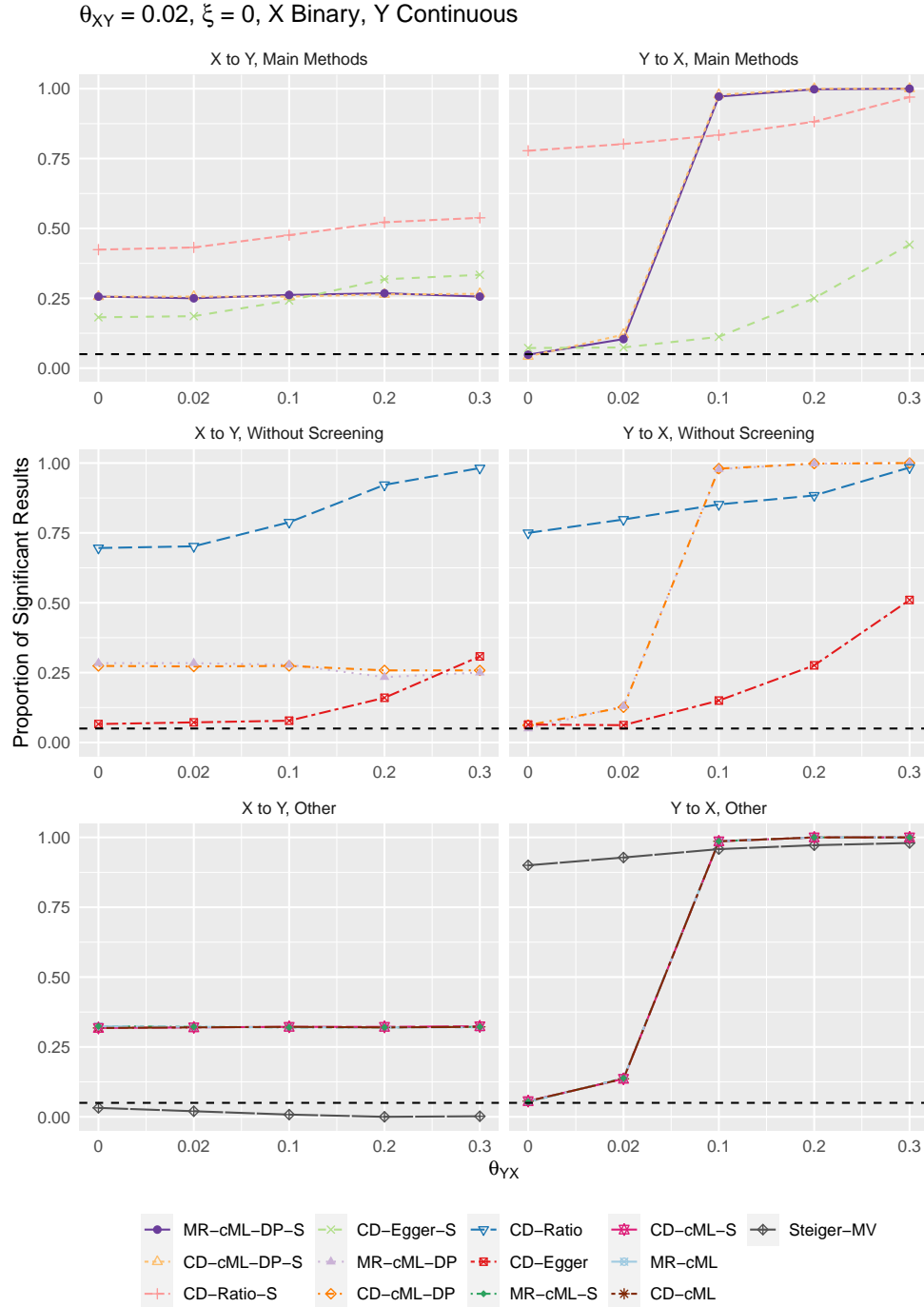
S11 Fig: When X is binary, Y is continuous, $\theta_{XY} = 0$ and $\xi = 0$, the proportions of significant simulation results obtained by the methods for direction $X \rightarrow Y$ (left column) and $Y \rightarrow X$ (right column). The first row shows results for four main methods: MR-cML-DP-S, CD-cML-DP-S, CD-Ratio-S, and CD-Egger-S; the second row shows results for four methods without screening: MR-cML-DP, CD-cML-DP, CD-Ratio, and CD-Egger; the third row shows results for other five methods.



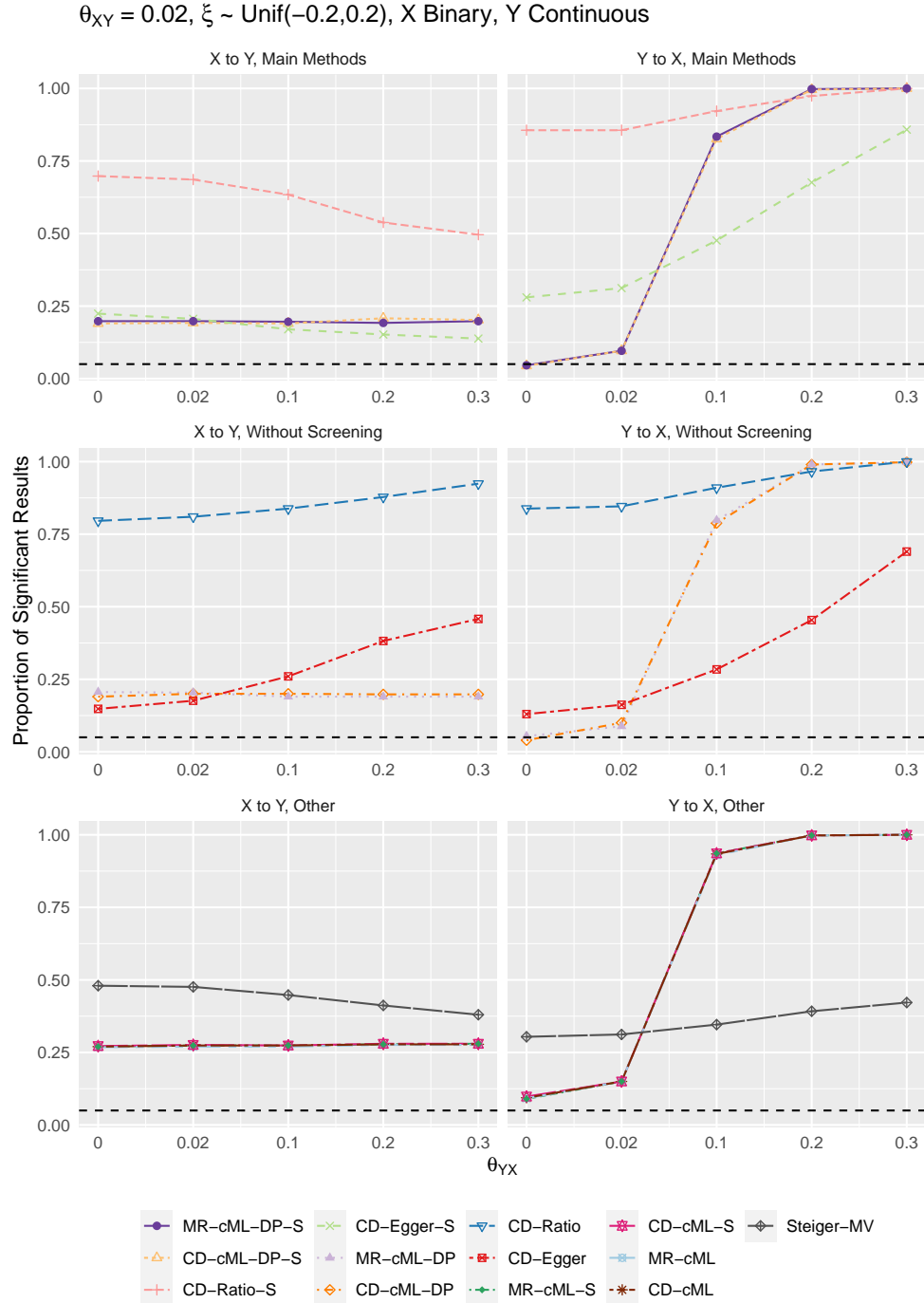
S12 Fig: When X is binary, Y is continuous, $\theta_{XY} = 0$ and $\xi \sim \text{Unif}(-0.2, 0.2)$, the proportions of significant simulation results obtained by the methods for direction $X \rightarrow Y$ (left column) and $Y \rightarrow X$ (right column). The first row shows results for four main methods: MR-cML-DP-S, CD-cML-DP-S, CD-Ratio-S, and CD-Egger-S; the second row shows results for four methods without screening: MR-cML-DP, CD-cML-DP, CD-Ratio, and CD-Egger; the third row shows results for other five methods.



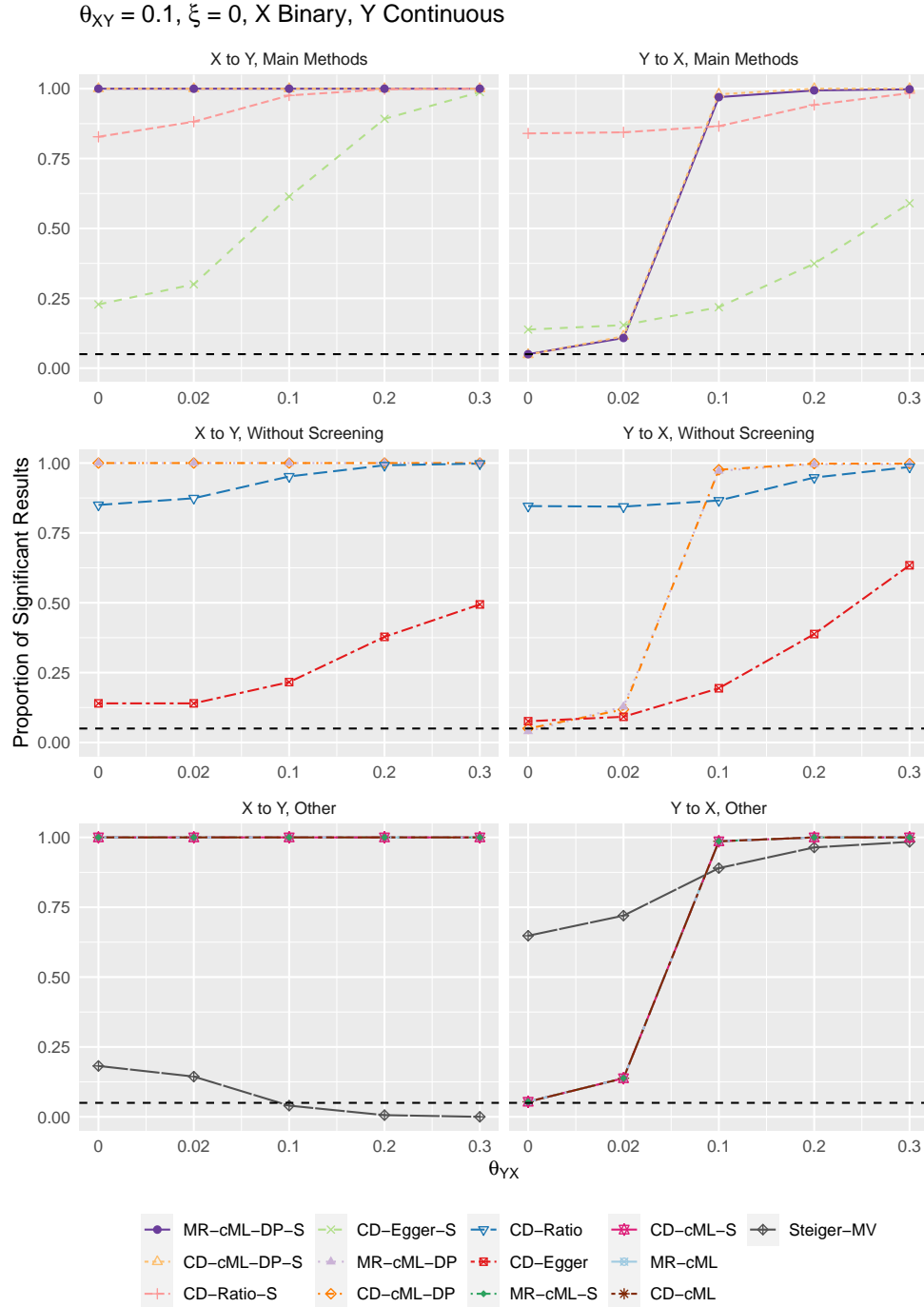
S13 Fig: When X is binary, Y is continuous, $\theta_{XY} = 0.02$ and $\xi = 0$, the proportions of significant simulation results obtained by the methods for direction $X \rightarrow Y$ (left column) and $Y \rightarrow X$ (right column). The first row shows results for four main methods: MR-cML-DP-S, CD-cML-DP-S, CD-Ratio-S, and CD-Egger-S; the second row shows results for four methods without screening: MR-cML-DP, CD-cML-DP, CD-Ratio, and CD-Egger; the third row shows results for other five methods.



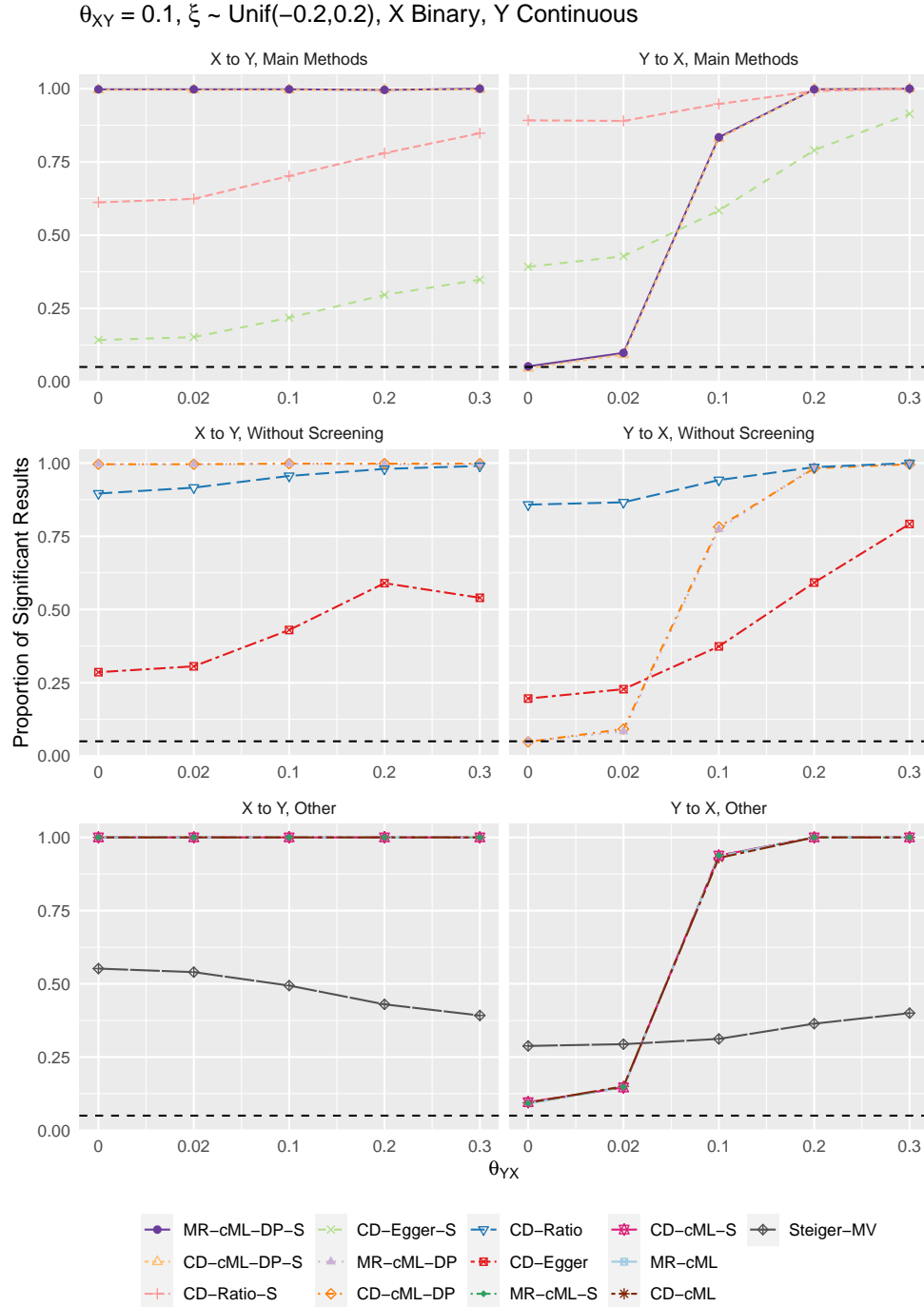
S14 Fig: When X is binary, Y is continuous, $\theta_{XY} = 0.02$ and $\xi \sim \text{Unif}(-0.2, 0.2)$, the proportions of significant simulation results obtained by the methods for direction $X \rightarrow Y$ (left column) and $Y \rightarrow X$ (right column). The first row shows results for four main methods: MR-cML-DP-S, CD-cML-DP-S, CD-Ratio-S, and CD-Egger-S; the second row shows results for four methods without screening: MR-cML-DP, CD-cML-DP, CD-Ratio, and CD-Egger; the third row shows results for other five methods.



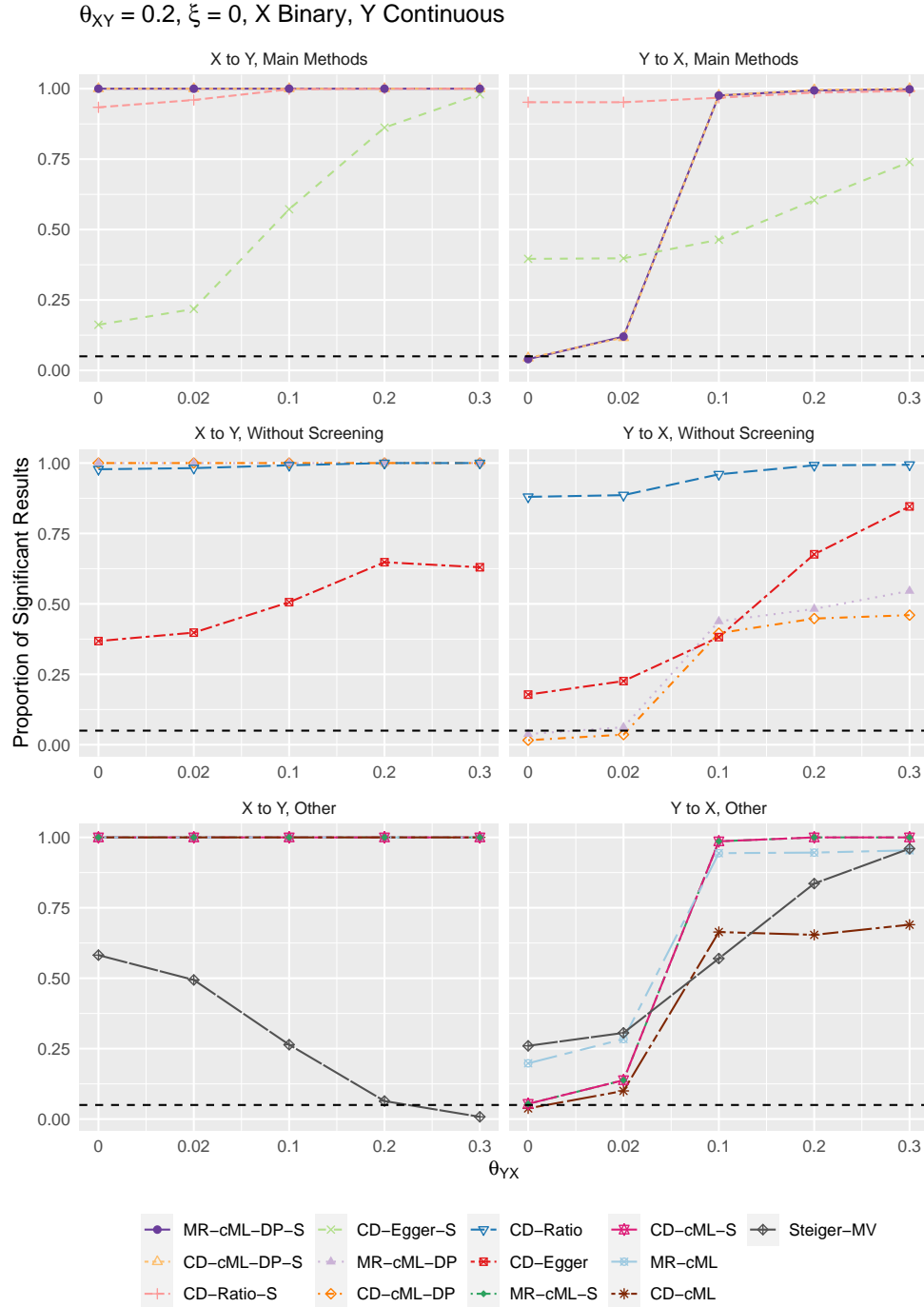
S15 Fig: When X is binary, Y is continuous, $\theta_{XY} = 0.1$ and $\xi = 0$, the proportions of significant simulation results obtained by the methods for direction $X \rightarrow Y$ (left column) and $Y \rightarrow X$ (right column). The first row shows results for four main methods: MR-cML-DP-S, CD-cML-DP-S, CD-Ratio-S, and CD-Egger-S; the second row shows results for four methods without screening: MR-cML-DP, CD-cML-DP, CD-Ratio, and CD-Egger; the third row shows results for other five methods.



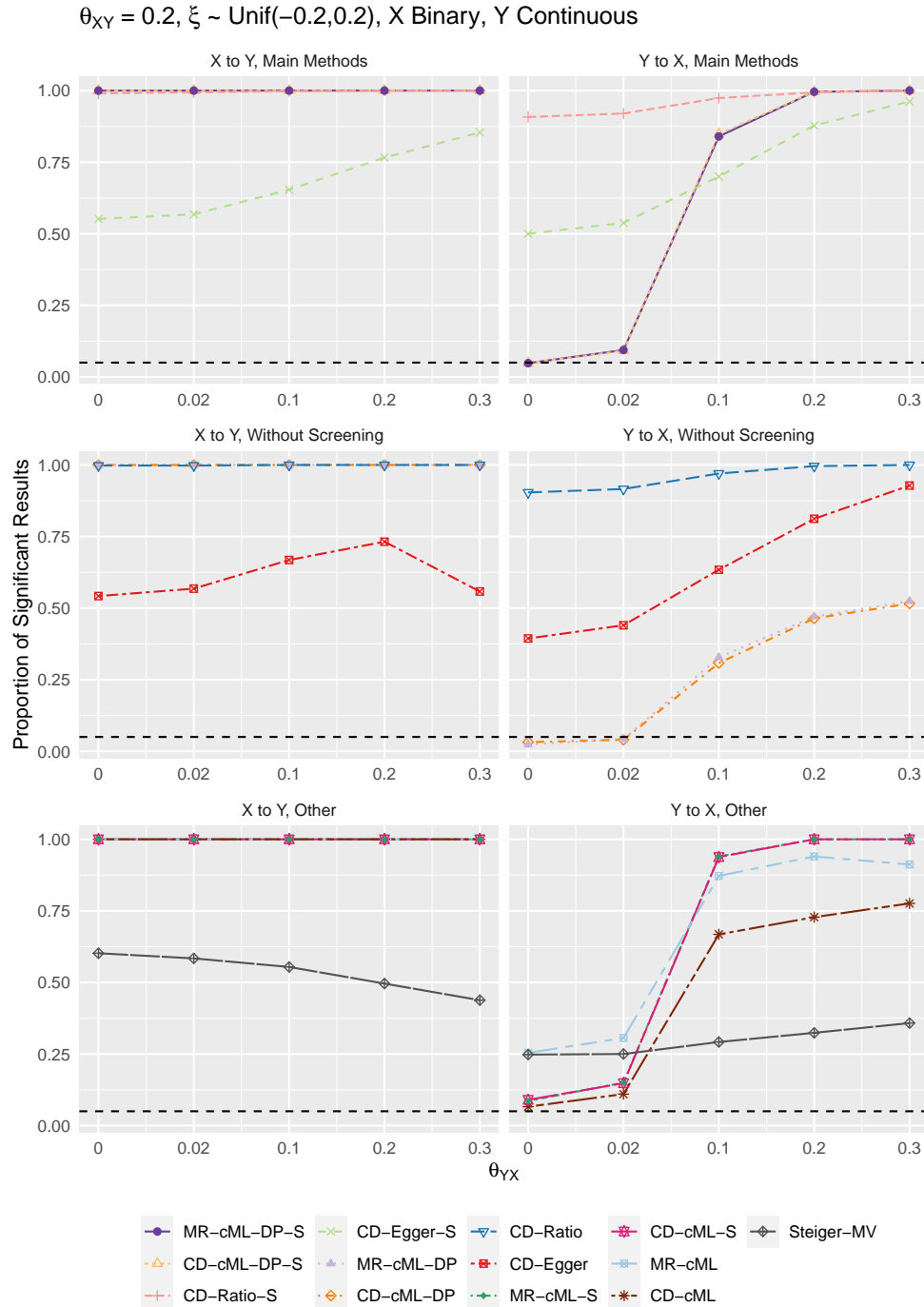
S16 Fig: When X is binary, Y is continuous, $\theta_{XY} = 0.1$ and $\xi \sim \text{Unif}(-0.2, 0.2)$, the proportions of significant simulation results obtained by the methods for direction $X \rightarrow Y$ (left column) and $Y \rightarrow X$ (right column). The first row shows results for four main methods: MR-cML-DP-S, CD-cML-DP-S, CD-Ratio-S, and CD-Egger-S; the second row shows results for four methods without screening: MR-cML-DP, CD-cML-DP, CD-Ratio, and CD-Egger; the third row shows results for other five methods.



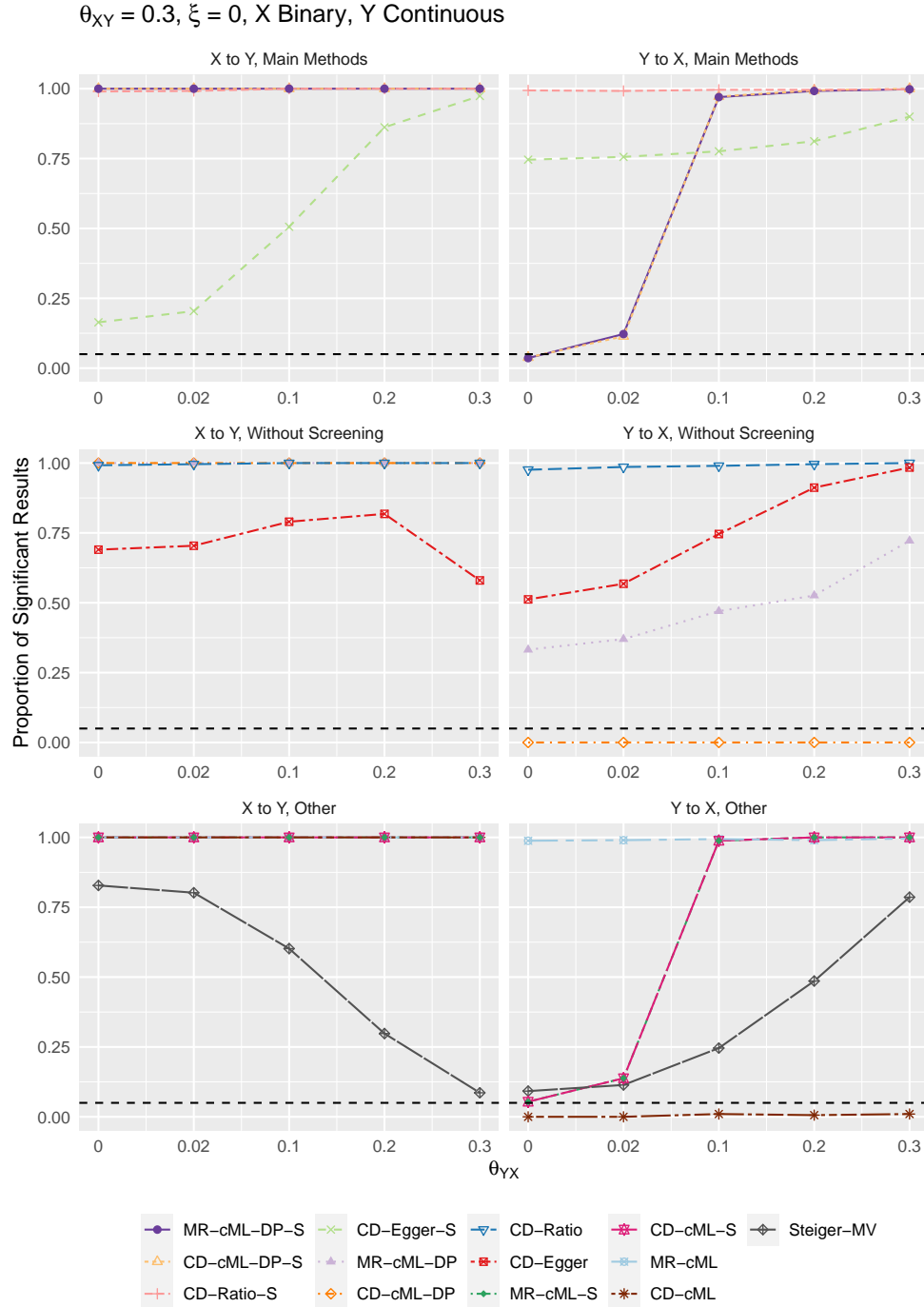
S17 Fig: When X is binary, Y is continuous, $\theta_{XY} = 0.2$ and $\xi = 0$, the proportions of significant simulation results obtained by the methods for direction $X \rightarrow Y$ (left column) and $Y \rightarrow X$ (right column). The first row shows results for four main methods: MR-cML-DP-S, CD-cML-DP-S, CD-Ratio-S, and CD-Egger-S; the second row shows results for four methods without screening: MR-cML-DP, CD-cML-DP, CD-Ratio, and CD-Egger; the third row shows results for other five methods.



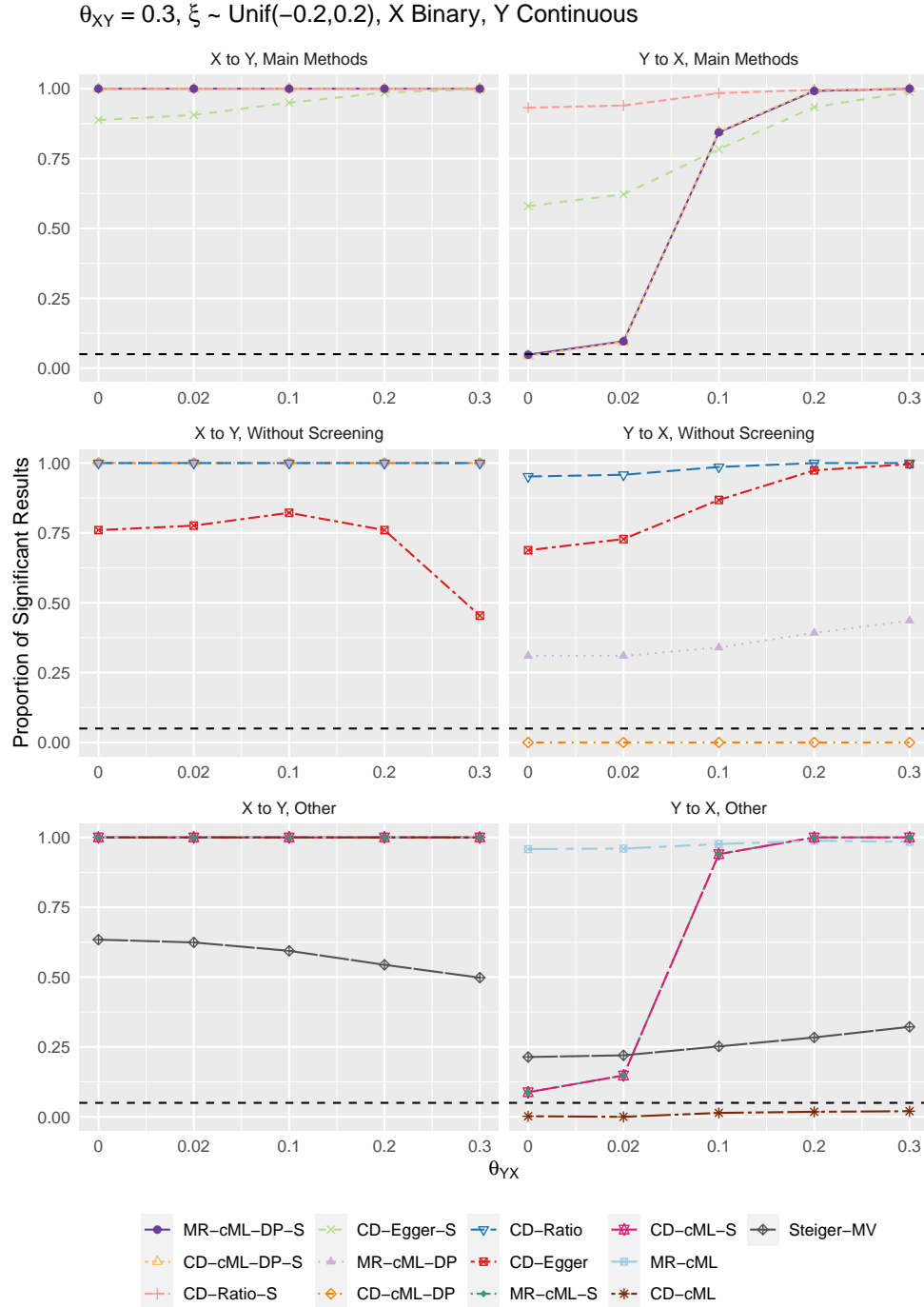
S18 Fig: When X is binary, Y is continuous, $\theta_{XY} = 0.2$ and $\xi \sim \text{Unif}(-0.2, 0.2)$, the proportions of significant simulation results obtained by the methods for direction $X \rightarrow Y$ (left column) and $Y \rightarrow X$ (right column). The first row shows results for four main methods: MR-cML-DP-S, CD-cML-DP-S, CD-Ratio-S, and CD-Egger-S; the second row shows results for four methods without screening: MR-cML-DP, CD-cML-DP, CD-Ratio, and CD-Egger; the third row shows results for other five methods.



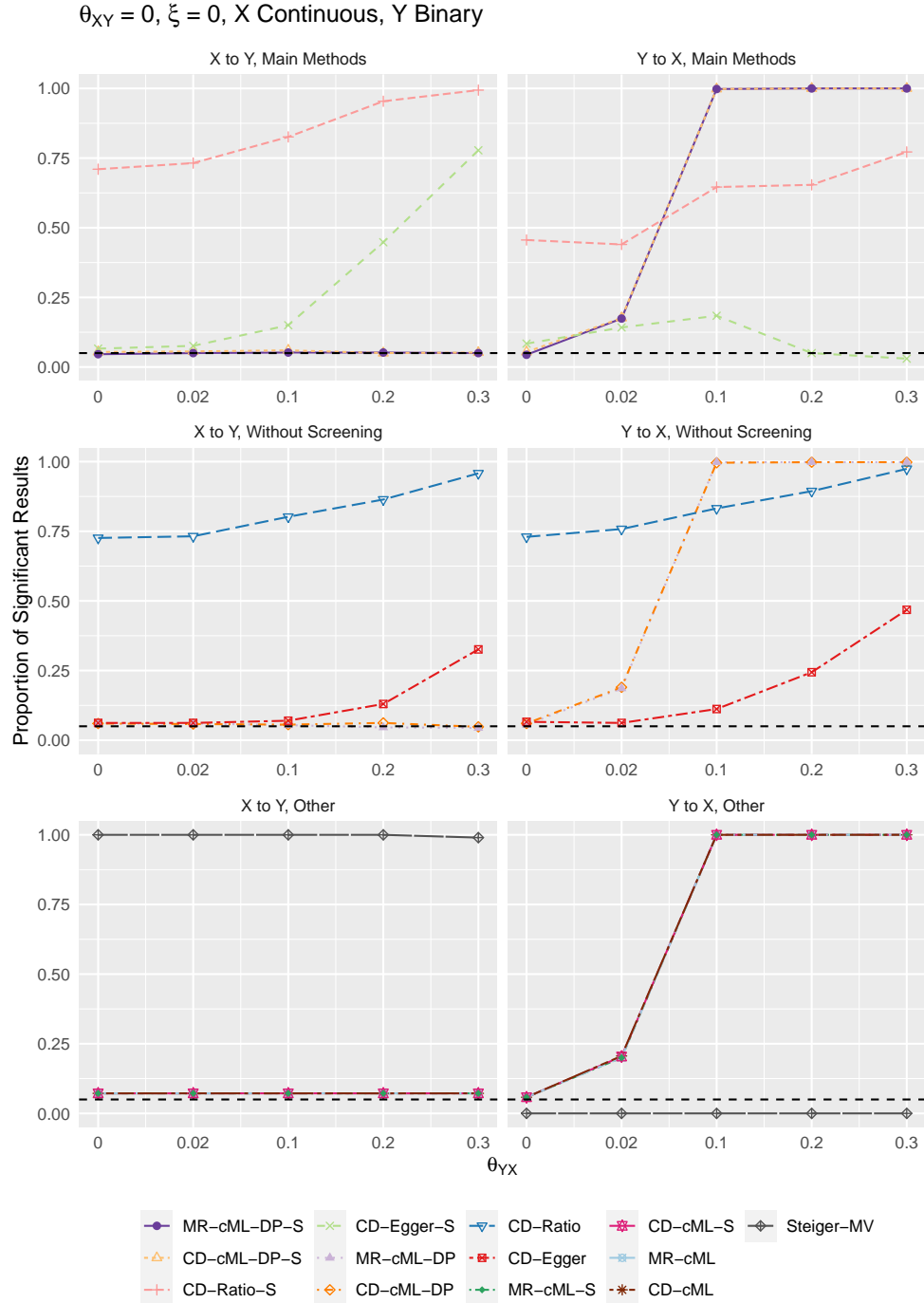
S19 Fig: When X is binary, Y is continuous, $\theta_{XY} = 0.3$ and $\xi = 0$, the proportions of significant simulation results obtained by the methods for direction $X \rightarrow Y$ (left column) and $Y \rightarrow X$ (right column). The first row shows results for four main methods: MR-cML-DP-S, CD-cML-DP-S, CD-Ratio-S, and CD-Egger-S; the second row shows results for four methods without screening: MR-cML-DP, CD-cML-DP, CD-Ratio, and CD-Egger; the third row shows results for other five methods.



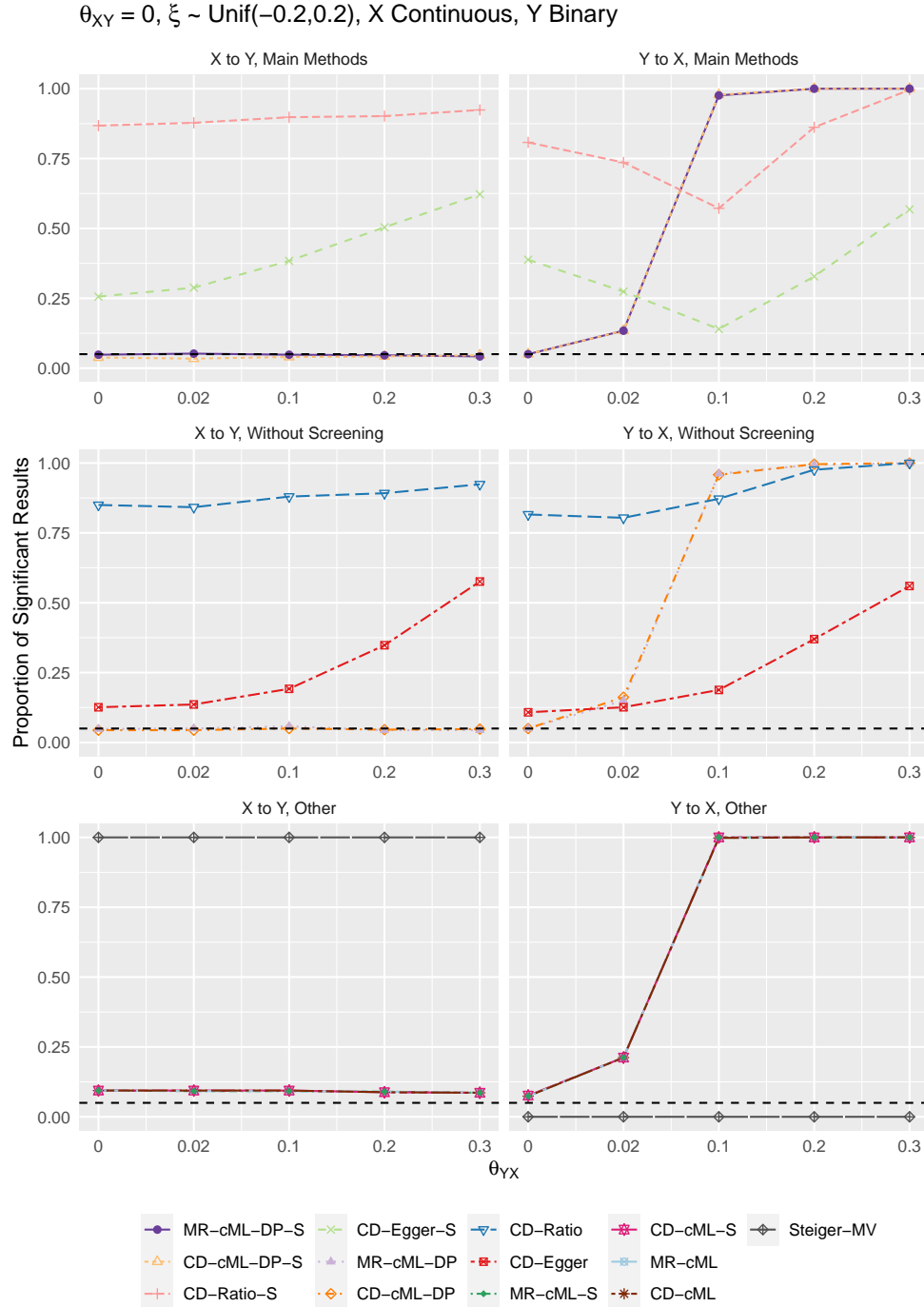
S20 Fig: When X is binary, Y is continuous, $\theta_{XY} = 0.3$ and $\xi \sim \text{Unif}(-0.2, 0.2)$, the proportions of significant simulation results obtained by the methods for direction $X \rightarrow Y$ (left column) and $Y \rightarrow X$ (right column). The first row shows results for four main methods: MR-cML-DP-S, CD-cML-DP-S, CD-Ratio-S, and CD-Egger-S; the second row shows results for four methods without screening: MR-cML-DP, CD-cML-DP, CD-Ratio, and CD-Egger; the third row shows results for other five methods.



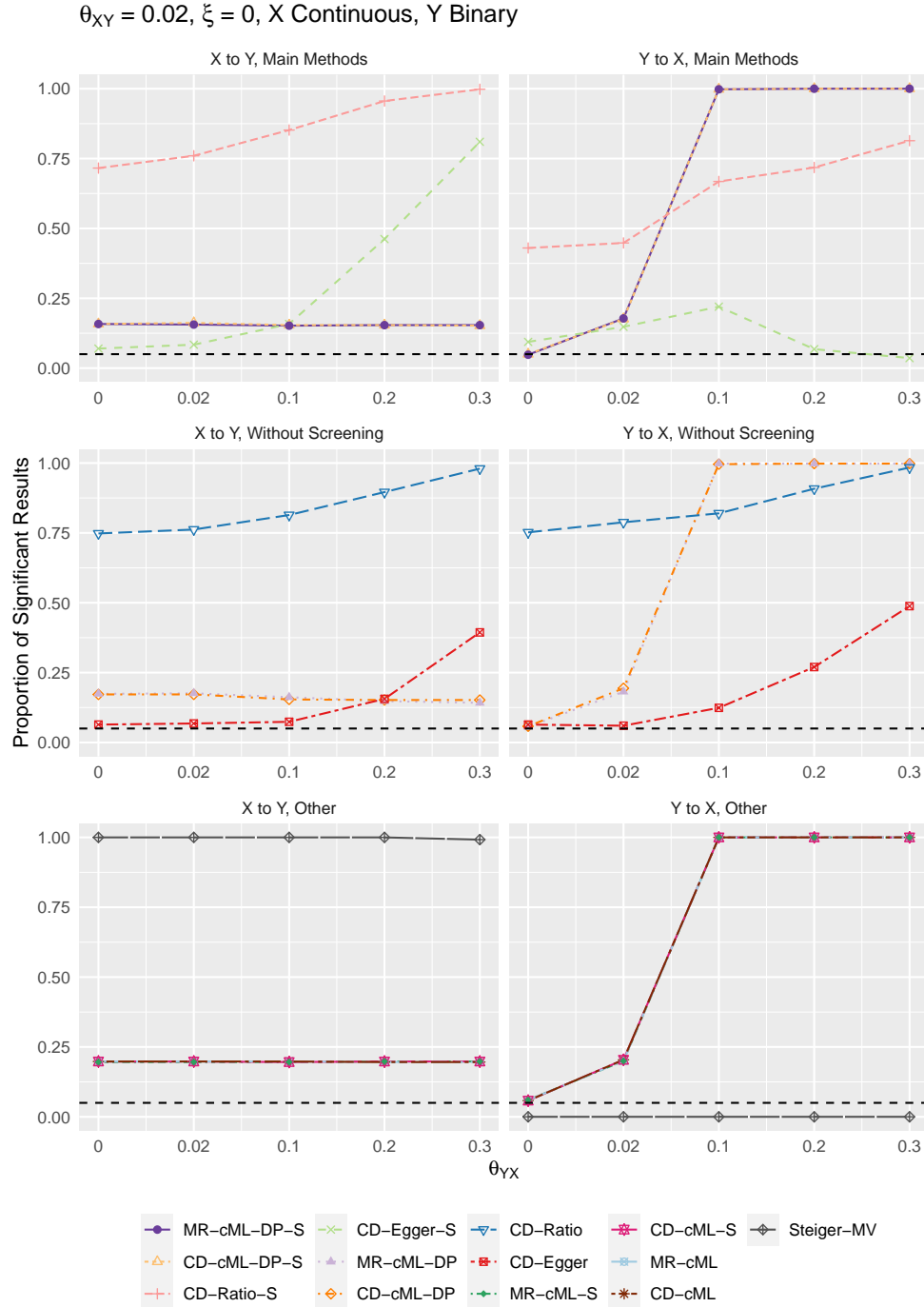
S21 Fig: When X is continuous, Y is binary, $\theta_{XY} = 0$ and $\xi = 0$, the proportions of significant simulation results obtained by the methods for direction $X \rightarrow Y$ (left column) and $Y \rightarrow X$ (right column). The first row shows results for four main methods: MR-cML-DP-S, CD-cML-DP-S, CD-Ratio-S, and CD-Egger-S; the second row shows results for four methods without screening: MR-cML-DP, CD-cML-DP, CD-Ratio, and CD-Egger; the third row shows results for other five methods.



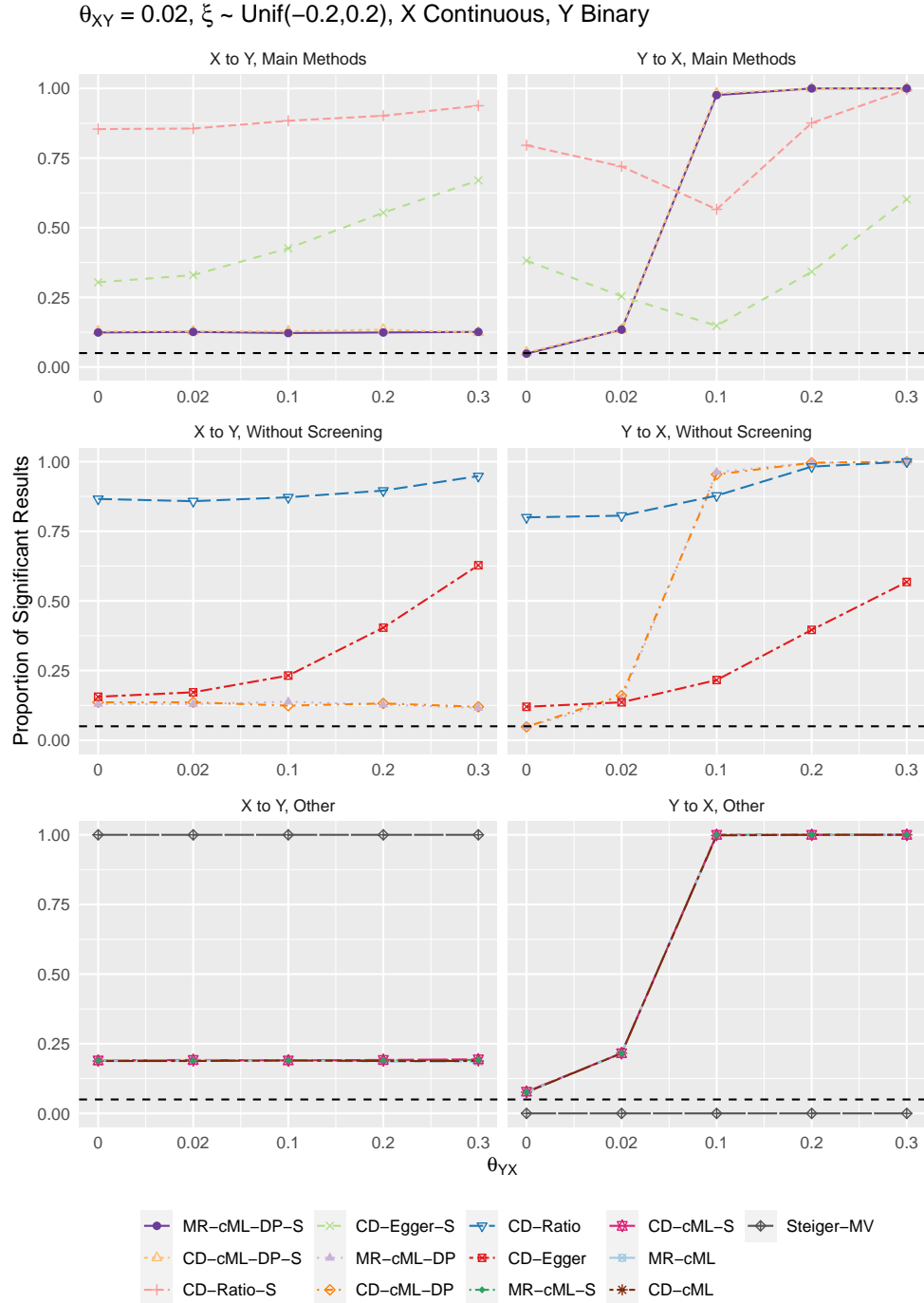
S22 Fig: When X is continuous, Y is binary, $\theta_{XY} = 0$ and $\xi \sim \text{Unif}(-0.2, 0.2)$, the proportions of significant simulation results obtained by the methods for direction $X \rightarrow Y$ (left column) and $Y \rightarrow X$ (right column). The first row shows results for four main methods: MR-cML-DP-S, CD-cML-DP-S, CD-Ratio-S, and CD-Egger-S; the second row shows results for four methods without screening: MR-cML-DP, CD-cML-DP, CD-Ratio, and CD-Egger; the third row shows results for other five methods.



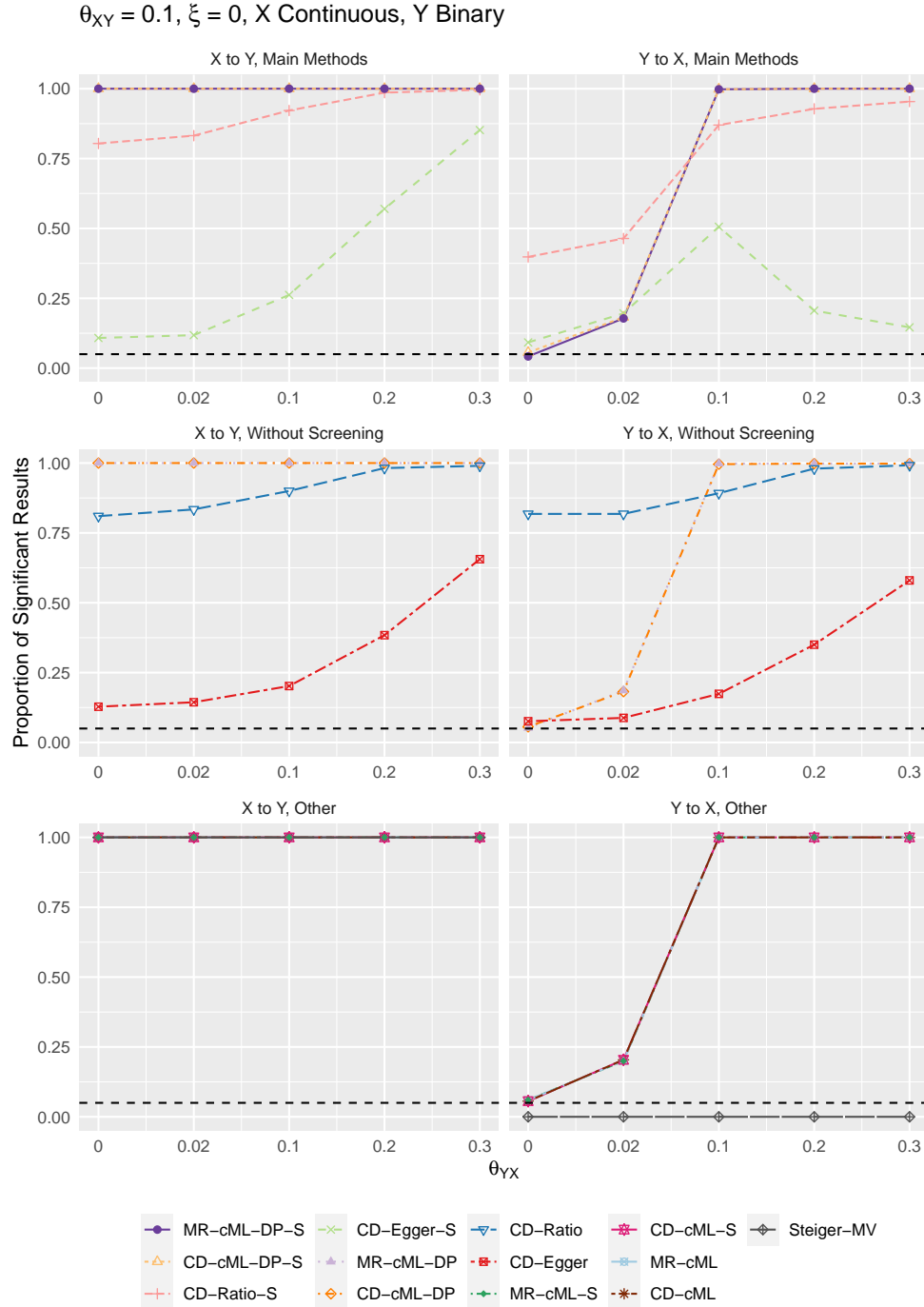
S23 Fig: When X is continuous, Y is binary, $\theta_{XY} = 0.02$ and $\xi = 0$, the proportions of significant simulation results obtained by the methods for direction $X \rightarrow Y$ (left column) and $Y \rightarrow X$ (right column). The first row shows results for four main methods: MR-cML-DP-S, CD-cML-DP-S, CD-Ratio-S, and CD-Egger-S; the second row shows results for four methods without screening: MR-cML-DP, CD-cML-DP, CD-Ratio, and CD-Egger; the third row shows results for other five methods.



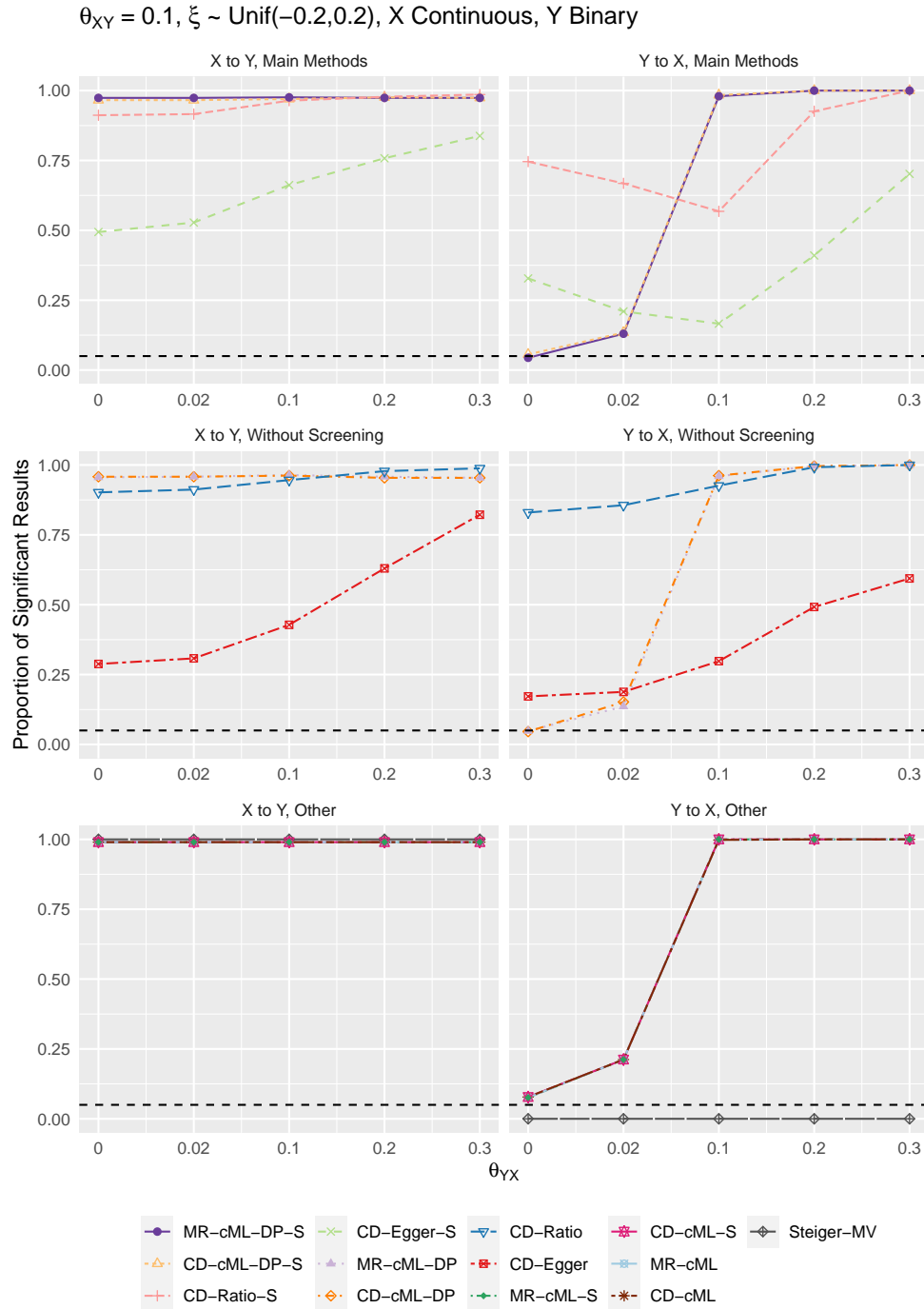
S24 Fig: When X is continuous, Y is binary, $\theta_{XY} = 0.02$ and $\xi \sim \text{Unif}(-0.2, 0.2)$, the proportions of significant simulation results obtained by the methods for direction $X \rightarrow Y$ (left column) and $Y \rightarrow X$ (right column). The first row shows results for four main methods: MR-cML-DP-S, CD-cML-DP-S, CD-Ratio-S, and CD-Egger-S; the second row shows results for four methods without screening: MR-cML-DP, CD-cML-DP, CD-Ratio, and CD-Egger; the third row shows results for other five methods.



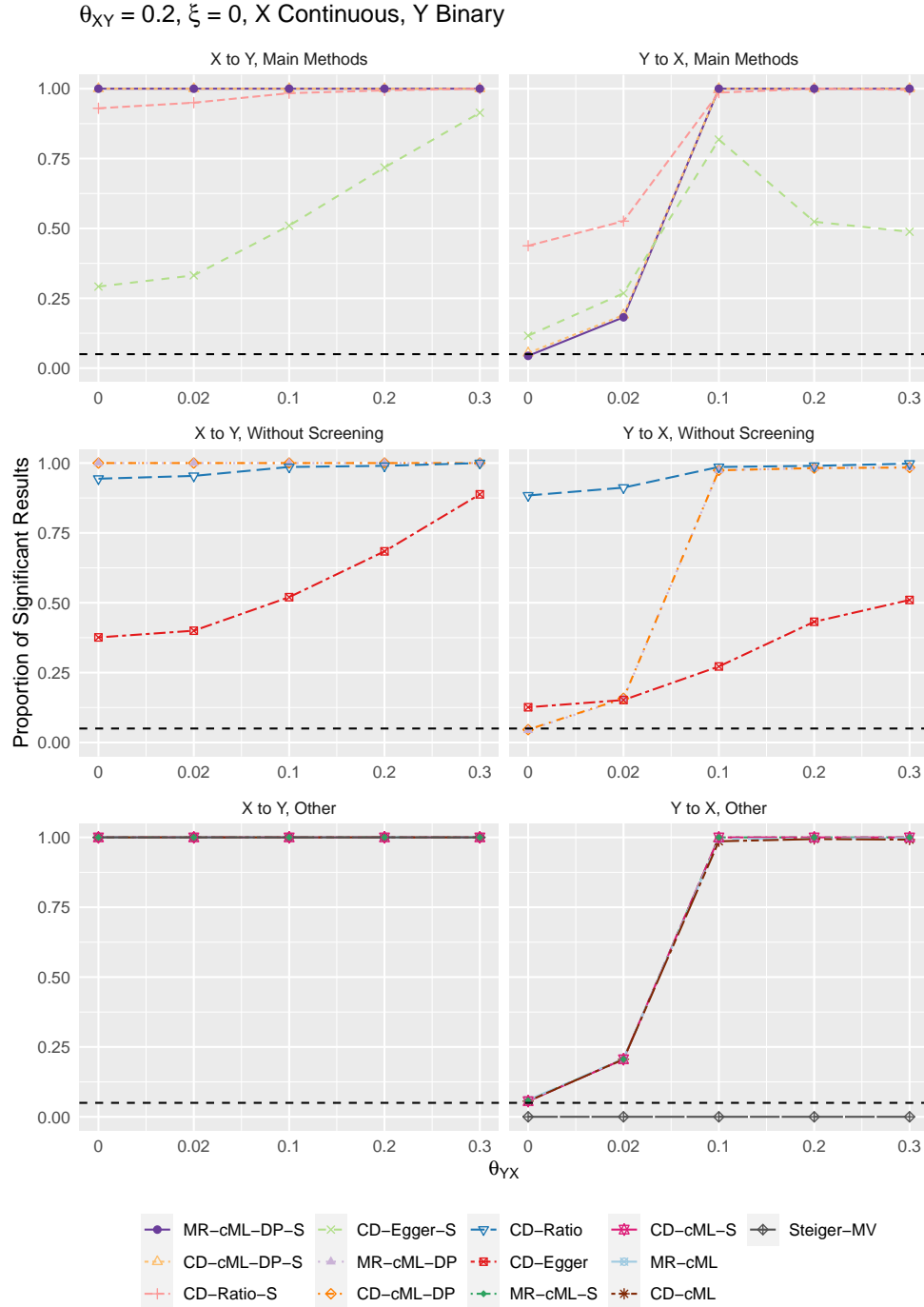
S25 Fig: When X is continuous, Y is binary, $\theta_{XY} = 0.1$ and $\xi = 0$, the proportions of significant simulation results obtained by the methods for direction $X \rightarrow Y$ (left column) and $Y \rightarrow X$ (right column). The first row shows results for four main methods: MR-cML-DP-S, CD-cML-DP-S, CD-Ratio-S, and CD-Egger-S; the second row shows results for four methods without screening: MR-cML-DP, CD-cML-DP, CD-Ratio, and CD-Egger; the third row shows results for other five methods.



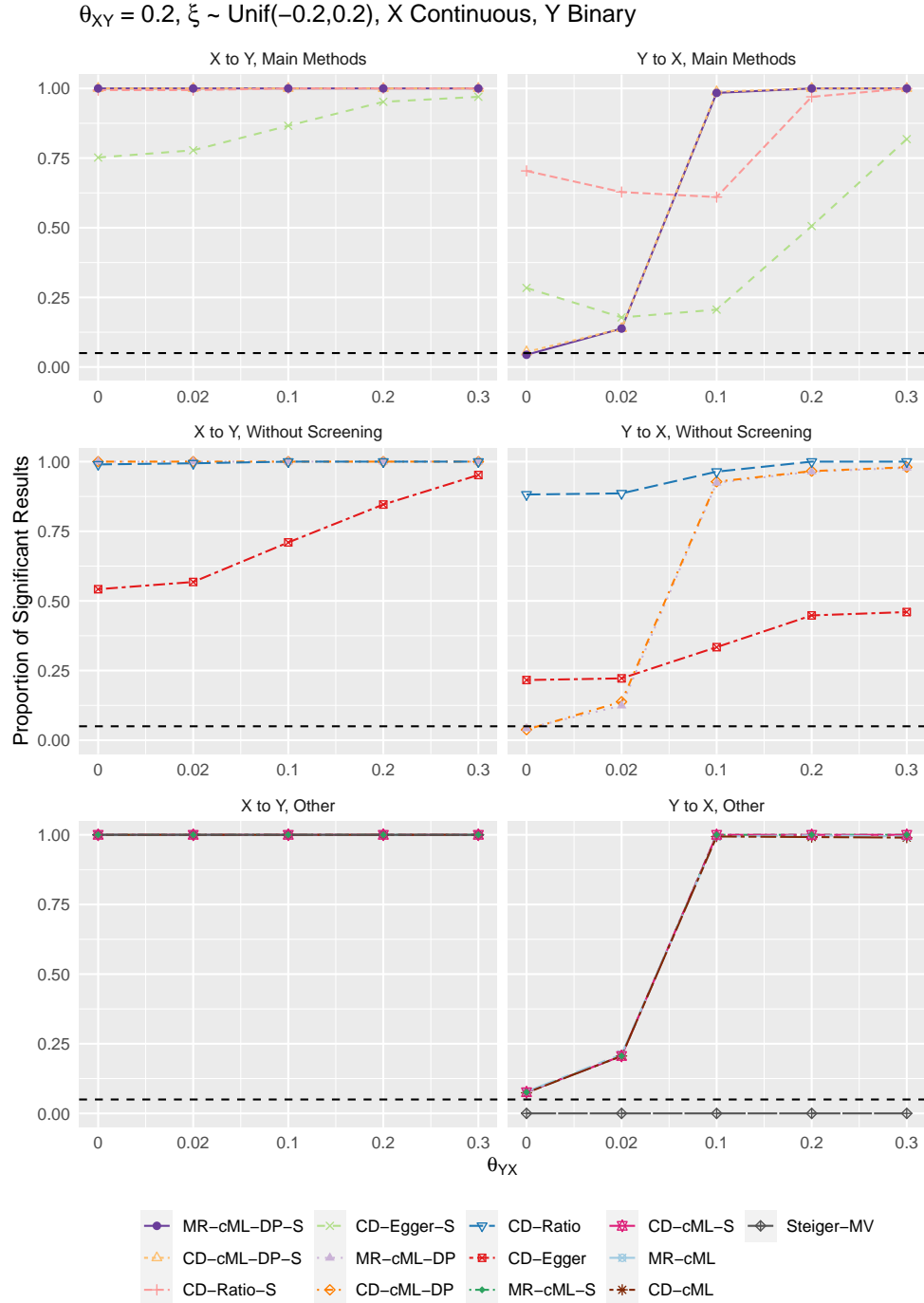
S26 Fig: When X is continuous, Y is binary, $\theta_{XY} = 0.1$ and $\xi \sim \text{Unif}(-0.2, 0.2)$, the proportions of significant simulation results obtained by the methods for direction $X \rightarrow Y$ (left column) and $Y \rightarrow X$ (right column). The first row shows results for four main methods: MR-cML-DP-S, CD-cML-DP-S, CD-Ratio-S, and CD-Egger-S; the second row shows results for four methods without screening: MR-cML-DP, CD-cML-DP, CD-Ratio, and CD-Egger; the third row shows results for other five methods.



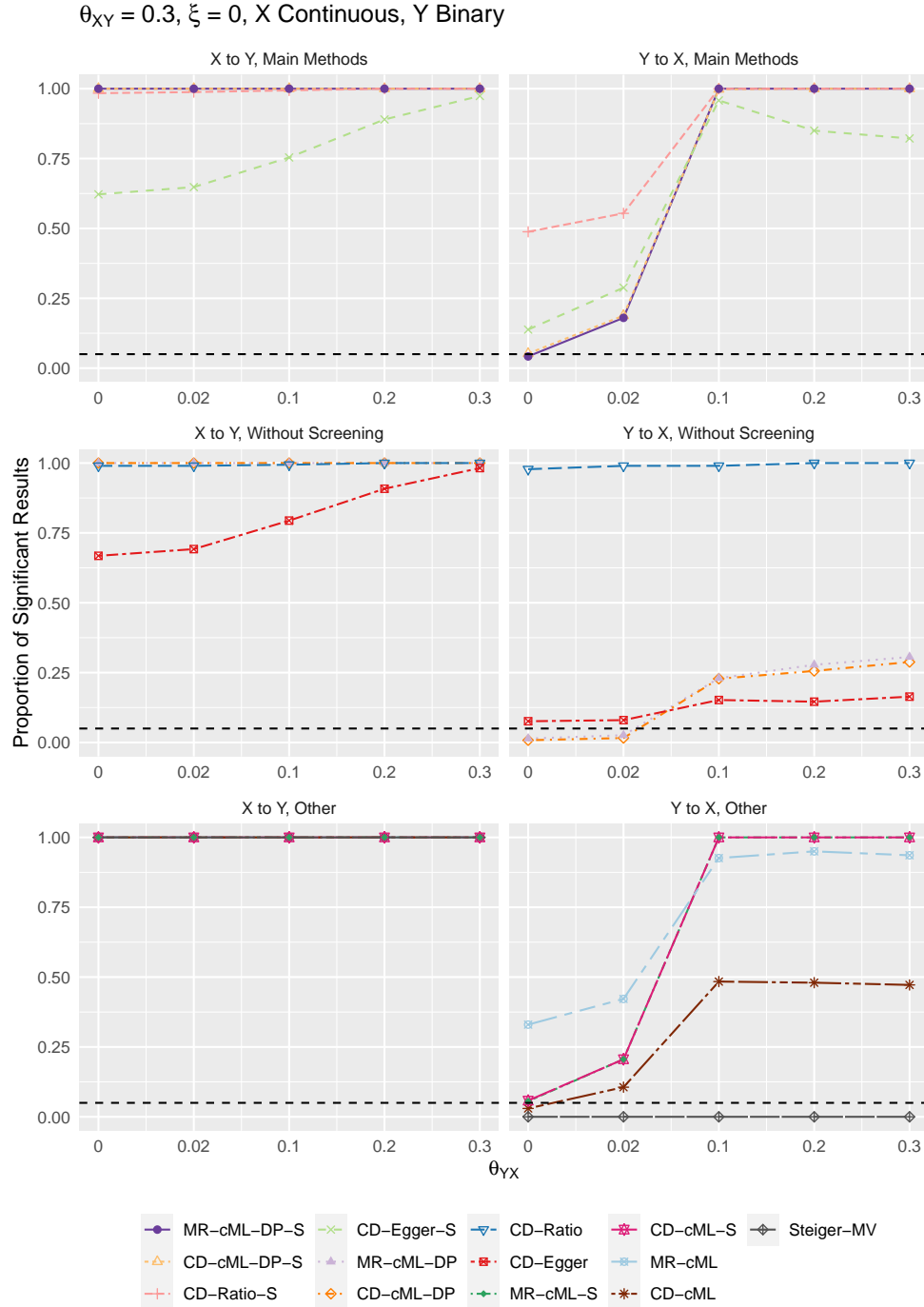
S27 Fig: When X is continuous, Y is binary, $\theta_{XY} = 0.2$ and $\xi = 0$, the proportions of significant simulation results obtained by the methods for direction $X \rightarrow Y$ (left column) and $Y \rightarrow X$ (right column). The first row shows results for four main methods: MR-cML-DP-S, CD-cML-DP-S, CD-Ratio-S, and CD-Egger-S; the second row shows results for four methods without screening: MR-cML-DP, CD-cML-DP, CD-Ratio, and CD-Egger; the third row shows results for other five methods.



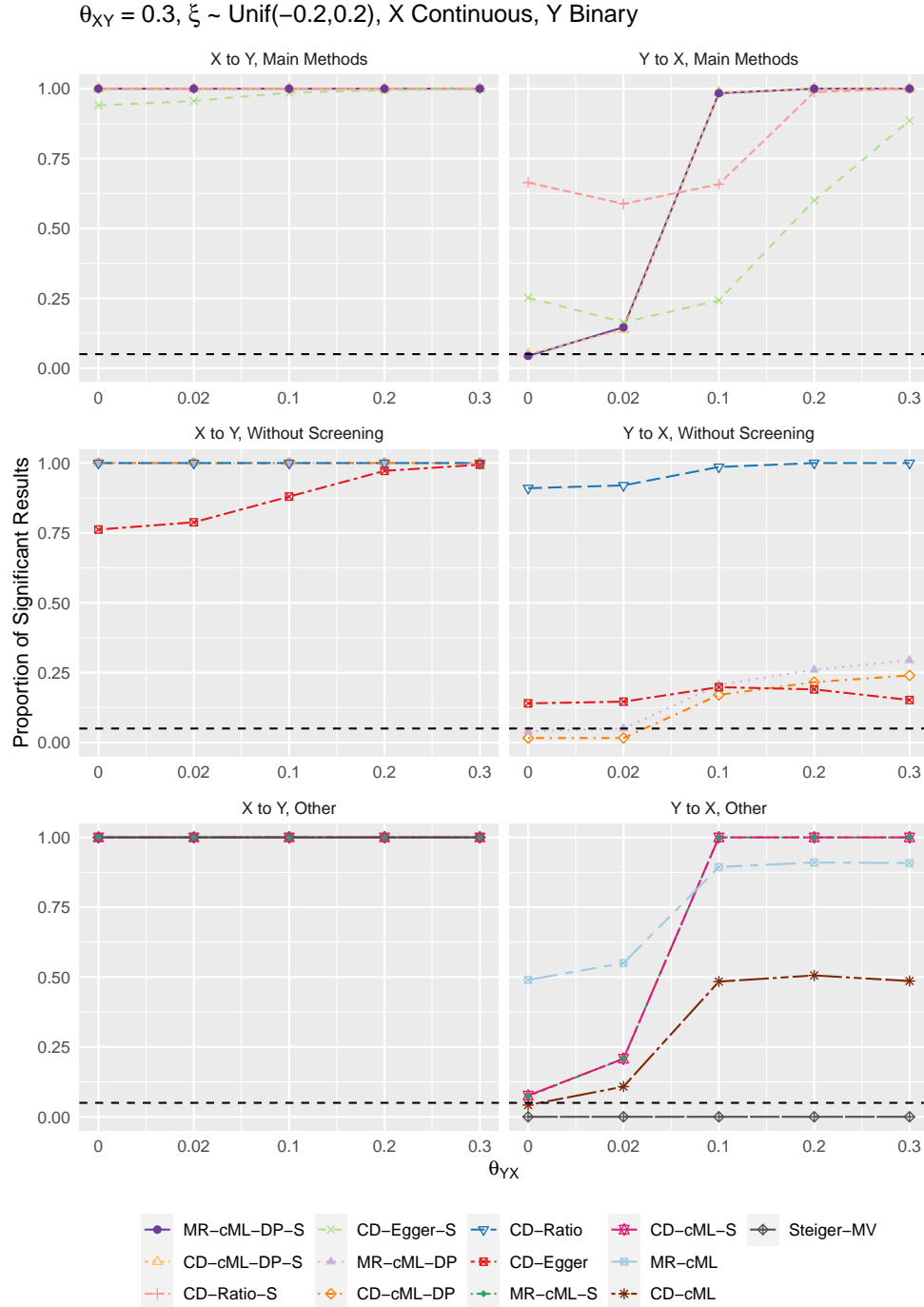
S28 Fig: When X is continuous, Y is binary, $\theta_{XY} = 0.2$ and $\xi \sim \text{Unif}(-0.2, 0.2)$, the proportions of significant simulation results obtained by the methods for direction $X \rightarrow Y$ (left column) and $Y \rightarrow X$ (right column). The first row shows results for four main methods: MR-cML-DP-S, CD-cML-DP-S, CD-Ratio-S, and CD-Egger-S; the second row shows results for four methods without screening: MR-cML-DP, CD-cML-DP, CD-Ratio, and CD-Egger; the third row shows results for other five methods.



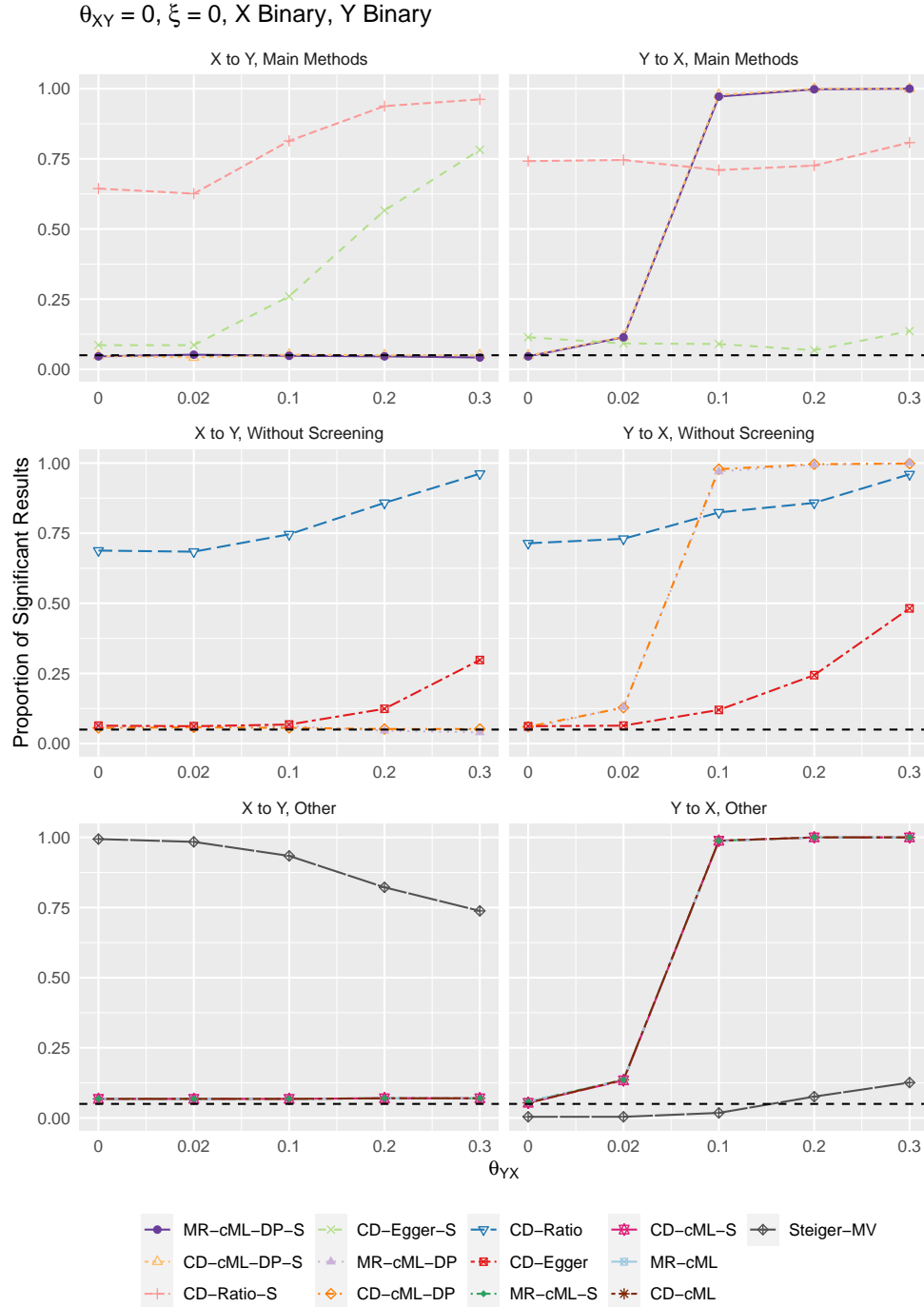
S29 Fig: When X is continuous, Y is binary, $\theta_{XY} = 0.3$ and $\xi = 0$, the proportions of significant simulation results obtained by the methods for direction $X \rightarrow Y$ (left column) and $Y \rightarrow X$ (right column). The first row shows results for four main methods: MR-cML-DP-S, CD-cML-DP-S, CD-Ratio-S, and CD-Egger-S; the second row shows results for four methods without screening: MR-cML-DP, CD-cML-DP, CD-Ratio, and CD-Egger; the third row shows results for other five methods.



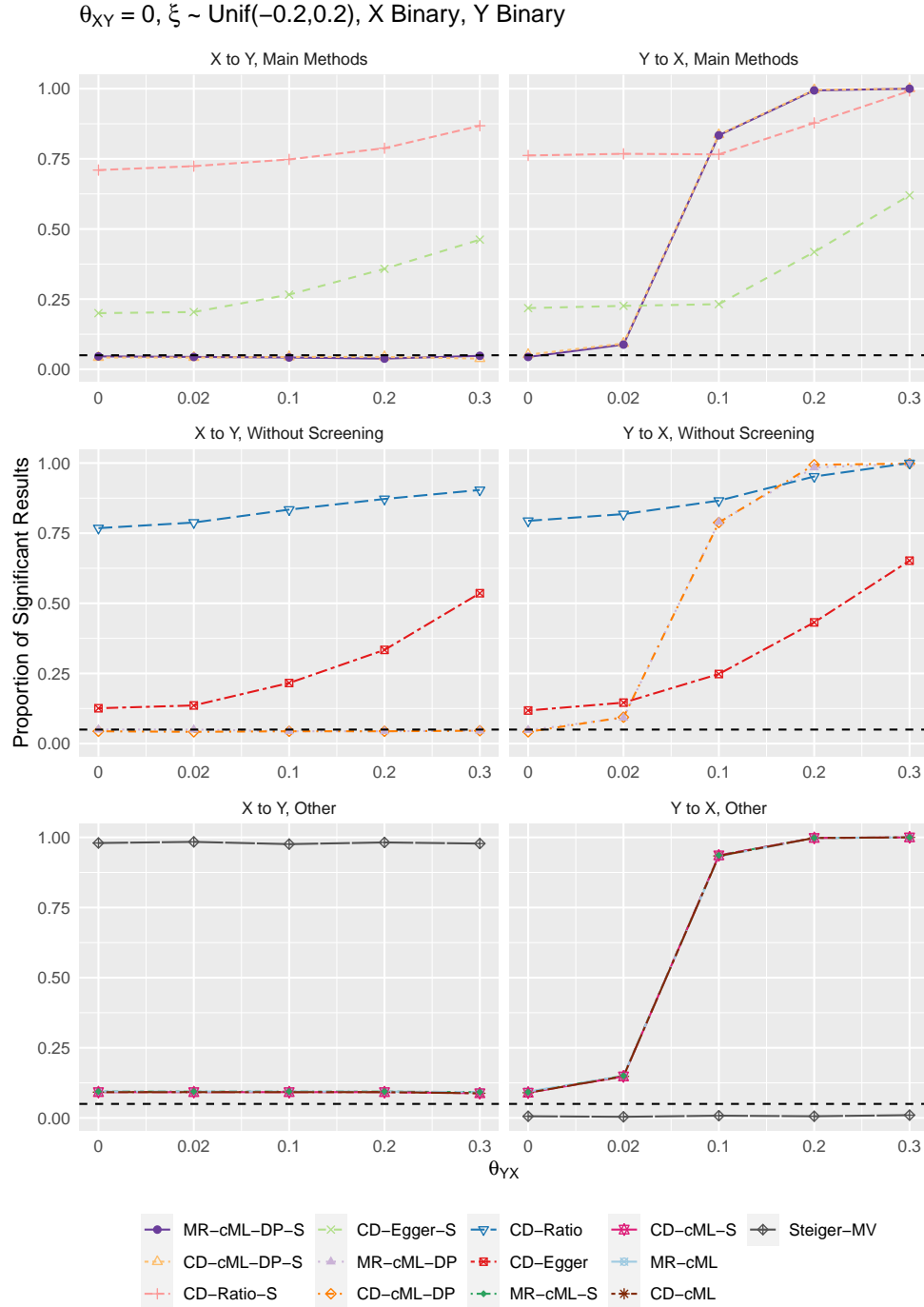
S30 Fig: When X is continuous, Y is binary, $\theta_{XY} = 0.3$ and $\xi \sim \text{Unif}(-0.2, 0.2)$, the proportions of significant simulation results obtained by the methods for direction $X \rightarrow Y$ (left column) and $Y \rightarrow X$ (right column). The first row shows results for four main methods: MR-cML-DP-S, CD-cML-DP-S, CD-Ratio-S, and CD-Egger-S; the second row shows results for four methods without screening: MR-cML-DP, CD-cML-DP, CD-Ratio, and CD-Egger; the third row shows results for other five methods.



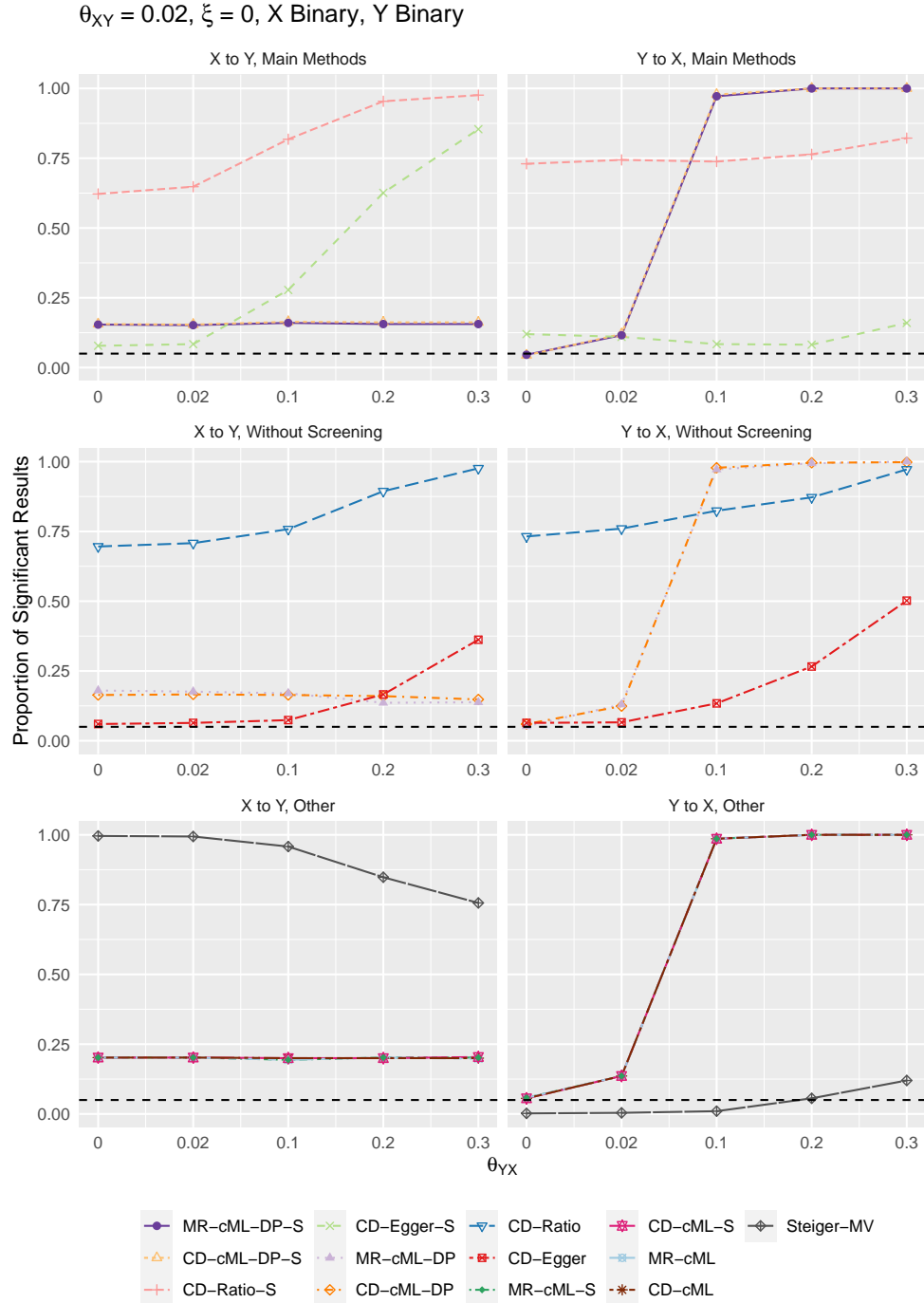
S31 Fig: When both X and Y are binary, $\theta_{XY} = 0$ and $\xi = 0$, the proportions of significant simulation results obtained by the methods for direction $X \rightarrow Y$ (left column) and $Y \rightarrow X$ (right column). The first row shows results for four main methods: MR-cML-DP-S, CD-cML-DP-S, CD-Ratio-S, and CD-Egger-S; the second row shows results for four methods without screening: MR-cML-DP, CD-cML-DP, CD-Ratio, and CD-Egger; the third row shows results for other five methods.



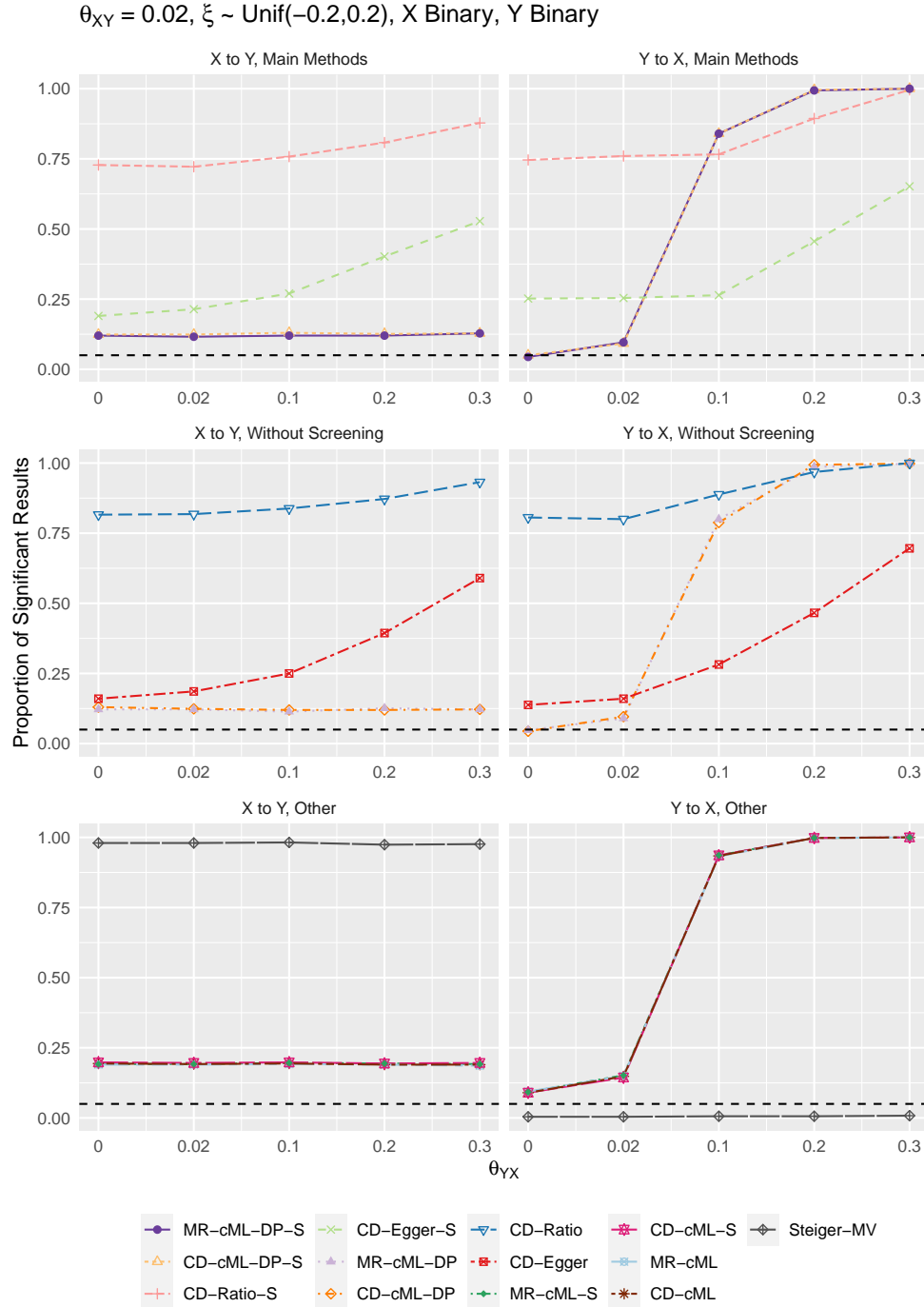
S32 Fig: When both X and Y are binary, $\theta_{XY} = 0$ and $\xi \sim \text{Unif}(-0.2, 0.2)$, the proportions of significant simulation results obtained by the methods for direction $X \rightarrow Y$ (left column) and $Y \rightarrow X$ (right column). The first row shows results for four main methods: MR-cML-DP-S, CD-cML-DP-S, CD-Ratio-S, and CD-Egger-S; the second row shows results for four methods without screening: MR-cML-DP, CD-cML-DP, CD-Ratio, and CD-Egger; the third row shows results for other five methods.



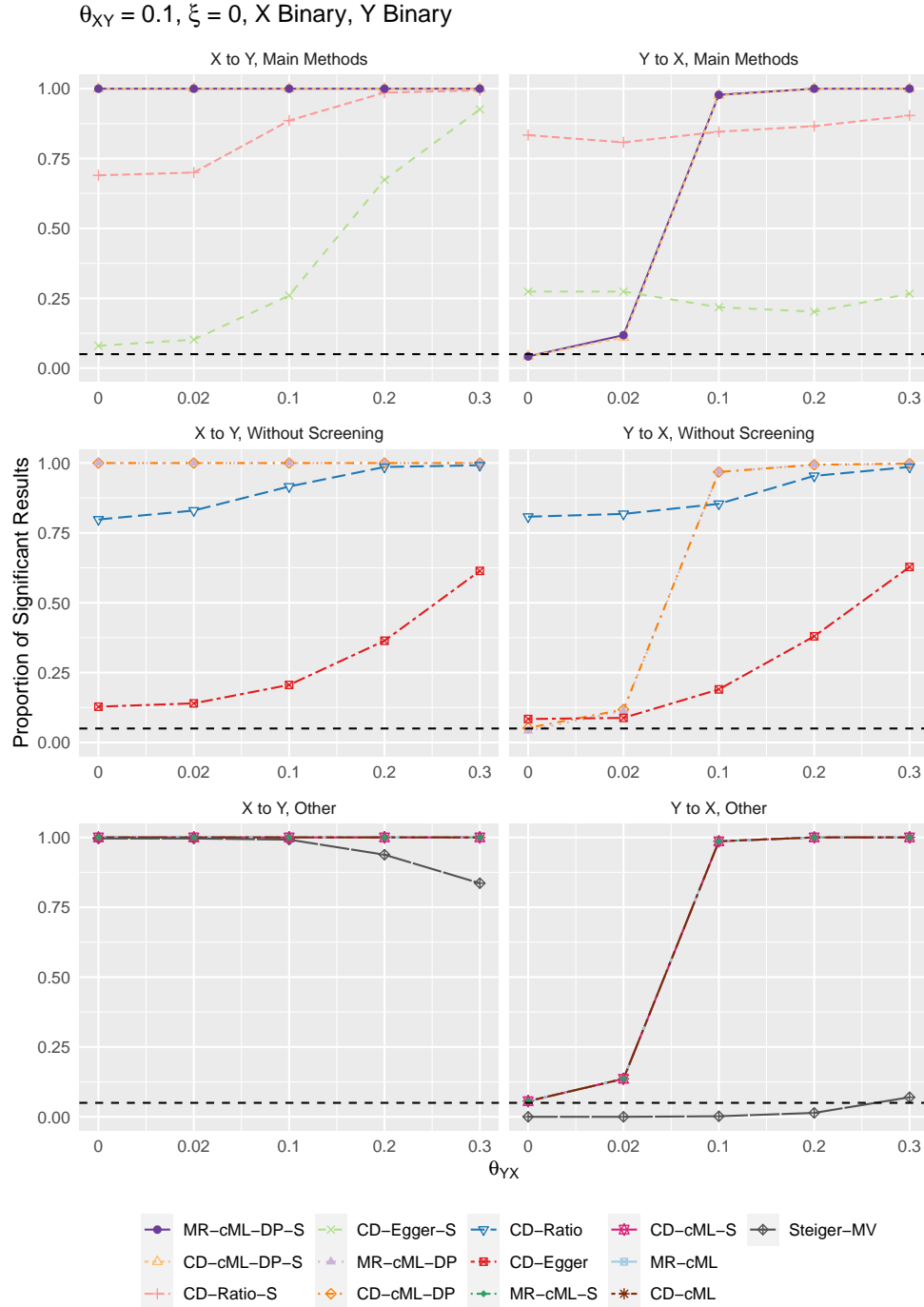
S33 Fig: When both X and Y are binary, $\theta_{XY} = 0.02$ and $\xi = 0$, the proportions of significant simulation results obtained by the methods for direction $X \rightarrow Y$ (left column) and $Y \rightarrow X$ (right column). The first row shows results for four main methods: MR-cML-DP-S, CD-cML-DP-S, CD-Ratio-S, and CD-Egger-S; the second row shows results for four methods without screening: MR-cML-DP, CD-cML-DP, CD-Ratio, and CD-Egger; the third row shows results for other five methods.



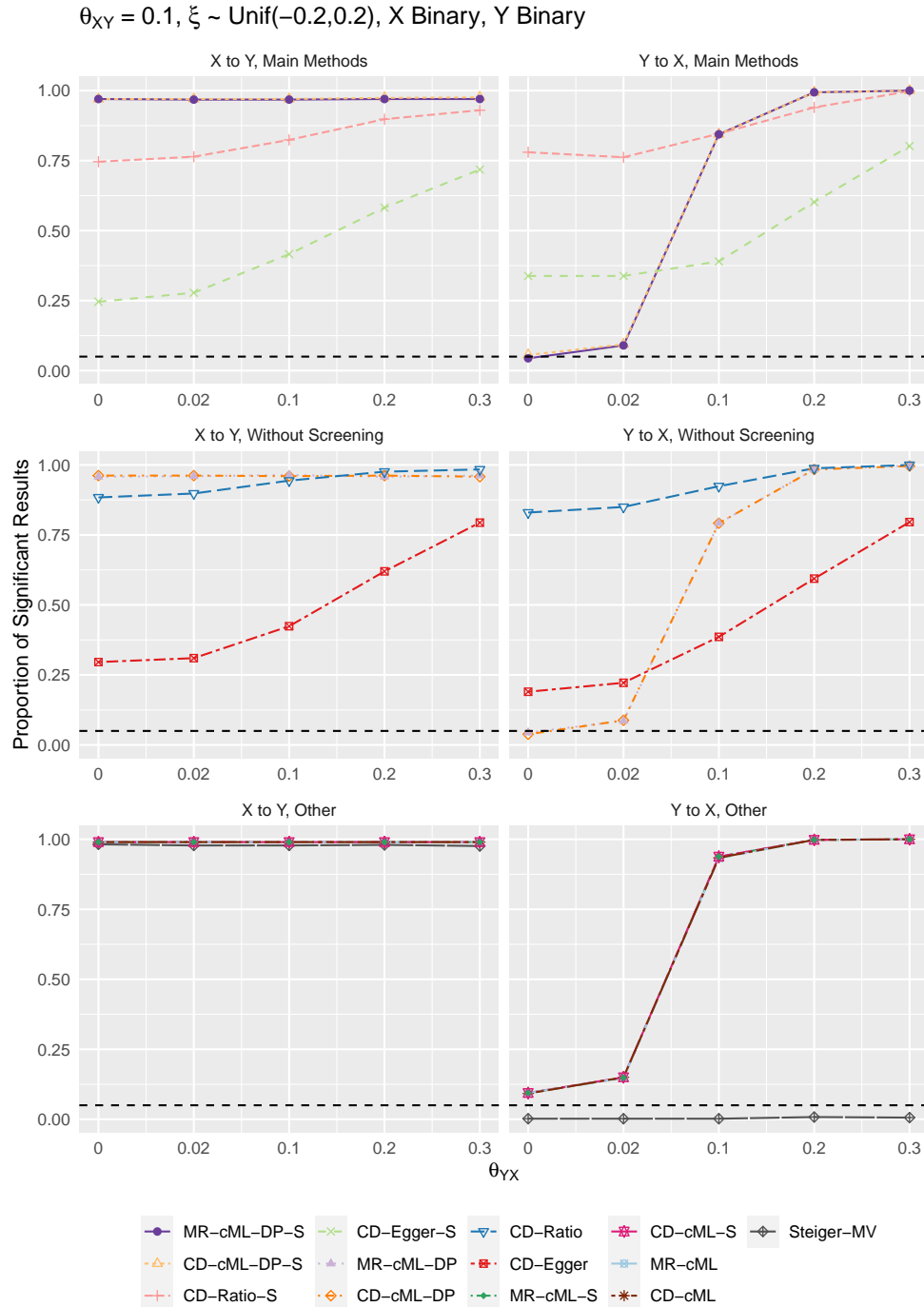
S34 Fig: When both X and Y are binary, $\theta_{XY} = 0.02$ and $\xi \sim \text{Unif}(-0.2, 0.2)$, the proportions of significant simulation results obtained by the methods for direction $X \rightarrow Y$ (left column) and $Y \rightarrow X$ (right column). The first row shows results for four main methods: MR-cML-DP-S, CD-cML-DP-S, CD-Ratio-S, and CD-Egger-S; the second row shows results for four methods without screening: MR-cML-DP, CD-cML-DP, CD-Ratio, and CD-Egger; the third row shows results for other five methods.



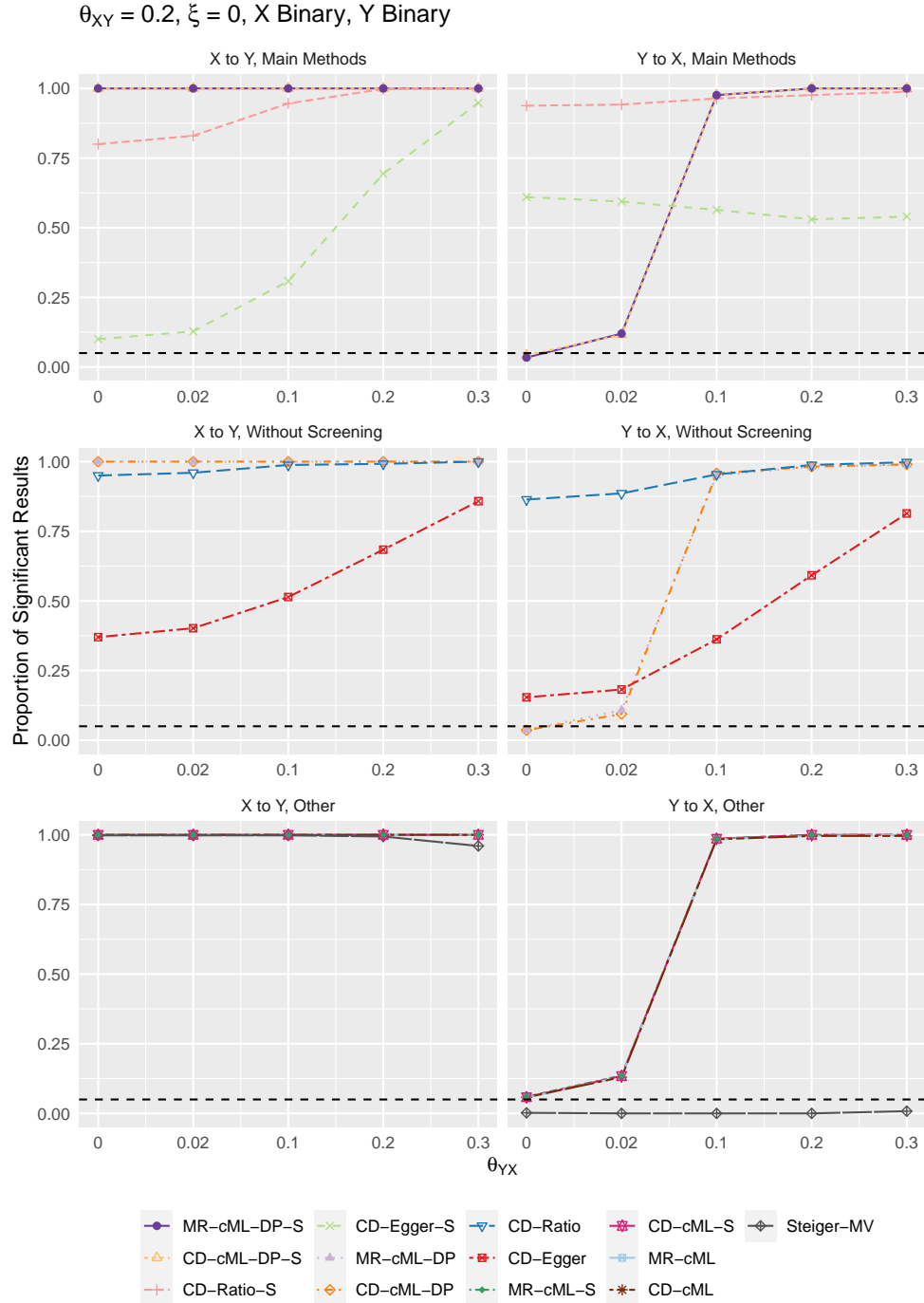
S35 Fig: When both X and Y are binary, $\theta_{XY} = 0.1$ and $\xi = 0$, the proportions of significant simulation results obtained by the methods for direction $X \rightarrow Y$ (left column) and $Y \rightarrow X$ (right column). The first row shows results for four main methods: MR-cML-DP-S, CD-cML-DP-S, CD-Ratio-S, and CD-Egger-S; the second row shows results for four methods without screening: MR-cML-DP, CD-cML-DP, CD-Ratio, and CD-Egger; the third row shows results for other five methods.



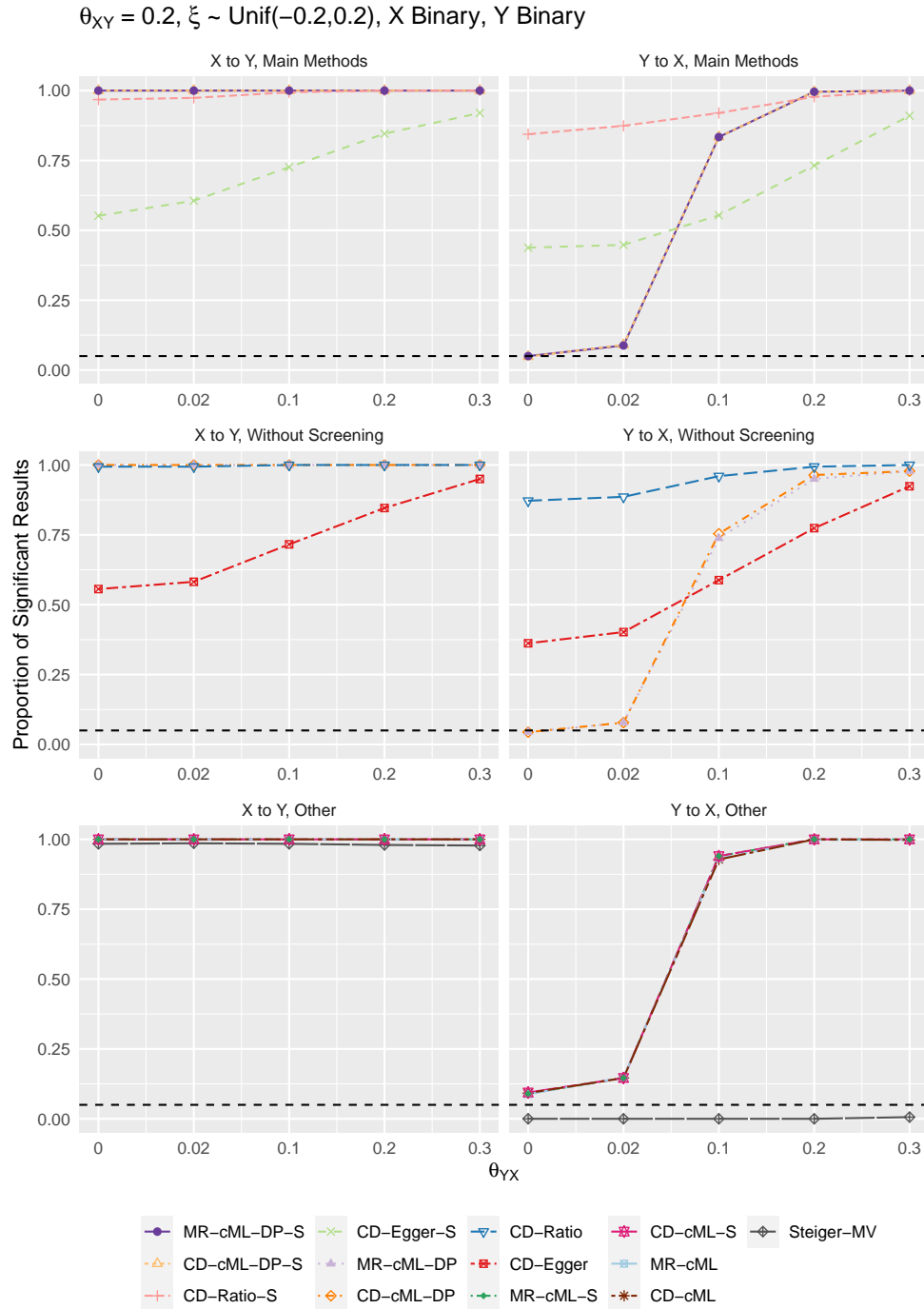
S36 Fig: When both X and Y are binary, $\theta_{XY} = 0.1$ and $\xi \sim \text{Unif}(-0.2, 0.2)$, the proportions of significant simulation results obtained by the methods for direction $X \rightarrow Y$ (left column) and $Y \rightarrow X$ (right column). The first row shows results for four main methods: MR-cML-DP-S, CD-cML-DP-S, CD-Ratio-S, and CD-Egger-S; the second row shows results for four methods without screening: MR-cML-DP, CD-cML-DP, CD-Ratio, and CD-Egger; the third row shows results for other five methods.



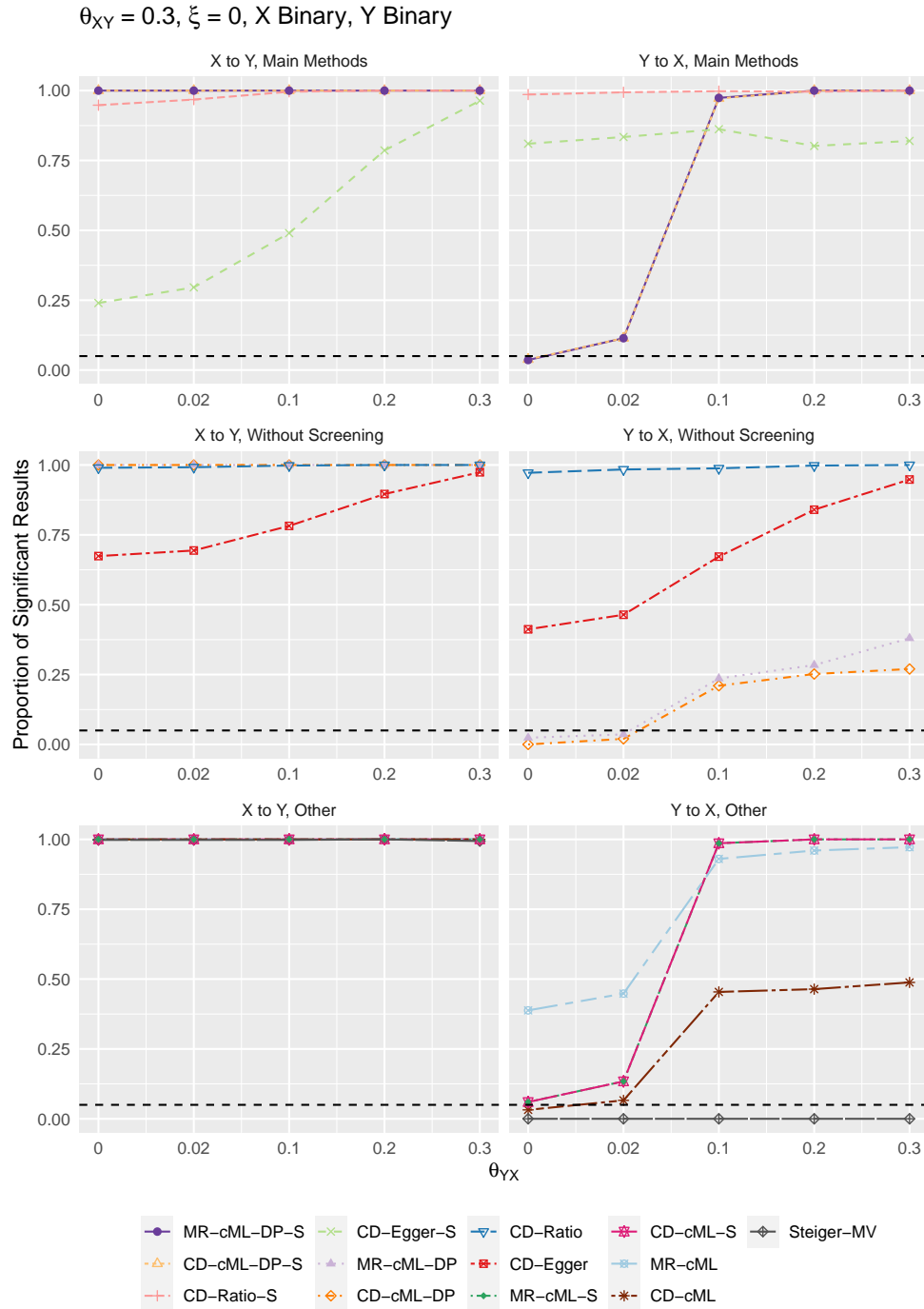
S37 Fig: When both X and Y are binary, $\theta_{XY} = 0.2$ and $\xi = 0$, the proportions of significant simulation results obtained by the methods for direction $X \rightarrow Y$ (left column) and $Y \rightarrow X$ (right column). The first row shows results for four main methods: MR-cML-DP-S, CD-cML-DP-S, CD-Ratio-S, and CD-Egger-S; the second row shows results for four methods without screening: MR-cML-DP, CD-cML-DP, CD-Ratio, and CD-Egger; the third row shows results for other five methods.



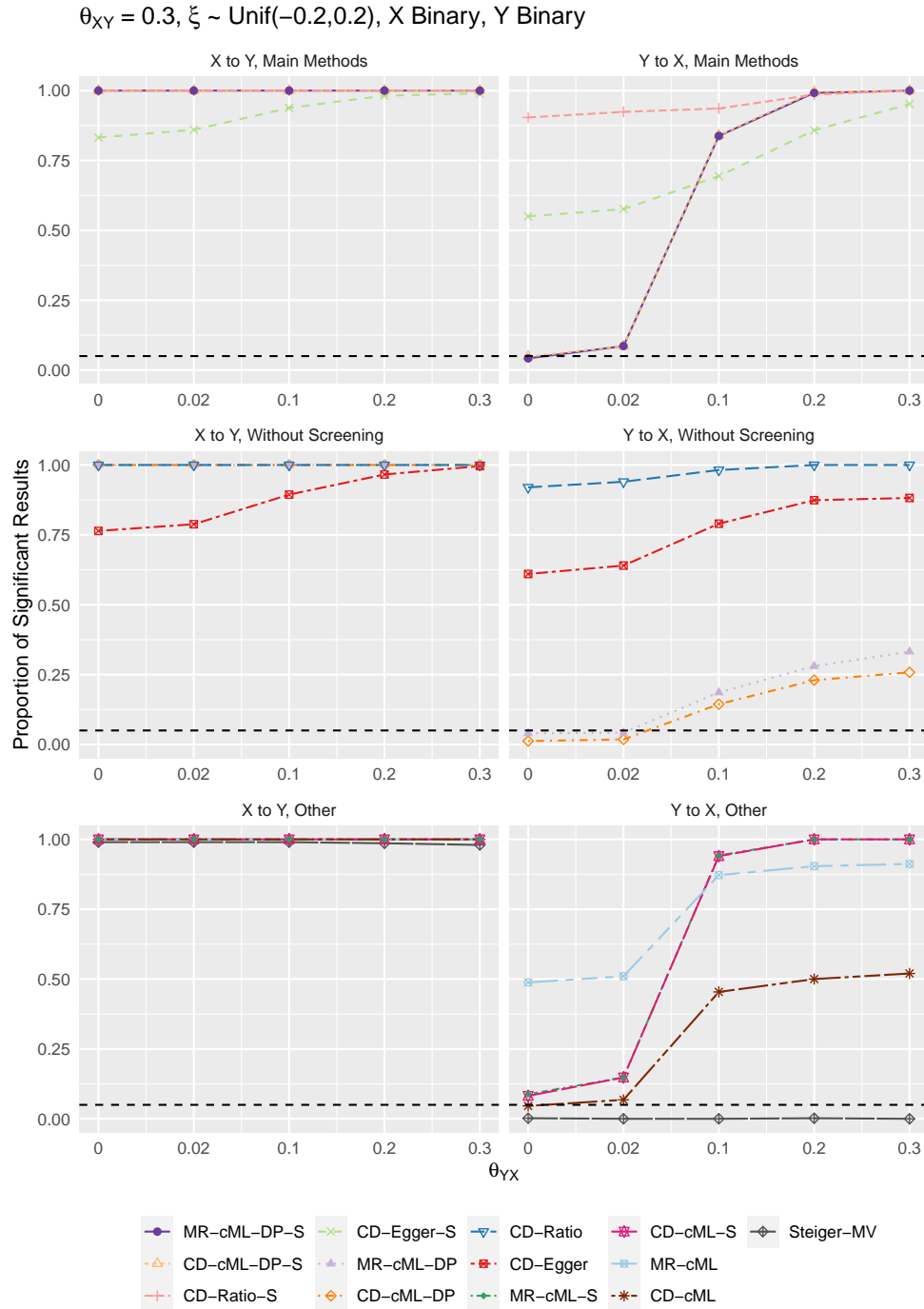
S38 Fig: When both X and Y are binary, $\theta_{XY} = 0.2$ and $\xi \sim \text{Unif}(-0.2, 0.2)$, the proportions of significant simulation results obtained by the methods for direction $X \rightarrow Y$ (left column) and $Y \rightarrow X$ (right column). The first row shows results for four main methods: MR-cML-DP-S, CD-cML-DP-S, CD-Ratio-S, and CD-Egger-S; the second row shows results for four methods without screening: MR-cML-DP, CD-cML-DP, CD-Ratio, and CD-Egger; the third row shows results for other five methods.



S39 Fig: When both X and Y are binary, $\theta_{XY} = 0.3$ and $\xi = 0$, the proportions of significant simulation results obtained by the methods for direction $X \rightarrow Y$ (left column) and $Y \rightarrow X$ (right column). The first row shows results for four main methods: MR-cML-DP-S, CD-cML-DP-S, CD-Ratio-S, and CD-Egger-S; the second row shows results for four methods without screening: MR-cML-DP, CD-cML-DP, CD-Ratio, and CD-Egger; the third row shows results for other five methods.



S40 Fig: When both X and Y are binary, $\theta_{XY} = 0.3$ and $\xi \sim \text{Unif}(-0.2, 0.2)$, the proportions of significant simulation results obtained by the methods for direction $X \rightarrow Y$ (left column) and $Y \rightarrow X$ (right column). The first row shows results for four main methods: MR-cML-DP-S, CD-cML-DP-S, CD-Ratio-S, and CD-Egger-S; the second row shows results for four methods without screening: MR-cML-DP, CD-cML-DP, CD-Ratio, and CD-Egger; the third row shows results for other five methods.



S2 Full Real Data Results

S2.1 48 Risk Factor-Disease Pairs

S1 Table: Inferring causal effects between first 6 risk factors and CAD. In each cell we show the Bonferroni adjusted $1-0.05/96 \approx 0.9995$ confidence intervals (CIs) of θ for the MR methods, and CIs of K for the CD methods; for Steiger’s method, we show the proportion of SNPs giving significant result. TRUE/FALSE in each cell indicates whether the result is significant or not, and the cells giving significant results are marked in red.

Method \ Direction	TG CAD to	CAD to TG	LDL to CAD	CAD to LDL	HDL to CAD	CAD to HDL	Height to CAD	CAD to Height	BMI to CAD	CAD to BMI	BF to CAD	CAD to BF
MR-cML-DP-S	(0.122, 0.563), TRUE	(-0.049, 0.079), FALSE	(0.184, 0.67), TRUE	(-0.101, 0.03), FALSE	(-0.557, 0.035), FALSE	(-0.058, 0.055), FALSE	(-0.166, -0.039), TRUE	(-0.021, 0.069), FALSE	(0.139, 0.49), TRUE	(-0.084, 0.003), FALSE	(-0.676, 0.948), FALSE	(-0.104, 0.019), FALSE
MR-cML-S	(0.278, 0.461), TRUE	(-0.022, 0.047), FALSE	(0.287, 0.499), TRUE	(-0.076, 0.014), FALSE	(-0.346, -0.179), TRUE	(-0.039, 0.039), FALSE	(-0.151, -0.05), TRUE	(-0.007, 0.053), FALSE	(0.171, 0.426), TRUE	(-0.067, -0.009), TRUE	(-0.159, 0.577), FALSE	(-0.08, 0.004), FALSE
CD-cML-DP-S	(0.02, 0.121), TRUE	(-0.157, 0.268), FALSE	(0.053, 0.159), TRUE	(-0.387, 0.116), FALSE	(-0.113, 0.005), FALSE	(-0.193, 0.213), FALSE	(-0.048, -0.011), TRUE	(-0.067, 0.212), FALSE	(0.047, 0.16), TRUE	(-0.205, 0.001), FALSE	(-0.144, 0.223), FALSE	(-0.349, 0.063), FALSE
CD-cML-S	(0.055, 0.093), TRUE	(-0.091, 0.187), FALSE	(0.096, 0.135), TRUE	(-0.297, 0.054), FALSE	(-0.074, -0.038), TRUE	(-0.131, 0.152), FALSE	(-0.043, -0.014), TRUE	(-0.033, 0.175), FALSE	(0.057, 0.139), TRUE	(-0.175, -0.022), TRUE	(-0.036, 0.143), FALSE	(-0.269, 0.012), FALSE
CD-Ratio-S	(0.046, 0.078), TRUE	(-0.056, 0.211), FALSE	(0.079, 0.106), TRUE	(-0.016, 0.267), FALSE	(-0.052, -0.023), TRUE	(-0.158, 0.115), FALSE	(-0.038, -0.01), TRUE	(-0.068, 0.124), FALSE	(0.052, 0.131), TRUE	(-0.161, -0.014), TRUE	(-0.054, 0.093), FALSE	(-0.253, 0.022), FALSE
CD-Egger-S	(0.036, 0.106), TRUE	(-0.146, 0.34), FALSE	(0.061, 0.12), TRUE	(-0.151, 0.513), FALSE	(-0.093, 0.001), FALSE	(-0.282, 0.174), FALSE	(-0.048, -0.004), TRUE	(-0.205, 0.178), FALSE	(0.032, 0.164), TRUE	(-0.213, 0.047), FALSE	(-0.168, 0.144), FALSE	(-0.287, 0.084), FALSE
MR-cML-DP	(0.122, 0.563), TRUE	(-0.048, 0.081), FALSE	(0.175, 0.698), TRUE	(-0.098, 0.03), FALSE	(-0.557, 0.035), FALSE	(-0.055, 0.054), FALSE	(-0.166, -0.039), TRUE	(-0.024, 0.074), FALSE	(0.139, 0.49), TRUE	(-0.084, 0.003), FALSE	(-0.676, 0.948), FALSE	(-0.104, 0.019), FALSE
MR-cML	(0.278, 0.461), TRUE	(-0.022, 0.047), FALSE	(0.225, 0.584), TRUE	(-0.076, 0.014), FALSE	(-0.346, -0.179), TRUE	(-0.039, 0.039), FALSE	(-0.151, -0.05), TRUE	(-0.007, 0.053), FALSE	(0.171, 0.426), TRUE	(-0.067, -0.009), TRUE	(-0.159, 0.577), FALSE	(-0.08, 0.004), FALSE
CD-cML-DP	(0.02, 0.121), TRUE	(-0.158, 0.281), FALSE	(0.053, 0.162), TRUE	(-0.362, 0.105), FALSE	(-0.113, 0.005), FALSE	(-0.176, 0.201), FALSE	(-0.048, -0.011), TRUE	(-0.075, 0.222), FALSE	(0.047, 0.16), TRUE	(-0.205, 0.001), FALSE	(-0.144, 0.223), FALSE	(-0.349, 0.063), FALSE
CD-cML	(0.055, 0.093), TRUE	(-0.091, 0.187), FALSE	(0.097, 0.135), TRUE	(-0.297, 0.054), FALSE	(-0.074, -0.038), TRUE	(-0.131, 0.152), FALSE	(-0.043, -0.014), TRUE	(-0.033, 0.175), FALSE	(0.057, 0.139), TRUE	(-0.175, -0.022), TRUE	(-0.036, 0.143), FALSE	(-0.269, 0.012), FALSE
CD-Ratio	(0.046, 0.078), TRUE	(-0.016, 0.25), FALSE	(0.081, 0.108), TRUE	(0.049, 0.327), TRUE	(-0.052, -0.023), TRUE	(-0.303, -0.04), TRUE	(-0.038, -0.01), TRUE	(-0.079, 0.112), FALSE	(0.052, 0.131), TRUE	(-0.161, -0.014), TRUE	(-0.054, 0.093), FALSE	(-0.253, 0.022), FALSE
CD-Egger	(0.036, 0.106), TRUE	(-0.156, 0.861), FALSE	(0.053, 0.152), TRUE	(-0.106, 2.214), FALSE	(-0.093, 0.001), FALSE	(-1.042, 0.144), FALSE	(-0.048, -0.004), TRUE	(-0.206, 0.201), FALSE	(0.032, 0.164), TRUE	(-0.213, 0.047), FALSE	(-0.168, 0.144), FALSE	(-0.287, 0.084), FALSE
LHC-MR	(0.052, 0.202), TRUE	(0.197, 0.726), TRUE	(0.089, 0.23), TRUE	(-0.333, 0.565), FALSE	(-0.184, -0.077), TRUE	(-0.643, -0.098), TRUE	(-0.094, -0.012), TRUE	(-0.498, 0.766), FALSE	(0.103, 0.258), TRUE	(-0.841, 0.621), FALSE	(0.106, 0.278), TRUE	(-0.29, 0.538), FALSE
Steiger	0.505, TRUE	0.184, FALSE	0.608, TRUE	0.128, FALSE	0.617, TRUE	0.141, FALSE	0.914, TRUE	0.073, FALSE	0.492, TRUE	0.407, FALSE	0.111, FALSE	0.25, FALSE

S2 Table: Inferring causal effects between second 6 risk factors and CAD. In each cell we show the Bonferroni adjusted 1-0.05/96 \approx 0.9995 confidence intervals (CIs) of θ for the MR methods, and CIs of K for the CD methods; for Steiger's method, we show the proportion of SNPs giving significant result. TRUE/FALSE in each cell indicates whether the result is significant or not, and the cells giving significant results are marked in red.

Method	Direction	BW CAD to	CAD BW to	DBP CAD to	CAD DBP to	SBP CAD to	CAD SBP to	FG CAD to	CAD FG to	Smoke to CAD	CAD to Smoke	Alcohol to CAD	CAD to Alcohol
MR-cML-DP-S		(-0.37, 0.152), FALSE	(-0.063, 0.027), FALSE	(0.055, 0.087), TRUE	(-0.978, 1.072), FALSE	(0.037, 0.053), TRUE	(-1.501, 4.369), FALSE	(0.126, 0.557), TRUE	(-0.028, 0.05), FALSE	(-0.166, 0.378), FALSE	(-0.072, 0.037), FALSE	(-0.212, 0.78), FALSE	(-0.014, 0.023), FALSE
MR-cML-S		(-0.263, 0.027), FALSE	(-0.05, 0.009), FALSE	(0.058, 0.075), TRUE	(-0.248, 0.147), FALSE	(0.04, 0.05), TRUE	(-0.345, 4.369), FALSE	(0.139, 0.547), TRUE	(-0.019, 0.04), FALSE	(-0.092, 0.311), FALSE	(-0.058, 0.026), FALSE	(0.017, 0.558), TRUE	(-0.01, 0.019), FALSE
CD-cML-DP-S		(-0.102, 0.043), FALSE	(-0.23, 0.098), FALSE	(0.16, 0.252), TRUE	(-0.328, 0.361), FALSE	(0.183, 0.265), TRUE	(-0.302, 0.862), FALSE	(0.019, 0.087), TRUE	(-0.187, 0.306), FALSE	(-0.089, 0.204), FALSE	(-0.132, 0.069), FALSE	(-0.06, 0.219), FALSE	(-0.053, 0.086), FALSE
CD-cML-S		(-0.072, 0.008), FALSE	(-0.182, 0.034), FALSE	(0.168, 0.217), TRUE	(-0.083, 0.056), FALSE	(0.198, 0.248), TRUE	(-0.273, 0.973), FALSE	(0.021, 0.085), TRUE	(-0.133, 0.243), FALSE	(-0.049, 0.168), FALSE	(-0.105, 0.05), FALSE	(0.004, 0.156), TRUE	(-0.038, 0.069), FALSE
CD-Ratio-S		(-0.066, 0.009), FALSE	(-0.181, 0.024), FALSE	(0.15, 0.195), TRUE	(-0.022, 0.088), FALSE	(0.171, 0.217), TRUE	(0.069, 0.176), TRUE	(0.012, 0.075), TRUE	(-0.135, 0.237), FALSE	(-0.027, 0.079), FALSE	(-0.094, 0.055), FALSE	(-0.018, 0.122), FALSE	(-0.03, 0.072), FALSE
CD-Egger-S		(-0.118, 0.038), FALSE	(-0.245, 0.057), FALSE	(0.142, 0.226), TRUE	(-0.183, 0.25), FALSE	(0.167, 0.251), TRUE	(-0.042, 0.327), FALSE	(-0.01, 0.108), FALSE	(-0.188, 0.291), FALSE	(-0.044, 0.114), FALSE	(-0.136, 0.12), FALSE	(-0.098, 0.187), FALSE	(-0.052, 0.094), FALSE
MR-cML-DP		(-0.37, 0.152), FALSE	(-0.065, 0.031), FALSE	(0.054, 0.088), TRUE	(-2.028, 2.379), FALSE	(0.036, 0.053), TRUE	(-2.254, 5.004), FALSE	(0.126, 0.557), TRUE	(-0.028, 0.05), FALSE	(-0.166, 0.378), FALSE	(-0.072, 0.037), FALSE	(-0.212, 0.78), FALSE	(-0.014, 0.023), FALSE
MR-cML		(-0.263, 0.027), FALSE	(-0.05, 0.009), FALSE	(0.058, 0.075), TRUE	(-0.248, 0.148), FALSE	(0.04, 0.05), TRUE	(1.914, 3.044), TRUE	(0.139, 0.547), TRUE	(-0.019, 0.04), FALSE	(-0.092, 0.311), FALSE	(-0.058, 0.026), FALSE	(0.017, 0.558), TRUE	(-0.01, 0.019), FALSE
CD-cML-DP		(-0.102, 0.043), FALSE	(-0.233, 0.113), FALSE	(0.159, 0.254), TRUE	(-0.635, 0.728), FALSE	(0.184, 0.263), TRUE	(-0.462, 1.001), FALSE	(0.019, 0.087), TRUE	(-0.187, 0.306), FALSE	(-0.089, 0.204), FALSE	(-0.132, 0.069), FALSE	(-0.06, 0.219), FALSE	(-0.053, 0.086), FALSE
CD-cML		(-0.072, 0.008), FALSE	(-0.182, 0.034), FALSE	(0.168, 0.217), TRUE	(-0.083, 0.056), FALSE	(0.198, 0.248), TRUE	(0.35, 0.62), TRUE	(0.021, 0.085), TRUE	(-0.133, 0.243), FALSE	(-0.049, 0.168), FALSE	(-0.105, 0.05), FALSE	(0.004, 0.156), TRUE	(-0.038, 0.069), FALSE
CD-Ratio		(-0.066, 0.009), FALSE	(-0.196, 0.008), FALSE	(0.151, 0.196), TRUE	(0.03, 0.137), TRUE	(0.173, 0.218), TRUE	(0.12, 0.225), TRUE	(0.012, 0.075), TRUE	(-0.135, 0.237), FALSE	(-0.027, 0.079), FALSE	(-0.094, 0.055), FALSE	(-0.018, 0.122), FALSE	(-0.03, 0.072), FALSE
CD-Egger		(-0.118, 0.038), FALSE	(-0.28, 0.049), FALSE	(0.142, 0.231), TRUE	(-0.189, 0.696), FALSE	(0.163, 0.258), TRUE	(0.038, 0.656), TRUE	(-0.01, 0.108), FALSE	(-0.188, 0.291), FALSE	(-0.044, 0.114), FALSE	(-0.136, 0.12), FALSE	(-0.098, 0.187), FALSE	(-0.052, 0.094), FALSE
LHC-MR		(-0.275, 0.065), FALSE	(-0.933, 0.353), FALSE	(0.171, 0.307), TRUE	(-1.115, 0.292), FALSE	(0.146, 0.385), TRUE	(-2.152, 1.499), FALSE	(0.029, 0.168), TRUE	(-0.715, -0.025), TRUE	(0.069, 0.3), TRUE	(0.057, 0.469), TRUE	(-0.261, 0.095), FALSE	(-0.219, 0.296), FALSE
Steiger		0.407, TRUE	0.296, FALSE	0.833, TRUE	0.055, FALSE	0.809, TRUE	0.071, FALSE	0.167, FALSE	0.097, FALSE	0.209, FALSE	0.64, TRUE	0.27, FALSE	0.69, TRUE

S3 Table: Inferring causal effects between first 6 risk factors and Stroke. In each cell we show the Bonferroni adjusted 1-0.05/96 \approx 0.9995 confidence intervals (CIs) of θ for the MR methods, and CIs of K for the CD methods; for Steiger's method, we show the proportion of SNPs giving significant result. TRUE/FALSE in each cell indicates whether the result is significant or not, and the cells giving significant results are marked in red.

Method	Direction	TG to Stroke	Stroke to TG	LDL to Stroke	Stroke to LDL	HDL to Stroke	Stroke to HDL	Height to Stroke	Stroke to Height	BMI to Stroke	Stroke to BMI	BF to Stroke	Stroke to BF
MR-cML-DP-S		(-0.109, 0.116), FALSE	(-0.029, 0.179), FALSE	(0.008, 0.2), TRUE	(-0.188, 0.14), FALSE	(-0.154, 0.029), FALSE	(-0.107, 0.111), FALSE	(-0.091, 0.062), FALSE	(-0.233, 0.137), FALSE	(-0.014, 0.299), FALSE	(-0.112, 0.11), FALSE	(-0.216, 0.45), FALSE	(-0.098, 0.104), FALSE
MR-cML-S		(-0.088, 0.088), FALSE	(-0.009, 0.155), FALSE	(0.044, 0.178), TRUE	(-0.141, 0.088), FALSE	(-0.138, 0.02), FALSE	(-0.087, 0.095), FALSE	(-0.069, 0.045), FALSE	(-0.161, 0.034), FALSE	(0.01, 0.293), TRUE	(-0.085, 0.085), FALSE	(-0.189, 0.399), FALSE	(-0.095, 0.093), FALSE
CD-cML-DP-S		(-0.022, 0.023), FALSE	(-0.15, 0.67), FALSE	(0.003, 0.045), TRUE	(-0.598, 0.431), FALSE	(-0.032, 0.005), FALSE	(-0.355, 0.444), FALSE	(-0.026, 0.018), FALSE	(-0.862, 0.499), FALSE	(-0.007, 0.094), FALSE	(-0.252, 0.266), FALSE	(-0.055, 0.115), FALSE	(-0.336, 0.367), FALSE
CD-cML-S		(-0.018, 0.017), FALSE	(-0.082, 0.601), FALSE	(0.01, 0.039), TRUE	(-0.456, 0.292), FALSE	(-0.028, 0.004), FALSE	(-0.293, 0.399), FALSE	(-0.019, 0.013), FALSE	(-0.597, 0.134), FALSE	(0.001, 0.091), TRUE	(-0.205, 0.22), FALSE	(-0.047, 0.102), FALSE	(-0.328, 0.332), FALSE
CD-Ratio-S		(-0.017, 0.018), FALSE	(-0.062, 0.562), FALSE	(0.008, 0.037), TRUE	(-0.359, 0.289), FALSE	(-0.03, 0.002), FALSE	(-0.295, 0.392), FALSE	(-0.024, 0.007), FALSE	(-0.387, 0.243), FALSE	(-0.002, 0.085), FALSE	(-0.243, 0.152), FALSE	(-0.048, 0.101), FALSE	(-0.325, 0.329), FALSE
CD-Egger-S		(-0.023, 0.025), FALSE	(-0.123, 0.677), FALSE	(0, 0.046), FALSE	(-0.476, 0.473), FALSE	(-0.039, 0.006), FALSE	(-0.357, 0.475), FALSE	(-0.03, 0.012), FALSE	(-0.765, 0.48), FALSE	(-0.021, 0.104), FALSE	(-0.387, 0.238), FALSE	(-0.051, 0.101), FALSE	(-0.316, 0.33), FALSE
MR-cML-DP		(-0.109, 0.116), FALSE	(-0.029, 0.179), FALSE	(0.008, 0.2), TRUE	(-0.188, 0.137), FALSE	(-0.154, 0.029), FALSE	(-0.117, 0.135), FALSE	(-0.091, 0.062), FALSE	(-0.212, 0.12), FALSE	(-0.014, 0.299), FALSE	(-0.112, 0.11), FALSE	(-0.216, 0.45), FALSE	(-0.098, 0.104), FALSE
MR-cML		(-0.088, 0.088), FALSE	(-0.009, 0.155), FALSE	(0.044, 0.178), TRUE	(-0.141, 0.088), FALSE	(-0.138, 0.02), FALSE	(-0.087, 0.095), FALSE	(-0.069, 0.045), FALSE	(-0.161, 0.034), FALSE	(0.01, 0.293), TRUE	(-0.085, 0.085), FALSE	(-0.189, 0.399), FALSE	(-0.095, 0.093), FALSE
CD-cML-DP		(-0.022, 0.023), FALSE	(-0.15, 0.67), FALSE	(0.003, 0.045), TRUE	(-0.576, 0.409), FALSE	(-0.032, 0.005), FALSE	(-0.393, 0.53), FALSE	(-0.026, 0.018), FALSE	(-0.787, 0.451), FALSE	(-0.007, 0.094), FALSE	(-0.252, 0.266), FALSE	(-0.055, 0.115), FALSE	(-0.336, 0.367), FALSE
CD-cML		(-0.018, 0.017), FALSE	(-0.082, 0.601), FALSE	(0.01, 0.039), TRUE	(-0.456, 0.292), FALSE	(-0.028, 0.004), FALSE	(-0.293, 0.399), FALSE	(-0.019, 0.013), FALSE	(-0.597, 0.134), FALSE	(0.001, 0.091), TRUE	(-0.205, 0.22), FALSE	(-0.047, 0.102), FALSE	(-0.328, 0.332), FALSE
CD-Ratio		(-0.017, 0.018), FALSE	(-0.062, 0.562), FALSE	(0.008, 0.037), TRUE	(-0.441, 0.194), FALSE	(-0.03, 0.002), FALSE	(-0.389, 0.283), FALSE	(-0.024, 0.007), FALSE	(-0.438, 0.189), FALSE	(-0.002, 0.085), FALSE	(-0.243, 0.152), FALSE	(-0.048, 0.101), FALSE	(-0.325, 0.329), FALSE
CD-Egger		(-0.023, 0.025), FALSE	(-0.123, 0.677), FALSE	(0, 0.046), FALSE	(-0.902, 0.45), FALSE	(-0.039, 0.006), FALSE	(-0.941, 0.553), FALSE	(-0.03, 0.012), FALSE	(-2.199, 0.934), FALSE	(-0.021, 0.104), FALSE	(-0.387, 0.238), FALSE	(-0.051, 0.101), FALSE	(-0.316, 0.33), FALSE
LHC-MR		(-0.009, 0.089), FALSE	(0.142, 0.999), TRUE	(0.02, 0.148), TRUE	(-0.666, 0.008), FALSE	(-0.089, 0.005), FALSE	(-0.948, -0.175), TRUE	(-0.011, 0.056), FALSE	(-2.448, 1.135), FALSE	(-0.059, 0.144), FALSE	(-0.073, 1.304), FALSE	(-0.035, 0.333), FALSE	(-0.574, 0.24), FALSE
Steiger		0.786, TRUE	0.086, FALSE	0.846, TRUE	0.066, FALSE	0.879, TRUE	0.061, FALSE	0.984, TRUE	0.011, FALSE	0.829, TRUE	0.132, FALSE	0.4, TRUE	0.32, FALSE

S4 Table: Inferring causal effects between second 6 risk factors and Stroke. In each cell we show the Bonferroni adjusted 1-0.05/96 \approx 0.9995 confidence intervals (CIs) of θ for the MR methods, and CIs of K for the CD methods; for Steiger's method, we show the proportion of SNPs giving significant result. TRUE/FALSE in each cell indicates whether the result is significant or not, and the cells giving significant results are marked in red.

Method	Direction	BW to Stroke	Stroke to BW	DBP to Stroke	Stroke to DBP	SBP to Stroke	Stroke to SBP	FG to Stroke	Stroke to FG	Smoke to Stroke	Stroke to Smoke	Alcohol to Stroke	Stroke to Alcohol
MR-cML-DP-S		(-0.287, 0.25), FALSE	(-0.163, 0.088), FALSE	(0.042, 0.069), TRUE	(-1.311, -0.019), TRUE	(0.03, 0.045), TRUE	(-1.638, 5.285), FALSE	(-0.279, 0.66), FALSE	(-0.049, 0.114), FALSE	(-0.103, 0.239), FALSE	(-0.108, 0.149), FALSE	(-0.063, 0.514), FALSE	(-0.038, 0.033), FALSE
MR-cML-S		(-0.208, 0.146), FALSE	(-0.103, 0.05), FALSE	(0.045, 0.064), TRUE	(-1.236, -0.104), TRUE	(0.031, 0.042), TRUE	(-0.119, 4.224), FALSE	(-0.083, 0.422), FALSE	(-0.034, 0.105), FALSE	(-0.045, 0.197), FALSE	(-0.086, 0.105), FALSE	(-0.029, 0.474), FALSE	(-0.034, 0.03), FALSE
CD-cML-DP-S		(-0.074, 0.062), FALSE	(-0.594, 0.328), FALSE	(0.116, 0.187), TRUE	(-0.489, -0.007), TRUE	(0.14, 0.212), TRUE	(-0.404, 1.127), FALSE	(-0.045, 0.099), FALSE	(-0.343, 0.741), FALSE	(-0.049, 0.113), FALSE	(-0.187, 0.293), FALSE	(-0.025, 0.164), FALSE	(-0.147, 0.124), FALSE
CD-cML-S		(-0.054, 0.036), FALSE	(-0.371, 0.188), FALSE	(0.127, 0.177), TRUE	(-0.46, -0.038), TRUE	(0.147, 0.198), TRUE	(-0.099, 0.906), FALSE	(-0.017, 0.075), FALSE	(-0.24, 0.684), FALSE	(-0.022, 0.094), FALSE	(-0.153, 0.217), FALSE	(-0.011, 0.145), FALSE	(-0.133, 0.114), FALSE
CD-Ratio-S		(-0.042, 0.039), FALSE	(-0.387, 0.105), FALSE	(0.114, 0.162), TRUE	(-0.208, 0.152), FALSE	(0.138, 0.187), TRUE	(-0.019, 0.356), FALSE	(-0.014, 0.054), FALSE	(-0.258, 0.654), FALSE	(-0.026, 0.087), FALSE	(-0.149, 0.21), FALSE	(-0.015, 0.137), FALSE	(-0.133, 0.114), FALSE
CD-Egger-S		(-0.063, 0.062), FALSE	(-0.581, 0.187), FALSE	(0.108, 0.18), TRUE	(-0.465, 0.708), FALSE	(0.132, 0.206), TRUE	(-0.314, 0.704), FALSE	(-0.026, 0.088), FALSE	(-0.285, 0.714), FALSE	(-0.052, 0.125), FALSE	(-0.235, 0.262), FALSE	(-0.056, 0.17), FALSE	(-0.13, 0.115), FALSE
MR-cML-DP		(-0.287, 0.25), FALSE	(-0.163, 0.088), FALSE	(0.042, 0.069), TRUE	(-1.371, 0.112), FALSE	(0.029, 0.044), TRUE	(4.192, 11.969), TRUE	(-0.279, 0.66), FALSE	(-0.049, 0.114), FALSE	(-0.103, 0.239), FALSE	(-0.108, 0.149), FALSE	(-0.063, 0.514), FALSE	(-0.038, 0.033), FALSE
MR-cML		(-0.208, 0.146), FALSE	(-0.103, 0.05), FALSE	(0.045, 0.064), TRUE	(-1.236, -0.103), TRUE	(0.031, 0.042), TRUE	(5.885, 10.424), TRUE	(-0.083, 0.422), FALSE	(-0.034, 0.105), FALSE	(-0.045, 0.197), FALSE	(-0.086, 0.105), FALSE	(-0.029, 0.474), FALSE	(-0.034, 0.03), FALSE
CD-cML-DP		(-0.074, 0.062), FALSE	(-0.594, 0.328), FALSE	(0.116, 0.187), TRUE	(-0.509, 0.041), FALSE	(0.14, 0.211), TRUE	(0.816, 2.51), FALSE	(-0.045, 0.099), FALSE	(-0.343, 0.741), FALSE	(-0.049, 0.113), FALSE	(-0.187, 0.293), FALSE	(-0.025, 0.164), FALSE	(-0.147, 0.124), FALSE
CD-cML		(-0.054, 0.036), FALSE	(-0.371, 0.188), FALSE	(0.127, 0.177), TRUE	(-0.46, -0.038), TRUE	(0.147, 0.198), TRUE	(1.235, 2.126), FALSE	(-0.017, 0.075), FALSE	(-0.24, 0.684), FALSE	(-0.022, 0.094), FALSE	(-0.153, 0.217), FALSE	(-0.011, 0.145), FALSE	(-0.133, 0.114), FALSE
CD-Ratio		(-0.042, 0.039), FALSE	(-0.387, 0.105), FALSE	(0.114, 0.162), TRUE	(-0.099, 0.253), FALSE	(0.139, 0.187), TRUE	(0.212, 0.557), TRUE	(-0.014, 0.054), FALSE	(-0.258, 0.654), FALSE	(-0.026, 0.087), FALSE	(-0.149, 0.21), FALSE	(-0.015, 0.137), FALSE	(-0.133, 0.114), FALSE
CD-Egger		(-0.063, 0.062), FALSE	(-0.581, 0.187), FALSE	(0.108, 0.18), TRUE	(-0.358, 2.127), FALSE	(0.133, 0.208), TRUE	(0.006, 1.689), FALSE	(-0.026, 0.088), FALSE	(-0.285, 0.714), FALSE	(-0.052, 0.125), FALSE	(-0.235, 0.262), FALSE	(-0.056, 0.17), FALSE	(-0.13, 0.115), FALSE
LHC-MR		(-0.196, 0.008), FALSE	(-0.041, 0.663), FALSE	(0.127, 0.213), TRUE	(0.043, 0.529), TRUE	(0.071, 0.291), TRUE	(-6.321, 6.806), FALSE	(0.029, 0.344), TRUE	(0.06, 0.775), TRUE	(-0.078, 0.191), FALSE	(-0.027, 0.943), FALSE	(-0.138, 0.267), FALSE	(-0.44, 0.161), FALSE
Steiger		0.73, TRUE	0.143, FALSE	0.909, TRUE	0.013, FALSE	0.907, TRUE	0.011, FALSE	0.462, FALSE	0.038, FALSE	0.553, TRUE	0.368, FALSE	0.633, TRUE	0.347, FALSE

S5 Table: Inferring causal effects between first 6 risk factors and T2D. In each cell we show the Bonferroni adjusted $1-0.05/96 \approx 0.9995$ confidence intervals (CIs) of θ for the MR methods, and CIs of K for the CD methods; for Steiger's method, we show the proportion of SNPs giving significant result. TRUE/FALSE in each cell indicates whether the result is significant or not, and the cells giving significant results are marked in red.

Method	Direction	TG to T2D	T2D to TG	LDL to T2D	T2D to LDL	HDL to T2D	T2D to HDL	Height to T2D	T2D to Height	BMI to T2D	T2D to BMI	BF to T2D	T2D to BF
MR-cML-DP-S		(-0.382, 0.483), FALSE	(-0.05, 0.15), FALSE	(-0.36, 0.082), FALSE	(-0.021, 0.045), FALSE	(-0.579, 0.165), FALSE	(-0.084, 0.049), FALSE	(-0.237, 0.145), FALSE	(-0.034, 0.057), FALSE	(0.426, 1.302), TRUE	(-0.105, -0.022), TRUE	(-0.17, 3.255), FALSE	(-0.094, 0.021), FALSE
MR-cML-S		(-0.172, 0.282), FALSE	(0.005, 0.11), TRUE	(-0.316, 0.029), FALSE	(-0.015, 0.042), FALSE	(-0.411, 0.002), FALSE	(-0.038, 0.018), FALSE	(-0.184, 0.09), FALSE	(-0.019, 0.043), FALSE	(0.484, 1.177), TRUE	(-0.094, -0.042), TRUE	(0.404, 2.836), TRUE	(-0.073, 0.004), FALSE
CD-cML-DP-S		(-0.229, 0.275), FALSE	(-0.062, 0.22), FALSE	(-0.217, 0.046), FALSE	(-0.029, 0.068), FALSE	(-0.327, 0.102), FALSE	(-0.118, 0.065), FALSE	(-0.189, 0.11), FALSE	(-0.04, 0.069), FALSE	(0.379, 1.223), FALSE	(-0.114, -0.02), TRUE	(-0.192, 2.647), FALSE	(-0.121, 0.024), FALSE
CD-cML-S		(-0.1, 0.152), FALSE	(-0.007, 0.162), FALSE	(-0.195, 0.013), FALSE	(-0.021, 0.064), FALSE	(-0.224, 0.011), FALSE	(-0.063, 0.027), FALSE	(-0.149, 0.071), FALSE	(-0.024, 0.052), FALSE	(0.435, 1.087), FALSE	(-0.098, -0.044), TRUE	(0.319, 2.27), FALSE	(-0.096, 0.001), FALSE
CD-Ratio-S		(-0.102, 0.127), FALSE	(0.009, 0.099), TRUE	(-0.167, 0.032), FALSE	(-0.021, 0.063), FALSE	(-0.198, 0.005), FALSE	(-0.076, 0.01), FALSE	(-0.131, 0.072), FALSE	(-0.025, 0.035), FALSE	(0.409, 1.043), FALSE	(-0.078, -0.03), TRUE	(-0.249, 1.168), FALSE	(-0.085, 0.001), FALSE
CD-Egger-S		(-0.166, 0.235), FALSE	(-0.041, 0.184), FALSE	(-0.203, 0.061), FALSE	(-0.02, 0.066), FALSE	(-0.258, 0.046), FALSE	(-0.172, 0.053), FALSE	(-0.179, 0.114), FALSE	(-0.025, 0.047), FALSE	(0.385, 1.182), FALSE	(-0.213, 0.148), FALSE	(-1.304, 2.297), FALSE	(-0.189, 0.116), FALSE
MR-cML-DP		(-0.382, 0.483), FALSE	(-0.05, 0.15), FALSE	(-0.36, 0.082), FALSE	(-0.021, 0.045), FALSE	(-0.569, 0.165), FALSE	(-0.084, 0.049), FALSE	(-0.237, 0.145), FALSE	(-0.034, 0.057), FALSE	(0.493, 1.358), TRUE	(-0.105, -0.022), TRUE	(0.395, 3.477), TRUE	(-0.094, 0.021), FALSE
MR-cML		(-0.172, 0.282), FALSE	(0.005, 0.11), TRUE	(-0.316, 0.029), FALSE	(-0.015, 0.042), FALSE	(-0.411, 0.002), FALSE	(-0.038, 0.018), FALSE	(-0.184, 0.09), FALSE	(-0.019, 0.043), FALSE	(0.586, 1.222), TRUE	(-0.094, -0.042), TRUE	(1.077, 2.983), TRUE	(-0.073, 0.004), FALSE
CD-cML-DP		(-0.229, 0.275), FALSE	(-0.062, 0.22), FALSE	(-0.217, 0.046), FALSE	(-0.029, 0.068), FALSE	(-0.326, 0.109), FALSE	(-0.118, 0.065), FALSE	(-0.189, 0.11), FALSE	(-0.04, 0.069), FALSE	(0.447, 1.274), FALSE	(-0.114, -0.02), TRUE	(0.384, 2.679), FALSE	(-0.121, 0.024), FALSE
CD-cML		(-0.1, 0.152), FALSE	(-0.007, 0.162), FALSE	(-0.195, 0.013), FALSE	(-0.021, 0.064), FALSE	(-0.224, 0.011), FALSE	(-0.063, 0.027), FALSE	(-0.149, 0.071), FALSE	(-0.024, 0.052), FALSE	(0.534, 1.131), FALSE	(-0.098, -0.044), TRUE	(0.843, 2.328), FALSE	(-0.096, 0.001), FALSE
CD-Ratio		(-0.102, 0.127), FALSE	(0.009, 0.099), TRUE	(-0.167, 0.032), FALSE	(-0.021, 0.063), FALSE	(-0.207, -0.005), TRUE	(-0.076, 0.01), FALSE	(-0.131, 0.072), FALSE	(-0.025, 0.035), FALSE	(0.483, 1.066), FALSE	(-0.078, -0.03), TRUE	(0.249, 1.457), FALSE	(-0.085, 0.001), FALSE
CD-Egger		(-0.166, 0.235), FALSE	(-0.041, 0.184), FALSE	(-0.203, 0.061), FALSE	(-0.02, 0.066), FALSE	(-0.291, 0.034), FALSE	(-0.172, 0.053), FALSE	(-0.179, 0.114), FALSE	(-0.025, 0.047), FALSE	(-0.061, 1.396), FALSE	(-0.213, 0.148), FALSE	(-0.456, 2.198), FALSE	(-0.189, 0.116), FALSE
LHC-MR		(-0.054, 1.011), FALSE	(0.065, 0.295), TRUE	(-0.12, 0.708), FALSE	(-0.185, 0.205), FALSE	(-0.917, -0.131), TRUE	(-0.171, 0.004), FALSE	(-0.609, 0.484), FALSE	(-0.261, 0.049), FALSE	(0.998, 1.002), TRUE	(-0.228, -0.001), TRUE	(0.92, 1.079), TRUE	(-1.112, 0.935), FALSE
Steiger		0.266, FALSE	0.172, FALSE	0.321, FALSE	0.111, FALSE	0.348, FALSE	0.13, FALSE	0.061, FALSE	0.034, FALSE	0, FALSE	0.171, FALSE	0, FALSE	0.6, TRUE

S6 Table: Inferring causal effects between second 6 risk factors and T2D. In each cell we show the Bonferroni adjusted 1-0.05/96 \approx 0.9995 confidence intervals (CIs) of θ for the MR methods, and CIs of K for the CD methods; for Steiger's method, we show the proportion of SNPs giving significant result. TRUE/FALSE in each cell indicates whether the result is significant or not, and the cells giving significant results are marked in red.

Method	Direction	BW to T2D	T2D to BW	DBP to T2D	T2D to DBP	SBP to T2D	T2D to SBP	FG to T2D	T2D to FG	Smoke to T2D	T2D to Smoke	Alcohol to T2D	T2D to Alcohol
MR-cML-DP-S		(-0.98, 0.226), FALSE	(-0.022, 0.054), FALSE	(-0.009, 0.056), FALSE	(-0.703, 0.412), FALSE	(0.005, 0.039), TRUE	(-0.531, 1.585), FALSE	(0.927, 3.134), TRUE	(0.032, 0.117), TRUE	(-0.568, 0.614), FALSE	(-0.062, 0.029), FALSE	(-0.852, 1.662), FALSE	(-0.045, 0.011), FALSE
MR-cML-S		(-0.831, 0.01), FALSE	(-0.015, 0.044), FALSE	(0, 0.044), TRUE	(-0.522, 0.041), FALSE	(0.009, 0.034), TRUE	(0.32, 1.067), TRUE	(1.167, 2.882), TRUE	(0.042, 0.106), TRUE	(-0.315, 0.244), FALSE	(-0.058, 0.023), FALSE	(-0.564, 1.372), FALSE	(-0.029, 0.001), FALSE
CD-cML-DP-S		(-0.749, 0.19), FALSE	(-0.028, 0.072), FALSE	(-0.06, 0.447), FALSE	(-0.09, 0.054), FALSE	(0.058, 0.539), TRUE	(-0.03, 0.109), FALSE	(0.411, 1.336), FALSE	(0.079, 0.261), TRUE	(-0.781, 0.842), FALSE	(-0.039, 0.02), FALSE	(-0.66, 1.192), FALSE	(-0.061, 0.017), FALSE
CD-cML-S		(-0.622, 0.012), FALSE	(-0.019, 0.059), FALSE	(0.006, 0.356), TRUE	(-0.065, 0.005), FALSE	(0.116, 0.466), TRUE	(0.024, 0.073), TRUE	(0.514, 1.218), FALSE	(0.099, 0.238), TRUE	(-0.481, 0.402), FALSE	(-0.036, 0.016), FALSE	(-0.438, 0.959), FALSE	(-0.037, 0.002), FALSE
CD-Ratio-S		(-0.562, 0.018), FALSE	(-0.044, 0.028), FALSE	(0.018, 0.352), TRUE	(-0.01, 0.024), FALSE	(0.13, 0.47), TRUE	(0.024, 0.062), TRUE	(0.215, 0.671), TRUE	(0.107, 0.235), TRUE	(-0.44, 0.383), FALSE	(-0.036, 0.015), FALSE	(-0.455, 0.831), FALSE	(-0.037, -0.001), TRUE
CD-Egger-S		(-0.724, 0.201), FALSE	(-0.177, 0.123), FALSE	(-0.035, 0.433), FALSE	(-0.038, 0.057), FALSE	(0.103, 0.539), TRUE	(0, 0.105), FALSE	(-0.055, 1.224), FALSE	(0.086, 0.276), TRUE	(-0.516, 0.501), FALSE	(-0.035, 0.016), FALSE	(-0.527, 1.036), FALSE	(-0.049, 0.006), FALSE
MR-cML-DP		(-1.031, 0.245), FALSE	(-0.022, 0.054), FALSE	(-0.008, 0.056), FALSE	(-0.703, 0.412), FALSE	(0.004, 0.039), TRUE	(-0.531, 1.585), FALSE	(0.847, 3.322), TRUE	(0.037, 0.11), TRUE	(-0.568, 0.614), FALSE	(-0.062, 0.029), FALSE	(-0.852, 1.662), FALSE	(-0.045, 0.011), FALSE
MR-cML		(-0.831, 0.01), FALSE	(-0.015, 0.044), FALSE	(0, 0.044), TRUE	(-0.522, 0.041), FALSE	(0.009, 0.034), TRUE	(0.32, 1.067), TRUE	(1.175, 2.874), TRUE	(0.042, 0.106), TRUE	(-0.315, 0.244), FALSE	(-0.058, 0.023), FALSE	(-0.564, 1.372), FALSE	(-0.029, 0.001), FALSE
CD-cML-DP		(-0.798, 0.21), FALSE	(-0.028, 0.072), FALSE	(-0.061, 0.452), FALSE	(-0.09, 0.054), FALSE	(0.061, 0.534), TRUE	(-0.03, 0.109), FALSE	(0.411, 1.427), FALSE	(0.088, 0.251), TRUE	(-0.781, 0.842), FALSE	(-0.039, 0.02), FALSE	(-0.66, 1.192), FALSE	(-0.061, 0.017), FALSE
CD-cML		(-0.622, 0.012), FALSE	(-0.019, 0.059), FALSE	(0.006, 0.356), TRUE	(-0.065, 0.005), FALSE	(0.116, 0.466), TRUE	(0.024, 0.073), TRUE	(0.603, 1.324), FALSE	(0.099, 0.238), TRUE	(-0.481, 0.402), FALSE	(-0.036, 0.016), FALSE	(-0.438, 0.959), FALSE	(-0.037, 0.002), FALSE
CD-Ratio		(-0.697, -0.13), TRUE	(-0.044, 0.028), FALSE	(0.022, 0.356), TRUE	(-0.01, 0.024), FALSE	(0.148, 0.487), TRUE	(0.024, 0.062), TRUE	(0.268, 0.719), TRUE	(0.115, 0.243), TRUE	(-0.44, 0.383), FALSE	(-0.036, 0.015), FALSE	(-0.455, 0.831), FALSE	(-0.037, -0.001), TRUE
CD-Egger		(-1.104, 0.172), FALSE	(-0.177, 0.123), FALSE	(-0.034, 0.462), FALSE	(-0.038, 0.057), FALSE	(0.09, 0.633), TRUE	(0, 0.105), FALSE	(-0.505, 1.715), FALSE	(-0.033, 0.442), FALSE	(-0.516, 0.501), FALSE	(-0.035, 0.016), FALSE	(-0.527, 1.036), FALSE	(-0.049, 0.006), FALSE
LHC-MR		(-1.622, 1.118), FALSE	(-0.49, 0.068), FALSE	(-0.11, 0.789), FALSE	(-0.021, 0.248), FALSE	(-0.016, 1.007), FALSE	(-0.081, 0.216), FALSE	(-0.227, 0.985), FALSE	(0.239, 0.5), TRUE	(-0.683, 1.675), FALSE	(-0.048, 0.118), FALSE	(-0.291, 1.227), FALSE	(-0.12, 0.029), FALSE
Steiger		0.038, FALSE	0.245, FALSE	0.005, FALSE	0.067, FALSE	0.005, FALSE	0.048, FALSE	0.091, FALSE	0.5, TRUE	0.032, FALSE	0.355, FALSE	0, FALSE	0.359, FALSE

S7 Table: Inferring causal effects between first 6 risk factors and Asthma. In each cell we show the Bonferroni adjusted 1-0.05/96 \approx 0.9995 confidence intervals (CIs) of θ for the MR methods, and CIs of K for the CD methods; for Steiger's method, we show the proportion of SNPs giving significant result. TRUE/FALSE in each cell indicates whether the result is significant or not, and the cells giving significant results are marked in red.

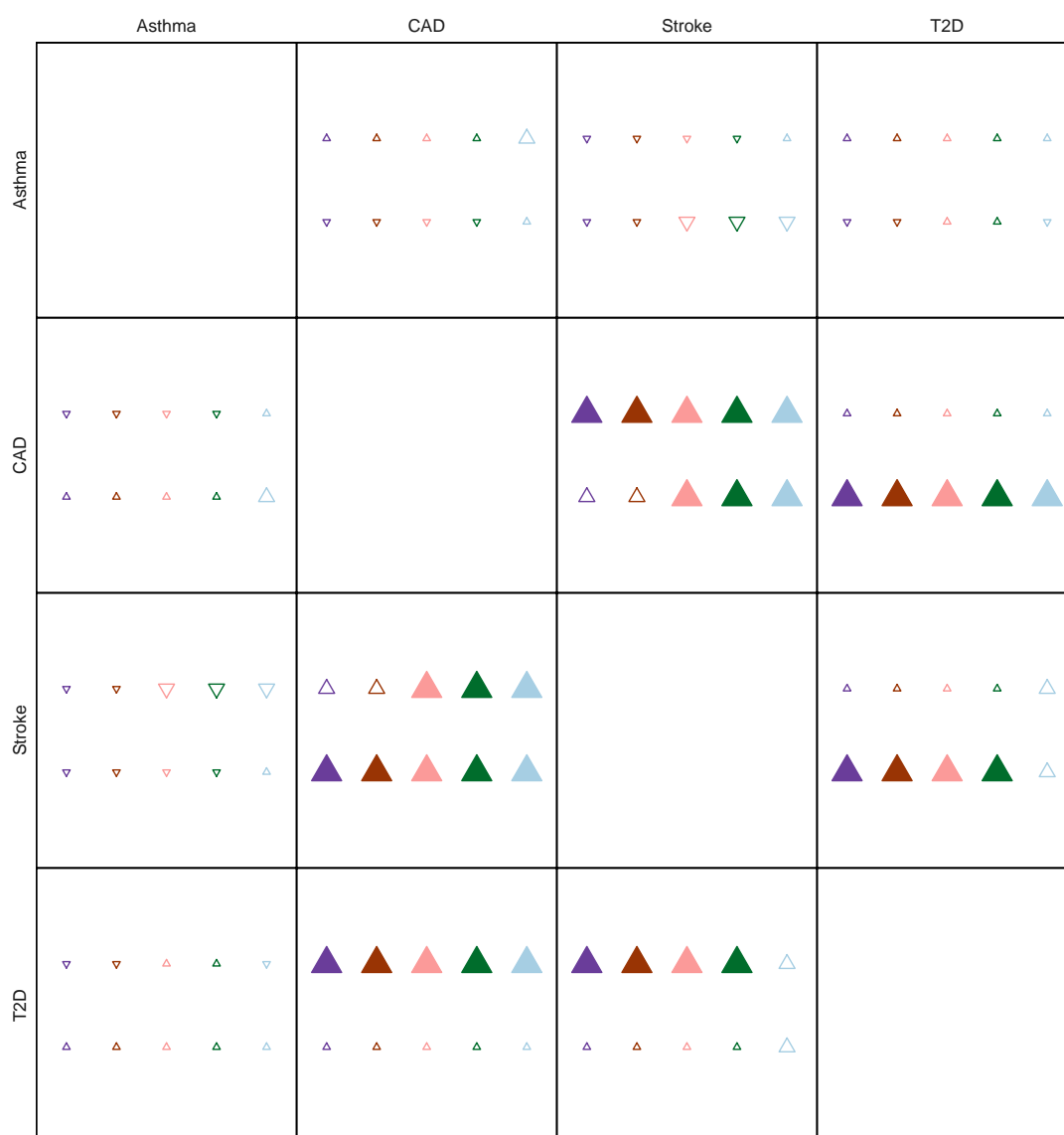
Method	Direction	TG to Asthma	Asthma to TG	LDL to Asthma	Asthma to LDL	HDL to Asthma	Asthma to HDL	Height to Asthma	Asthma to Height	BMI to Asthma	Asthma to BMI	BF to Asthma	Asthma to BF
MR-cML-DP-S		(-0.305, 0.185), FALSE	(-0.056, 0.077), FALSE	(-0.152, 0.143), FALSE	(-0.064, 0.035), FALSE	(-0.204, 0.164), FALSE	(-0.036, 0.059), FALSE	(-0.088, 0.131), FALSE	(-0.038, 0.023), FALSE	(-0.14, 0.41), FALSE	(-0.034, 0.028), FALSE	(-0.392, 0.645), FALSE	(-0.03, 0.061), FALSE
MR-cML-S		(-0.222, 0.094), FALSE	(-0.037, 0.055), FALSE	(-0.13, 0.106), FALSE	(-0.055, 0.031), FALSE	(-0.154, 0.114), FALSE	(-0.033, 0.055), FALSE	(-0.058, 0.122), FALSE	(-0.04, 0.023), FALSE	(-0.092, 0.348), FALSE	(-0.033, 0.026), FALSE	(-0.38, 0.618), FALSE	(-0.028, 0.058), FALSE
CD-cML-DP-S		(-0.068, 0.041), FALSE	(-0.173, 0.24), FALSE	(-0.037, 0.036), FALSE	(-0.196, 0.113), FALSE	(-0.049, 0.039), FALSE	(-0.112, 0.183), FALSE	(-0.029, 0.043), FALSE	(-0.116, 0.073), FALSE	(-0.049, 0.153), FALSE	(-0.078, 0.065), FALSE	(-0.113, 0.19), FALSE	(-0.091, 0.177), FALSE
CD-cML-S		(-0.05, 0.021), FALSE	(-0.117, 0.174), FALSE	(-0.032, 0.027), FALSE	(-0.165, 0.102), FALSE	(-0.036, 0.026), FALSE	(-0.1, 0.17), FALSE	(-0.019, 0.04), FALSE	(-0.121, 0.072), FALSE	(-0.032, 0.131), FALSE	(-0.076, 0.06), FALSE	(-0.108, 0.182), FALSE	(-0.084, 0.17), FALSE
CD-Ratio-S		(-0.053, 0.012), FALSE	(-0.113, 0.146), FALSE	(-0.025, 0.032), FALSE	(-0.186, 0.053), FALSE	(-0.029, 0.03), FALSE	(-0.181, 0.068), FALSE	(-0.026, 0.031), FALSE	(-0.118, 0.072), FALSE	(-0.033, 0.129), FALSE	(-0.077, 0.06), FALSE	(-0.11, 0.179), FALSE	(-0.084, 0.169), FALSE
CD-Egger-S		(-0.07, 0.024), FALSE	(-0.177, 0.201), FALSE	(-0.04, 0.042), FALSE	(-0.231, 0.081), FALSE	(-0.04, 0.043), FALSE	(-0.334, 0.182), FALSE	(-0.035, 0.043), FALSE	(-0.114, 0.111), FALSE	(-0.04, 0.137), FALSE	(-0.076, 0.062), FALSE	(-0.13, 0.167), FALSE	(-0.085, 0.169), FALSE
MR-cML-DP		(-0.305, 0.185), FALSE	(-0.056, 0.077), FALSE	(-0.152, 0.143), FALSE	(-0.064, 0.035), FALSE	(-0.189, 0.15), FALSE	(-0.036, 0.059), FALSE	(-0.088, 0.131), FALSE	(-0.043, 0.023), FALSE	(-0.14, 0.41), FALSE	(-0.034, 0.028), FALSE	(-0.392, 0.645), FALSE	(-0.03, 0.061), FALSE
MR-cML		(-0.222, 0.094), FALSE	(-0.037, 0.055), FALSE	(-0.13, 0.106), FALSE	(-0.055, 0.031), FALSE	(-0.154, 0.114), FALSE	(-0.033, 0.055), FALSE	(-0.058, 0.122), FALSE	(-0.04, 0.023), FALSE	(-0.092, 0.348), FALSE	(-0.033, 0.026), FALSE	(-0.38, 0.618), FALSE	(-0.028, 0.058), FALSE
CD-cML-DP		(-0.068, 0.041), FALSE	(-0.173, 0.24), FALSE	(-0.037, 0.036), FALSE	(-0.196, 0.113), FALSE	(-0.045, 0.036), FALSE	(-0.112, 0.183), FALSE	(-0.029, 0.043), FALSE	(-0.132, 0.073), FALSE	(-0.049, 0.153), FALSE	(-0.078, 0.065), FALSE	(-0.113, 0.19), FALSE	(-0.091, 0.177), FALSE
CD-cML		(-0.05, 0.021), FALSE	(-0.117, 0.174), FALSE	(-0.032, 0.027), FALSE	(-0.165, 0.102), FALSE	(-0.036, 0.026), FALSE	(-0.1, 0.17), FALSE	(-0.019, 0.04), FALSE	(-0.121, 0.072), FALSE	(-0.032, 0.131), FALSE	(-0.076, 0.06), FALSE	(-0.108, 0.182), FALSE	(-0.084, 0.17), FALSE
CD-Ratio		(-0.053, 0.012), FALSE	(-0.113, 0.146), FALSE	(-0.025, 0.032), FALSE	(-0.186, 0.053), FALSE	(-0.031, 0.029), FALSE	(-0.181, 0.068), FALSE	(-0.026, 0.031), FALSE	(-0.132, 0.056), FALSE	(-0.033, 0.129), FALSE	(-0.077, 0.06), FALSE	(-0.11, 0.179), FALSE	(-0.084, 0.169), FALSE
CD-Egger		(-0.07, 0.024), FALSE	(-0.177, 0.201), FALSE	(-0.04, 0.042), FALSE	(-0.231, 0.081), FALSE	(-0.068, 0.053), FALSE	(-0.334, 0.182), FALSE	(-0.035, 0.043), FALSE	(-0.458, 0.311), FALSE	(-0.04, 0.137), FALSE	(-0.076, 0.062), FALSE	(-0.13, 0.167), FALSE	(-0.085, 0.169), FALSE
LHC-MR		(-0.298, 0.059), FALSE	(-0.663, 0.317), FALSE	(-0.18, 0.061), FALSE	(-0.175, 0.312), FALSE	(-0.042, 0.278), FALSE	(-0.836, 0.137), FALSE	(-0.152, 0.107), FALSE	(-0.792, 0.09), FALSE	(-0.087, 0.167), FALSE	(-0.076, 0.133), FALSE	(-0.278, 0.073), FALSE	(-0.524, 0.4), FALSE
Steiger		0.8, TRUE	0.2, FALSE	0.807, TRUE	0.182, FALSE	0.845, TRUE	0.155, FALSE	0.903, TRUE	0.024, FALSE	0.714, TRUE	0.208, FALSE	0.346, FALSE	0.654, TRUE

S8 Table: Inferring causal effects between second 6 risk factors and Asthma. In each cell we show the Bonferroni adjusted $1-0.05/96 \approx 0.9995$ confidence intervals (CIs) of θ for the MR methods, and CIs of K for the CD methods; for Steiger's method, we show the proportion of SNPs giving significant result. TRUE/FALSE in each cell indicates whether the result is significant or not, and the cells giving significant results are marked in red.

Method \ Direction	BW to Asthma	Asthma to BW	DBP to Asthma	Asthma to DBP	SBP to Asthma	Asthma to SBP	FG to Asthma	Asthma to FG	Smoke to Asthma	Asthma to Smoke	Alcohol to Asthma	Asthma to Alcohol
MR-cML-DP-S	(-0.233, 0.479), FALSE	(-0.043, 0.023), FALSE	(-0.023, 0.018), FALSE	(-0.443, 0.222), FALSE	(-0.01, 0.012), FALSE	(-0.646, 0.331), FALSE	(-0.722, 0.371), FALSE	(-0.022, 0.05), FALSE	(-0.16, 0.201), FALSE	(-0.052, 0.044), FALSE	(-0.864, 0.609), FALSE	(-0.027, 0.017), FALSE
MR-cML-S	(-0.14, 0.393), FALSE	(-0.041, 0.021), FALSE	(-0.018, 0.012), FALSE	(-0.355, 0.069), FALSE	(-0.008, 0.009), FALSE	(-0.536, 0.159), FALSE	(-0.558, 0.184), FALSE	(-0.016, 0.045), FALSE	(-0.167, 0.222), FALSE	(-0.047, 0.041), FALSE	(-0.75, 0.525), FALSE	(-0.022, 0.011), FALSE
CD-cML-DP-S	(-0.068, 0.147), FALSE	(-0.141, 0.076), FALSE	(-0.075, 0.057), FALSE	(-0.132, 0.067), FALSE	(-0.058, 0.066), FALSE	(-0.116, 0.059), FALSE	(-0.126, 0.065), FALSE	(-0.128, 0.289), FALSE	(-0.097, 0.123), FALSE	(-0.084, 0.073), FALSE	(-0.257, 0.192), FALSE	(-0.088, 0.056), FALSE
CD-cML-S	(-0.04, 0.121), FALSE	(-0.133, 0.066), FALSE	(-0.057, 0.039), FALSE	(-0.106, 0.022), FALSE	(-0.046, 0.052), FALSE	(-0.095, 0.028), FALSE	(-0.098, 0.032), FALSE	(-0.096, 0.261), FALSE	(-0.102, 0.136), FALSE	(-0.077, 0.067), FALSE	(-0.223, 0.168), FALSE	(-0.07, 0.036), FALSE
CD-Ratio-S	(-0.048, 0.11), FALSE	(-0.131, 0.038), FALSE	(-0.056, 0.03), FALSE	(-0.079, 0.03), FALSE	(-0.044, 0.051), FALSE	(-0.053, 0.053), FALSE	(-0.084, 0.042), FALSE	(-0.1, 0.24), FALSE	(-0.101, 0.136), FALSE	(-0.076, 0.067), FALSE	(-0.223, 0.167), FALSE	(-0.062, 0.038), FALSE
CD-Egger-S	(-0.077, 0.134), FALSE	(-0.131, 0.065), FALSE	(-0.068, 0.052), FALSE	(-0.126, 0.065), FALSE	(-0.053, 0.065), FALSE	(-0.096, 0.11), FALSE	(-0.174, 0.098), FALSE	(-0.142, 0.265), FALSE	(-0.112, 0.131), FALSE	(-0.077, 0.068), FALSE	(-0.26, 0.197), FALSE	(-0.076, 0.06), FALSE
MR-cML-DP	(-0.233, 0.479), FALSE	(-0.043, 0.023), FALSE	(-0.023, 0.018), FALSE	(-0.443, 0.222), FALSE	(-0.01, 0.012), FALSE	(-0.646, 0.331), FALSE	(-0.722, 0.371), FALSE	(-0.022, 0.05), FALSE	(-0.16, 0.201), FALSE	(-0.052, 0.044), FALSE	(-0.864, 0.609), FALSE	(-0.027, 0.017), FALSE
MR-cML	(-0.14, 0.393), FALSE	(-0.041, 0.021), FALSE	(-0.018, 0.012), FALSE	(-0.355, 0.069), FALSE	(-0.008, 0.009), FALSE	(-0.536, 0.159), FALSE	(-0.558, 0.184), FALSE	(-0.016, 0.045), FALSE	(-0.167, 0.222), FALSE	(-0.047, 0.041), FALSE	(-0.75, 0.525), FALSE	(-0.022, 0.011), FALSE
CD-cML-DP	(-0.068, 0.147), FALSE	(-0.141, 0.076), FALSE	(-0.075, 0.057), FALSE	(-0.132, 0.067), FALSE	(-0.058, 0.066), FALSE	(-0.116, 0.059), FALSE	(-0.126, 0.065), FALSE	(-0.128, 0.289), FALSE	(-0.097, 0.123), FALSE	(-0.084, 0.073), FALSE	(-0.257, 0.192), FALSE	(-0.088, 0.056), FALSE
CD-cML	(-0.04, 0.121), FALSE	(-0.133, 0.066), FALSE	(-0.057, 0.039), FALSE	(-0.106, 0.022), FALSE	(-0.046, 0.052), FALSE	(-0.095, 0.028), FALSE	(-0.098, 0.032), FALSE	(-0.096, 0.261), FALSE	(-0.102, 0.136), FALSE	(-0.077, 0.067), FALSE	(-0.223, 0.168), FALSE	(-0.07, 0.036), FALSE
CD-Ratio	(-0.048, 0.11), FALSE	(-0.131, 0.067), FALSE	(-0.056, 0.038), FALSE	(-0.079, 0.03), FALSE	(-0.044, 0.051), FALSE	(-0.053, 0.053), FALSE	(-0.084, 0.042), FALSE	(-0.1, 0.24), FALSE	(-0.101, 0.136), FALSE	(-0.076, 0.067), FALSE	(-0.223, 0.167), FALSE	(-0.062, 0.038), FALSE
CD-Egger	(-0.077, 0.134), FALSE	(-0.131, 0.065), FALSE	(-0.068, 0.052), FALSE	(-0.126, 0.065), FALSE	(-0.053, 0.065), FALSE	(-0.096, 0.11), FALSE	(-0.174, 0.098), FALSE	(-0.142, 0.265), FALSE	(-0.112, 0.131), FALSE	(-0.077, 0.068), FALSE	(-0.26, 0.197), FALSE	(-0.076, 0.06), FALSE
LHC-MR	(-0.292, 0.175), FALSE	(-0.494, 0.211), FALSE	(-0.128, 0.148), FALSE	(-0.144, 0.388), FALSE	(-0.093, 0.174), FALSE	(-0.042, 0.223), FALSE	(-2.037, 2.356), FALSE	(-1.804, 1.328), FALSE	(-0.197, 0.139), FALSE	(-0.136, 0.172), FALSE	(-0.279, 0.079), FALSE	(-0.162, 0.063), FALSE
Steiger	0.712, TRUE	0.271, FALSE	0.5, TRUE	0.024, FALSE	0.513, TRUE	0.031, FALSE	0.414, FALSE	0.517, TRUE	0.471, FALSE	0.5, TRUE	0.357, FALSE	0.405, TRUE

S2.2 Pairs of 4 Diseases

S41 Fig: Causal relationship between pairs of 4 diseases.



S9 Table: Inferring causal effects between pairs of 4 diseases. In each cell we show the Bonferroni adjusted $1-0.05/12 \approx 0.996$ confidence intervals (CIs) of θ for the MR methods, and CIs of K for the CD methods; for Steiger’s method, we show the proportion of SNPs giving significant result. TRUE/FALSE in each cell indicates whether the result is significant or not, and the cells giving significant results are marked in red.

Method	Direction	CAD to Stroke	Stroke to CAD	CAD to T2D	T2D to CAD	CAD to Asthma	Asthma to CAD	Stroke to T2D	T2D to Stroke	Stroke to Asthma	Asthma to Stroke	T2D to Asthma	Asthma to T2D
MR-cML-DP-S		(0.102, 0.318), TRUE	(-0.032, 0.414), FALSE	(-0.221, 0.233), FALSE	(0.009, 0.134), TRUE	(-0.179, 0.17), FALSE	(-0.043, 0.099), FALSE	(-0.313, 0.523), FALSE	(0.011, 0.144), TRUE	(-0.442, 0.132), FALSE	(-0.077, 0.044), FALSE	(-0.126, 0.095), FALSE	(-0.209, 0.233), FALSE
MR-cML-S		(0.135, 0.25), TRUE	(0.05, 0.309), TRUE	(-0.094, 0.165), FALSE	(0.019, 0.111), TRUE	(-0.125, 0.13), FALSE	(-0.019, 0.084), FALSE	(-0.223, 0.473), FALSE	(0.023, 0.124), TRUE	(-0.397, 0.068), FALSE	(-0.069, 0.04), FALSE	(-0.096, 0.072), FALSE	(-0.117, 0.145), FALSE
CD-cML-DP-S		(0.099, 0.29), TRUE	(-0.022, 0.432), FALSE	(-0.592, 0.623), FALSE	(0.003, 0.048), TRUE	(-0.196, 0.175), FALSE	(-0.039, 0.087), FALSE	(-0.878, 1.387), FALSE	(0.003, 0.048), TRUE	(-0.511, 0.174), FALSE	(-0.065, 0.035), FALSE	(-0.049, 0.04), FALSE	(-0.496, 0.565), FALSE
CD-cML-S		(0.131, 0.232), TRUE	(0.057, 0.323), TRUE	(-0.278, 0.449), FALSE	(0.007, 0.039), TRUE	(-0.139, 0.095), FALSE	(-0.017, 0.074), FALSE	(-0.674, 1.276), FALSE	(0.007, 0.041), TRUE	(-0.449, 0.097), FALSE	(-0.058, 0.032), FALSE	(-0.037, 0.03), FALSE	(-0.281, 0.347), FALSE
CD-Ratio-S		(0.124, 0.219), TRUE	(0.088, 0.322), TRUE	(-0.278, 0.385), FALSE	(0.009, 0.037), TRUE	(-0.141, 0.06), FALSE	(-0.025, 0.058), FALSE	(-0.44, 1.175), FALSE	(0.006, 0.039), TRUE	(-0.401, 0.043), FALSE	(-0.058, 0.032), FALSE	(-0.03, 0.03), FALSE	(-0.277, 0.305), FALSE
CD-Egger-S		(0.108, 0.271), TRUE	(0.002, 0.525), TRUE	(-0.47, 0.636), FALSE	(0.005, 0.044), TRUE	(-0.176, 0.111), FALSE	(-0.071, 0.142), FALSE	(-0.784, 1.365), FALSE	(0.006, 0.042), TRUE	(-0.535, 0.078), FALSE	(-0.058, 0.034), FALSE	(-0.043, 0.046), FALSE	(-0.355, 0.382), FALSE
MR-cML-DP		(0.098, 0.327), TRUE	(-0.021, 0.417), FALSE	(-0.221, 0.233), FALSE	(0.009, 0.134), TRUE	(-0.178, 0.165), FALSE	(-0.043, 0.099), FALSE	(-0.313, 0.523), FALSE	(0.011, 0.144), TRUE	(-0.442, 0.132), FALSE	(-0.077, 0.044), FALSE	(-0.126, 0.095), FALSE	(-0.209, 0.233), FALSE
MR-cML		(0.135, 0.25), TRUE	(0.05, 0.309), TRUE	(-0.094, 0.165), FALSE	(0.019, 0.111), TRUE	(-0.125, 0.13), FALSE	(-0.019, 0.084), FALSE	(-0.223, 0.473), FALSE	(0.023, 0.124), TRUE	(-0.397, 0.068), FALSE	(-0.069, 0.04), FALSE	(-0.096, 0.072), FALSE	(-0.117, 0.145), FALSE
CD-cML-DP		(0.093, 0.303), TRUE	(-0.028, 0.456), FALSE	(-0.592, 0.623), FALSE	(0.003, 0.048), TRUE	(-0.199, 0.173), FALSE	(-0.039, 0.087), FALSE	(-0.878, 1.387), FALSE	(0.003, 0.048), TRUE	(-0.511, 0.174), FALSE	(-0.065, 0.035), FALSE	(-0.049, 0.04), FALSE	(-0.496, 0.565), FALSE
CD-cML		(0.131, 0.232), TRUE	(0.057, 0.323), TRUE	(-0.278, 0.449), FALSE	(0.007, 0.039), TRUE	(-0.139, 0.095), FALSE	(-0.017, 0.074), FALSE	(-0.674, 1.276), FALSE	(0.007, 0.041), TRUE	(-0.449, 0.097), FALSE	(-0.058, 0.032), FALSE	(-0.037, 0.03), FALSE	(-0.281, 0.347), FALSE
CD-Ratio		(0.131, 0.225), TRUE	(0.123, 0.353), TRUE	(-0.278, 0.385), FALSE	(0.009, 0.037), TRUE	(-0.139, 0.061), FALSE	(-0.025, 0.058), FALSE	(-0.44, 1.175), FALSE	(0.006, 0.039), TRUE	(-0.401, 0.043), FALSE	(-0.058, 0.032), FALSE	(-0.03, 0.03), FALSE	(-0.277, 0.305), FALSE
CD-Egger		(0.115, 0.293), TRUE	(0.001, 0.61), TRUE	(-0.47, 0.636), FALSE	(0.005, 0.044), TRUE	(-0.257, 0.128), FALSE	(-0.071, 0.142), FALSE	(-0.784, 1.365), FALSE	(0.006, 0.042), TRUE	(-0.535, 0.078), FALSE	(-0.058, 0.034), FALSE	(-0.043, 0.046), FALSE	(-0.355, 0.382), FALSE
LHC-MR		(0.135, 0.386), TRUE	(0.372, 0.759), TRUE	(-0.332, 1.551), FALSE	(0.013, 0.106), TRUE	(-0.138, 0.243), FALSE	(-0.043, 0.23), FALSE	(-0.095, 1.009), FALSE	(-0.032, 0.197), FALSE	(-1.182, 0.442), FALSE	(-0.298, 0.419), FALSE	(-0.201, 0.059), FALSE	(-0.286, 1.613), FALSE
Steiger		0.768, TRUE	0.146, FALSE	0.014, FALSE	0.25, FALSE	0.411, TRUE	0.233, FALSE	0, FALSE	0.5, FALSE	0.312, FALSE	0.531, TRUE	0.414, FALSE	0, FALSE

S2.3 Links to GWAS Summary Datasets

We downloaded the GWAS summary datasets from the IEU GWAS database [1], which are the same as the data included in R package TwoSampleMR. The links are shown in S10 Table.

S10 Table: Links for downloading GWAS summary datasets to be used in real data analysis.

Trait	Link
TG	https://gwas.mrcieu.ac.uk/files/ebi-a-GCST002216/ebi-a-GCST002216.vcf.gz
LDL	https://gwas.mrcieu.ac.uk/files/ebi-a-GCST002222/ebi-a-GCST002222.vcf.gz
HDL	https://gwas.mrcieu.ac.uk/files/ebi-a-GCST002223/ebi-a-GCST002223.vcf.gz
Height	https://gwas.mrcieu.ac.uk/files/ieu-a-89/ieu-a-89.vcf.gz
BMI	https://gwas.mrcieu.ac.uk/files/ieu-a-835/ieu-a-835.vcf.gz
BF	https://gwas.mrcieu.ac.uk/files/ieu-a-999/ieu-a-999.vcf.gz
BW	https://gwas.mrcieu.ac.uk/files/ieu-a-1083/ieu-a-1083.vcf.gz
DBP	https://gwas.mrcieu.ac.uk/files/ieu-b-39/ieu-b-39.vcf.gz
SBP	https://gwas.mrcieu.ac.uk/files/ieu-b-38/ieu-b-38.vcf.gz
FG	https://gwas.mrcieu.ac.uk/files/ebi-a-GCST000568/ebi-a-GCST000568.vcf.gz
Smoke	https://gwas.mrcieu.ac.uk/files/ieu-b-25/ieu-b-25.vcf.gz
Alcohol	https://gwas.mrcieu.ac.uk/files/ieu-b-73/ieu-b-73.vcf.gz
CAD	https://gwas.mrcieu.ac.uk/files/ebi-a-GCST005195/ebi-a-GCST005195.vcf.gz
Stroke	https://gwas.mrcieu.ac.uk/files/ebi-a-GCST005838/ebi-a-GCST005838.vcf.gz
T2D	https://gwas.mrcieu.ac.uk/files/ieu-a-26/ieu-a-26.vcf.gz
Asthma	https://gwas.mrcieu.ac.uk/files/ebi-a-GCST006862/ebi-a-GCST006862.vcf.gz

S3 Theoretical Results

S3.1 Proof of Theorem 1

Theorem 1. Under Assumptions 1 and 2, if $m_{XY}^0 \in \mathcal{M}$, we have $P(\hat{m}_I = m_{XY}^0) \rightarrow 1$ and $P(\hat{B}_{XY}(\hat{m}_I) = B_{XY}^0) \rightarrow 1$ as $N_1, N_2 \rightarrow \infty$. Furthermore, the cMLE $\hat{K}_{XY} := \hat{K}_{XY}(\hat{m}_I)$ is consistent and asymptotically normal:

$$\sqrt{V}(\hat{K}_{XY} - K_{XY}) \xrightarrow{d} N(0, 1), \text{ as } N_1, N_2 \rightarrow \infty,$$

where

$$V = \sum_{g \in (B_{XY}^0)^c} \frac{\rho_{Xg}^2}{\sigma_{Xg}^2 \cdot K_{XY}^2 + \sigma_{Yg}^2}.$$

Proof. First, we show $P(\hat{B}_{XY}(m_{XY}^0) = B_{XY}^0) \rightarrow 1$, which is equivalent to show for any $B_1 \subseteq \{1, \dots, m\}$ such that $|B_1| = m_{XY}^0$ and $B_1 \neq B_{XY}^0$, $P(\hat{B}_{XY}(m_{XY}^0) = B_1) \rightarrow 0$ as $N_1, N_2 \rightarrow \infty$. We have

$$\begin{aligned} & P(\hat{B}_{XY}(m_{XY}^0) = B_1) \\ & \leq P\left(\min_{\tilde{K}, \tilde{\rho}_{Xg}} \sum_{g \in B_1^c} \left(\frac{(r_{Xg} - \tilde{\rho}_{Xg})^2}{\text{SE}(r_{Xg})^2} + \frac{(r_{Yg} - \tilde{K}\tilde{\rho}_{Xg})^2}{\text{SE}(r_{Yg})^2} \right) \leq \min_{\tilde{K}, \tilde{\rho}_{Xg}} \sum_{g \in (B_{XY}^0)^c} \left(\frac{(r_{Xg} - \tilde{\rho}_{Xg})^2}{\text{SE}(r_{Xg})^2} + \frac{(r_{Yg} - \tilde{K}\tilde{\rho}_{Xg})^2}{\text{SE}(r_{Yg})^2} \right)\right) \\ & \leq P\left(\min_{\tilde{K}, \tilde{\rho}_{Xg}} \sum_{g \in B_1^c} \left(\frac{(r_{Xg} - \tilde{\rho}_{Xg})^2}{\text{SE}(r_{Xg})^2} + \frac{(r_{Yg} - \tilde{K}\tilde{\rho}_{Xg})^2}{\text{SE}(r_{Yg})^2} \right) \leq \sum_{g \in (B_{XY}^0)^c} \left(\frac{(r_{Xg} - \rho_{Xg})^2}{\text{SE}(r_{Xg})^2} + \frac{(r_{Yg} - K_{XY}\rho_{Xg})^2}{\text{SE}(r_{Yg})^2} \right)\right). \end{aligned}$$

Note that, for $g \in (B_{XY}^0)^c$, $\frac{r_{Xg} - \rho_{Xg}}{\text{SE}(r_{Xg})} \sim N(0, 1)$ and $\frac{r_{Yg} - K_{XY}\rho_{Xg}}{\text{SE}(r_{Yg})} \sim N(0, 1)$. So for any $\varepsilon > 0$, there exists $C > 0$ such that

$$P\left(\sum_{g \in (B_{XY}^0)^c} \left(\frac{(r_{Xg} - \rho_{Xg})^2}{\text{SE}(r_{Xg})^2} + \frac{(r_{Yg} - K_{XY}\rho_{Xg})^2}{\text{SE}(r_{Yg})^2} \right) > C\right) < \frac{\varepsilon}{2}. \quad (1)$$

And we have

$$\begin{aligned} P\left(\min_{\tilde{K}, \tilde{\rho}_{Xg}} \sum_{g \in B_1^c} \left(\frac{(r_{Xg} - \tilde{\rho}_{Xg})^2}{\text{SE}(r_{Xg})^2} + \frac{(r_{Yg} - \tilde{K}\tilde{\rho}_{Xg})^2}{\text{SE}(r_{Yg})^2} \right) \leq \sum_{g \in (B_{XY}^0)^c} \left(\frac{(r_{Xg} - \rho_{Xg})^2}{\text{SE}(r_{Xg})^2} + \frac{(r_{Yg} - K_{XY}\rho_{Xg})^2}{\text{SE}(r_{Yg})^2} \right)\right) \\ \leq P\left(\min_{\tilde{K}, \tilde{\rho}_{Xg}} \sum_{g \in B_1^c} \left(\frac{(r_{Xg} - \tilde{\rho}_{Xg})^2}{\text{SE}(r_{Xg})^2} + \frac{(r_{Yg} - \tilde{K}\tilde{\rho}_{Xg})^2}{\text{SE}(r_{Yg})^2} \right) \leq C\right) + P\left(\sum_{g \in (B_{XY}^0)^c} \left(\frac{(r_{Xg} - \rho_{Xg})^2}{\text{SE}(r_{Xg})^2} + \frac{(r_{Yg} - K_{XY}\rho_{Xg})^2}{\text{SE}(r_{Yg})^2} \right) > C\right). \end{aligned}$$

After profiling out $\tilde{\rho}_{Xg}$'s, we get

$$\min_{\tilde{K}, \tilde{\rho}_{Xg}} \sum_{g \in B_1^c} \left(\frac{(r_{Xg} - \tilde{\rho}_{Xg})^2}{\text{SE}(r_{Xg})^2} + \frac{(r_{Yg} - \tilde{K}\tilde{\rho}_{Xg})^2}{\text{SE}(r_{Yg})^2} \right) = \min_{\tilde{K}} \sum_{g \in B_1^c} \frac{(r_{Yg} - \tilde{K} \cdot r_{Xg})^2}{\text{SE}(r_{Yg})^2 + \tilde{K}^2 \text{SE}(r_{Xg})^2},$$

so

$$\begin{aligned} P\left(\min_{\tilde{K}, \tilde{\rho}_{Xg}} \sum_{g \in B_1^c} \left(\frac{(r_{Xg} - \tilde{\rho}_{Xg})^2}{\text{SE}(r_{Xg})^2} + \frac{(r_{Yg} - \tilde{K}\tilde{\rho}_{Xg})^2}{\text{SE}(r_{Yg})^2} \right) \leq C\right) \\ = P\left(\min_{\tilde{K}} \sum_{g \in B_1^c} \frac{(r_{Yg} - \tilde{K} \cdot r_{Xg})^2}{\text{SE}(r_{Yg})^2 + \tilde{K}^2 \text{SE}(r_{Xg})^2} \leq C\right). \end{aligned}$$

We have $\frac{r_{Yg} - \tilde{K} \cdot r_{Xg}}{\sqrt{\text{SE}(r_{Yg})^2 + \tilde{K}^2 \text{SE}(r_{Xg})^2}} \sim N\left(\frac{K_{XY} \cdot \rho_{Xg} + b_{XYg} - \tilde{K} \cdot \rho_{Xg}}{\sqrt{\text{SE}(r_{Yg})^2 + \tilde{K}^2 \text{SE}(r_{Xg})^2}}, 1\right)$, so $\sum_{g \in B_1^c} \frac{(r_{Yg} - \tilde{K} \cdot r_{Xg})^2}{\text{SE}(r_{Yg})^2 + \tilde{K}^2 \text{SE}(r_{Xg})^2}$ follows non-central χ^2 distribution with degrees of freedom $(m - m_{XY}^0)$ and non-centrality parameter $\lambda_{\tilde{K}}$ depending on \tilde{K}

$$\lambda_{\tilde{K}} = \sum_{g \in B_1^c} \frac{(K_{XY} \cdot \rho_{Xg} + b_{XYg} - \tilde{K} \cdot \rho_{Xg})^2}{\text{SE}(r_{Yg})^2 + \tilde{K}^2 \text{SE}(r_{Xg})^2}.$$

With Assumption 2, we get

$$\lambda_{\tilde{K}} \geq \sum_{g \in B_1^c} \frac{(K_{XY} \cdot \rho_{Xg} + b_{XYg} - \tilde{K} \cdot \rho_{Xg})^2}{\frac{u_Y}{N_2} + \tilde{K}^2 \cdot \frac{u_X}{l_n \cdot N_2}} = N_2 \cdot \sum_{g \in B_1^c} \frac{(K_{XY} \cdot \rho_{Xg} + b_{XYg} - \tilde{K} \cdot \rho_{Xg})^2}{u_Y + \tilde{K}^2 \cdot \frac{u_X}{l_n}}.$$

With Assumption 1, we know

$$\min_{\tilde{K}} \sum_{g \in B_1^c} \frac{(K_{XY} \cdot \rho_{Xg} + b_{XYg} - \tilde{K} \cdot \rho_{Xg})^2}{u_Y + \tilde{K}^2 \cdot \frac{u_X}{l_n}} = v > 0,$$

here v is a constant. This is because, with Assumption 1, there is no \tilde{K} making $K_{XY} \cdot \rho_{Xg} + b_{XYg} - \tilde{K} \cdot \rho_{Xg} = 0$ for all $g \in B_1^c$ simultaneously. So we have $\min_{\tilde{K}} \lambda_{\tilde{K}} \geq N_2 \cdot v$. Then as N_2 large enough, we have

$$P\left(\min_{\tilde{K}} \sum_{g \in B_1^c} \frac{(r_{Yg} - \tilde{K} \cdot r_{Xg})^2}{\text{SE}(r_{Yg})^2 + \tilde{K}^2 \text{SE}(r_{Xg})^2} \leq C\right) \leq \frac{\varepsilon}{2}. \quad (2)$$

Combining (1) and (2), we get $P(\hat{B}_{XY}(m_{XY}^0) = B_{XY}^0) \rightarrow 1$ as $N_1, N_2 \rightarrow \infty$.

Next, we show $P(\hat{m}_I = m_{XY}^0) \rightarrow 1$. For any $m_1 < m_{XY}^0$, we have

$$\begin{aligned} P(\hat{m}_I = m_1) &\leq P(\text{BIC}(m_1) \leq \text{BIC}(m_{XY}^0)) \\ &= P(-2 \cdot L(\hat{K}_{XY}(m_1), \hat{\rho}_{Xg}(m_1), \hat{b}_{XYg}(m_1)) + \log(n) \cdot m_1 \leq -2 \cdot L(\hat{K}_{XY}(m_{XY}^0), \hat{\rho}_{Xg}(m_{XY}^0), \hat{b}_{XYg}(m_{XY}^0)) + \log(n) \cdot m_{XY}^0) \\ &= P(2 \cdot L(\hat{K}_{XY}(m_{XY}^0), \hat{\rho}_{Xg}(m_{XY}^0), \hat{b}_{XYg}(m_{XY}^0)) - 2 \cdot L(\hat{K}_{XY}(m_1), \hat{\rho}_{Xg}(m_1), \hat{b}_{XYg}(m_1)) \leq \log(n)(m_{XY}^0 - m_1)). \end{aligned}$$

As we have shown $P(\hat{B}_{XY}(m_{XY}^0) = B_{XY}^0) \rightarrow 1$, with probability goes to 1 we have

$$\begin{aligned} &2 \cdot L(\hat{K}_{XY}(m_{XY}^0), \hat{\rho}_{Xg}(m_{XY}^0), \hat{b}_{XYg}(m_{XY}^0)) - 2 \cdot L(\hat{K}_{XY}(m_1), \hat{\rho}_{Xg}(m_1), \hat{b}_{XYg}(m_1)) \\ &= \min_{\tilde{K}, \tilde{\rho}_{Xg}} \sum_{g \in \hat{B}_{m_1}^c} \left(\frac{(r_{Xg} - \tilde{\rho}_{Xg})^2}{\text{SE}(r_{Xg})^2} + \frac{(r_{Yg} - \tilde{K}\tilde{\rho}_{Xg})^2}{\text{SE}(r_{Yg})^2} \right) - \min_{\tilde{K}, \tilde{\rho}_{Xg}} \sum_{g \in (B_{XY}^0)^c} \left(\frac{(r_{Xg} - \tilde{\rho}_{Xg})^2}{\text{SE}(r_{Xg})^2} + \frac{(r_{Yg} - \tilde{K}\tilde{\rho}_{Xg})^2}{\text{SE}(r_{Yg})^2} \right) \\ &\geq \min_{\tilde{K}, \tilde{\rho}_{Xg}} \sum_{g \in \hat{B}_{m_1}^c} \left(\frac{(r_{Xg} - \tilde{\rho}_{Xg})^2}{\text{SE}(r_{Xg})^2} + \frac{(r_{Yg} - \tilde{K}\tilde{\rho}_{Xg})^2}{\text{SE}(r_{Yg})^2} \right) - \sum_{g \in (B_{XY}^0)^c} \left(\frac{(r_{Xg} - \rho_{Xg})^2}{\text{SE}(r_{Xg})^2} + \frac{(r_{Yg} - K_{XY}\rho_{Xg})^2}{\text{SE}(r_{Yg})^2} \right). \end{aligned}$$

Then we get

$$\begin{aligned} &P(\hat{m}_I = m_1) \\ &\leq P\left(\min_{\tilde{K}, \tilde{\rho}_{Xg}} \sum_{g \in \hat{B}_{m_1}^c} \left(\frac{(r_{Xg} - \tilde{\rho}_{Xg})^2}{\text{SE}(r_{Xg})^2} + \frac{(r_{Yg} - \tilde{K}\tilde{\rho}_{Xg})^2}{\text{SE}(r_{Yg})^2} \right) \leq \sum_{g \in (B_{XY}^0)^c} \left(\frac{(r_{Xg} - \rho_{Xg})^2}{\text{SE}(r_{Xg})^2} + \frac{(r_{Yg} - K_{XY}\rho_{Xg})^2}{\text{SE}(r_{Yg})^2} \right) + \log(n)(m_{XY}^0 - m_1)\right) \\ &\leq \sum_{|B|=m_1} P\left(\min_{\tilde{K}, \tilde{\rho}_{Xg}} \sum_{g \in B^c} \left(\frac{(r_{Xg} - \tilde{\rho}_{Xg})^2}{\text{SE}(r_{Xg})^2} + \frac{(r_{Yg} - \tilde{K}\tilde{\rho}_{Xg})^2}{\text{SE}(r_{Yg})^2} \right) \leq \sum_{g \in (B_{XY}^0)^c} \left(\frac{(r_{Xg} - \rho_{Xg})^2}{\text{SE}(r_{Xg})^2} + \frac{(r_{Yg} - K_{XY}\rho_{Xg})^2}{\text{SE}(r_{Yg})^2} \right) + \log(n)(m_{XY}^0 - m_1)\right). \end{aligned}$$

Similar as above, we get

$$\min_{\tilde{K}, \tilde{\rho}_{Xg}} \sum_{g \in B^c} \left(\frac{(r_{Xg} - \tilde{\rho}_{Xg})^2}{\text{SE}(r_{Xg})^2} + \frac{(r_{Yg} - \tilde{K}\tilde{\rho}_{Xg})^2}{\text{SE}(r_{Yg})^2} \right) = \min_{\tilde{K}} \sum_{g \in B^c} \frac{(r_{Yg} - \tilde{K} \cdot r_{Xg})^2}{\text{SE}(r_{Yg})^2 + \tilde{K}^2 \text{SE}(r_{Xg})^2},$$

and $\sum_{g \in B^c} \frac{(r_{Yg} - \tilde{K} \cdot r_{Xg})^2}{\text{SE}(r_{Yg})^2 + \tilde{K}^2 \text{SE}(r_{Xg})^2}$ follows non-central χ^2 distribution with degrees of freedom $(m - m_1)$ and non-centrality parameter $\lambda_{\tilde{K}}$ depending on \tilde{K}

$$\lambda_{\tilde{K}} = \sum_{g \in B^c} \frac{(K_{XY} \cdot \rho_{Xg} + b_{XYg} - \tilde{K} \cdot \rho_{Xg})^2}{\text{SE}(r_{Yg})^2 + \tilde{K}^2 \text{SE}(r_{Xg})^2}.$$

Similarly, since $m_1 < m_{XY}^0$, with Assumption 2 we have $\lambda_{\tilde{K}} \geq N_2 \cdot v$ for some constant v , so for any $|B| = m_1$, we get

$$P\left(\min_{\tilde{K}, \tilde{\rho}_{Xg}} \sum_{g \in B^c} \left(\frac{(r_{Xg} - \tilde{\rho}_{Xg})^2}{\text{SE}(r_{Xg})^2} + \frac{(r_{Yg} - \tilde{K}\tilde{\rho}_{Xg})^2}{\text{SE}(r_{Yg})^2} \right) \leq \sum_{g \in (B_{XY}^0)^c} \left(\frac{(r_{Xg} - \rho_{Xg})^2}{\text{SE}(r_{Xg})^2} + \frac{(r_{Yg} - K_{XY}\rho_{Xg})^2}{\text{SE}(r_{Yg})^2} \right) + \log(n)(m_{XY}^0 - m_1)\right) \rightarrow 0.$$

This gives us $P(\hat{m}_I = m_1) \rightarrow 0$ for any $m_1 < m_{XY}^0$. For any $m_1 > m_{XY}^0$, we have

$$\begin{aligned} &P(\hat{m}_I = m_1) \\ &\leq P\left(\log(n)(m_1 - m_{XY}^0) \leq \sum_{g \in (B_{XY}^0)^c} \left(\frac{(r_{Xg} - \rho_{Xg})^2}{\text{SE}(r_{Xg})^2} + \frac{(r_{Yg} - K_{XY}\rho_{Xg})^2}{\text{SE}(r_{Yg})^2} \right) - \min_{\tilde{K}, \tilde{\rho}_{Xg}} \sum_{g \in \hat{B}_{m_1}^c} \left(\frac{(r_{Xg} - \tilde{\rho}_{Xg})^2}{\text{SE}(r_{Xg})^2} + \frac{(r_{Yg} - \tilde{K}\tilde{\rho}_{Xg})^2}{\text{SE}(r_{Yg})^2} \right)\right) \\ &\leq P\left(\log(n)(m_1 - m_{XY}^0) \leq \sum_{g \in (B_{XY}^0)^c} \left(\frac{(r_{Xg} - \rho_{Xg})^2}{\text{SE}(r_{Xg})^2} + \frac{(r_{Yg} - K_{XY}\rho_{Xg})^2}{\text{SE}(r_{Yg})^2} \right)\right) \end{aligned}$$

Since $\sum_{g \in (B_{XY}^0)^c} \left(\frac{(r_{Xg} - \rho_{Xg})^2}{\text{SE}(r_{Xg})^2} + \frac{(r_{Yg} - K_{XY}\rho_{Xg})^2}{\text{SE}(r_{Yg})^2} \right)$ is a central χ^2 distribution with degrees of freedom $2(m - m_{XY}^0)$, we get $P(\hat{m}_I = m_1) \rightarrow 0$ for any $m_1 > m_{XY}^0$. So we have $P(\hat{m}_I = m_{XY}^0) \rightarrow 1$ as $N_1, N_2 \rightarrow \infty$.

As $P(\hat{B}_{XY}(\hat{m}_I) = B_{XY}^0) \rightarrow 1$, we could consistently select all invalid IVs. Following Theorem 3.2 in [4], we have

$$\frac{V}{\sqrt{V_1}}(\hat{K}_{XY} - K_{XY}) \xrightarrow{d} N(0, 1), \text{ as } N_1, N_2 \rightarrow \infty,$$

where

$$V = \sum_{g \in (B_{XY}^0)^c} \frac{\rho_{Xg}^2 \sigma_{Xg}^2 + \rho_{Yg}^2 \sigma_{Yg}^2}{(\sigma_{Xg}^2 \cdot K_{XY}^2 + \sigma_{Yg}^2)^2} = \sum_{g \in (B_{XY}^0)^c} \frac{\rho_{Xg}^2}{\sigma_{Xg}^2 \cdot K_{XY}^2 + \sigma_{Yg}^2},$$

and

$$V_1 = \sum_{g \in (B_{XY}^0)^c} \frac{\rho_{Xg}^2 \sigma_{Xg}^2 + \rho_{Yg}^2 \sigma_{Yg}^2 + \sigma_{Xg}^2 \sigma_{Yg}^2}{(\sigma_{Xg}^2 \cdot K_{XY}^2 + \sigma_{Yg}^2)^2}.$$

In our model ρ_{Xg} 's and ρ_{Yg} 's are fixed constants, σ_{Xg}^2 's and σ_{Yg}^2 's are $O(1/n)$, so we have $V/V_1 \rightarrow 1$, and

$$\sqrt{V}(\hat{K}_{XY} - K_{XY}) \xrightarrow{d} N(0, 1), \text{ as } N_1, N_2 \rightarrow \infty.$$

□

S3.2 Proof of Theorem 2

First we introduce the definition of “converge weakly”, as Definition 2.2 in [2].

Definition 2.2 by Xiong et al. [2]. $F(\cdot)$ is a distribution function, $F_n(\cdot)$ is random distribution function that depends on some random variable. We say $F_n(\cdot)$ converges weakly to $F(\cdot)$ in probability if for each continuous point x of $F(\cdot)$, $F_n(x) \xrightarrow{P} F(x)$ as $n \rightarrow \infty$. This is denoted by $F_n(\cdot) \xrightarrow{w.P} F(\cdot)$.

Now we show the proof of Theorem 2.

Theorem 2. Under Assumptions 1 and 2, conditional on the original GWAS summary data, $\sqrt{V}(\hat{K}_{XY}^{(t)} - \hat{K}_{XY}) \xrightarrow{w.P} N(0, 1)$ as $N_1, N_2 \rightarrow \infty$.

Proof. Denote $\tilde{B} = \{i : \tilde{b}_{XYg} \neq 0\}$ as the set of estimated invalid IVs with non-zero direct effects based on perturbed data. First we show that $P(\tilde{B} = B_{XY}^0 | \mathcal{D}) \xrightarrow{P} 1$, which is equivalent to for any $\varepsilon > 0, \delta > 0$, there exists n such that when $n_1 > n, n_2 > n$ we have $P(P(\tilde{B} = B_{XY}^0 | \mathcal{D}) < 1 - \varepsilon) < \delta$. Following similar argument in Theorem 1, we could get the unconditional probability $P(\tilde{B} = B_{XY}^0) \rightarrow 1$. Suppose we could find a pair of $\varepsilon_0 > 0, \delta_0 > 0$ such that $P(P(\tilde{B} = B_{XY}^0 | \mathcal{D}) < 1 - \varepsilon_0) < \delta_0$ for arbitrarily large n_1, n_2 , then we can get

$$P(\tilde{B} = B_{XY}^0) = \int_{\mathcal{D}} P(\tilde{B} = B_{XY}^0 | \mathcal{D}) dF(\mathcal{D}) < 1 - \varepsilon_0 \delta_0,$$

contradicts that $P(\tilde{B} = B_{XY}^0) \rightarrow 1$, thus we have shown that $P(\tilde{B} = B_{XY}^0 | \mathcal{D}) \xrightarrow{P} 1$. Now we could focus on the case that $\tilde{B} = \hat{B} = B_{XY}^0$, for simplicity we use \tilde{K}, \hat{K} to represent $\hat{K}_{XY}^{(t)}, \hat{K}_{XY}$. Similar to [4], after profiling out ρ_{Xg} 's in the original log-likelihood function, we have

$$\tilde{K} = \arg \min_K \sum_{g \in (B_{XY}^0)^c} \frac{(\tilde{r}_{Yg} - K \cdot \tilde{r}_{Xg})^2}{\sigma_{Xg}^2 \cdot K^2 + \sigma_{Yg}^2}, \quad \hat{K} = \arg \min_K \sum_{g \in (B_{XY}^0)^c} \frac{(r_{Yg} - K \cdot r_{Xg})^2}{\sigma_{Xg}^2 \cdot K^2 + \sigma_{Yg}^2}. \quad (3)$$

Denote

$$f(K) = \sum_{g \in (B_{XY}^0)^c} \frac{(\tilde{r}_{Yg} - K \cdot \tilde{r}_{Xg})^2}{\sigma_{Xg}^2 \cdot K^2 + \sigma_{Yg}^2},$$

and

$$\begin{aligned} \phi(K) &= \frac{\partial f(K)}{\partial K} = \sum_{g \in (B_{XY}^0)^c} \frac{(\tilde{r}_{Yg} - K \cdot \tilde{r}_{Xg})(K \tilde{r}_{Yg} \sigma_{Xg}^2 + \tilde{r}_{Xg} \sigma_{Yg}^2)}{(\sigma_{Xg}^2 K^2 + \sigma_{Yg}^2)^2} \\ &= \sum_{g \in (B_{XY}^0)^c} \frac{(r_{Yg} - K r_{Xg})(K r_{Yg} \sigma_{Xg}^2 + r_{Xg} \sigma_{Yg}^2) + (r_{Yg} - K r_{Xg})(K \xi_g \sigma_{Xg}^2 + \varepsilon_g \sigma_{Yg}^2) + (\xi_g - K \varepsilon_g)(K r_{Yg} \sigma_{Xg}^2 + r_{Xg} \sigma_{Yg}^2 + K \xi_g \sigma_{Xg}^2 + \varepsilon_g \sigma_{Yg}^2)}{(\sigma_{Xg}^2 K^2 + \sigma_{Yg}^2)^2}, \end{aligned}$$

here $\xi_g = \tilde{r}_{Yg} - r_{Yg} \sim N(0, \sigma_{Yg}^2)$, $\varepsilon_g = \tilde{r}_{Xg} - r_{Xg} \sim N(0, \sigma_{Xg}^2)$. We have

$$0 = \phi(\tilde{K}) = \phi(\hat{K}) + \phi'(\hat{K})(\tilde{K} - \hat{K}) + \frac{1}{2} \phi''(K^*)(\tilde{K} - \hat{K})^2,$$

with K^* is between \tilde{K} and \hat{K} , thus

$$\sqrt{V}(\tilde{K} - \hat{K}) = \frac{-\phi(\hat{K})/\sqrt{V}}{\phi'(\hat{K})/V + (1/2)(\tilde{K} - \hat{K})\phi''(K^*)/V}.$$

Next we show $\phi(\hat{K})/\sqrt{V} | \mathcal{D} \xrightarrow{w.P} N(0, 1)$. From equation (6), we can get

$$\phi(\hat{K}) = \sum_{g \in (B_{XY}^0)^c} \frac{(r_{Yg} - \hat{K} r_{Xg})(\hat{K} \xi_g \sigma_{Xg}^2 + \varepsilon_g \sigma_{Yg}^2) + (\xi_g - \hat{K} \varepsilon_g)(\hat{K} r_{Yg} \sigma_{Xg}^2 + r_{Xg} \sigma_{Yg}^2 + \hat{K} \xi_g \sigma_{Xg}^2 + \varepsilon_g \sigma_{Yg}^2)}{(\sigma_{Xg}^2 \hat{K}^2 + \sigma_{Yg}^2)^2}.$$

Note that ξ_g 's and ε_g 's are $O_p(1/\sqrt{n})$, $n = \min(N_1, N_2)$, thus

$$\phi(\hat{K}) = \sum_{g \in (B_{XY}^0)^c} \frac{\xi_g(r_{Yg} \hat{K} \sigma_{Xg}^2 - \hat{K}^2 r_{Xg} \sigma_{Xg}^2 + \hat{K} r_{Yg} \sigma_{Xg}^2 + r_{Xg} \sigma_{Yg}^2) + \varepsilon_g(r_{Yg} \sigma_{Yg}^2 - \hat{K} r_{Xg} \sigma_{Yg}^2 - \hat{K}^2 r_{Yg} \sigma_{Xg}^2 - \hat{K} r_{Xg} \sigma_{Yg}^2)}{(\sigma_{Xg}^2 \hat{K}^2 + \sigma_{Yg}^2)^2} + O_p(1), \quad (4)$$

thus $\phi(\hat{K})/\sqrt{V} | \mathcal{D} = N(0, V^*/V) | \mathcal{D} + O_p(1/\sqrt{n})$, with

$$V^* = \sum_{g \in (B_{XY}^0)^c} \frac{\sigma_{Yg}^2(r_{Yg} \hat{K} \sigma_{Xg}^2 - \hat{K}^2 r_{Xg} \sigma_{Xg}^2 + \hat{K} r_{Yg} \sigma_{Xg}^2 + r_{Xg} \sigma_{Yg}^2)^2 + \sigma_{Xg}^2(r_{Yg} \sigma_{Yg}^2 - \hat{K} r_{Xg} \sigma_{Yg}^2 - \hat{K}^2 r_{Yg} \sigma_{Xg}^2 - \hat{K} r_{Xg} \sigma_{Yg}^2)^2}{(\sigma_{Xg}^2 \hat{K}^2 + \sigma_{Yg}^2)^4},$$

as $r_{Xg} \xrightarrow{P} \rho_{Xi}$, $r_{Yg} \xrightarrow{P} \rho_{Yi}$, $\hat{K} \xrightarrow{P} K_0$, we can get $V^*/V \xrightarrow{P} 1$, thus we get $\phi(\hat{K})/\sqrt{V} | \mathcal{D} \xrightarrow{w.P} N(0, 1)$.

Next we show $-\phi'(\hat{K})/V | \mathcal{D} \xrightarrow{w.P} 1$. After some calculation we get

$$\phi'(K) = \sum_{g \in (B_{XY}^0)^c} \frac{2\sigma_{Xg}^4 \tilde{r}_{Xg} \tilde{r}_{Yg} \cdot K^3 + 3(\sigma_{Xg}^2 \sigma_{Yg}^2 \tilde{r}_{Xg}^2 - \sigma_{Xg}^4 \tilde{r}_{Yg}^2) K^2 - 6\sigma_{Xg}^2 \sigma_{Yg}^2 \tilde{r}_{Xg} \tilde{r}_{Yg} K + (\sigma_{Xg}^2 \sigma_{Yg}^2 \tilde{r}_{Yg}^2 - \tilde{r}_{Xg}^2 \sigma_{Yg}^4)}{(\sigma_{Xg}^2 K^2 + \sigma_{Yg}^2)^3}, \quad (5)$$

as $\tilde{r}_{Xg} \xrightarrow{P} \rho_{Xi}$, $\tilde{r}_{Yg} \xrightarrow{P} \rho_{Yi}$, $\hat{K} \xrightarrow{P} K_0$, we get $-\phi'(\hat{K})/V \xrightarrow{P} 1$, with Theorem 3.3 in [2], $-\phi'(\hat{K})/V|\mathcal{D} \xrightarrow{w.P} 1$.

Based on equation (8), we can see $\phi''(K)$ has its numerator of order n^5 and its denominator of order n^6 , thus $\phi''(K^*)/V = O_p(1)$. As $\tilde{K} \xrightarrow{P} K_0$, $\hat{K} \xrightarrow{P} K_0$, we have $\tilde{K} - \hat{K} \xrightarrow{P} 0$, again with Theorem 3.3 in [2] we get $\tilde{K} - \hat{K}|\mathcal{D} \xrightarrow{w.P} 0$. Thus we can get $\frac{1}{2}\phi''(K^*)(\tilde{K} - \hat{K})|\mathcal{D} \xrightarrow{w.P} 0$. Now with Theorem 3.2 in [2], we can get $\sqrt{V}(\tilde{K} - \hat{K})|\mathcal{D} \xrightarrow{w.P} N(0, 1)$, completing the proof. \square

S3.3 MR-cML with Data Perturbation

Now we show that the data perturbation scheme is also consistent for MR-cML in [3]. We use the following notations: the true effects on X are β_{Xi} 's, and those on Y are β_{Yi} 's; the estimated/observed effects on X are $\hat{\beta}_{Xi} \sim N(\beta_{Xi}, \sigma_{Xi}^2)$, and those on Y are $\hat{\beta}_{Yi} \sim N(\beta_{Yi}, \sigma_{Yi}^2)$. Here σ_{Xi} 's and σ_{Yi} 's are the true standard deviations; in practice we have the standard errors $\hat{\sigma}_{Xi}$'s and $\hat{\sigma}_{Yi}$'s as their estimates from GWAS datasets, thus approximately we have $\hat{\beta}_{Xi} \sim N(\beta_{Xi}, \hat{\sigma}_{Xi}^2)$ and $\hat{\beta}_{Yi} \sim N(\beta_{Yi}, \hat{\sigma}_{Yi}^2)$. For simplicity and without ambiguity, we treat the standard errors $\hat{\sigma}_{Xi}$'s and $\hat{\sigma}_{Yi}$'s as the true values of σ_{Xi} 's and σ_{Yi} 's in the following. The perturbed effects on X are $\tilde{\beta}_{Xi} \sim N(\hat{\beta}_{Xi}, \sigma_{Xi}^2)$, and the perturbed effects on Y are $\tilde{\beta}_{Yi} \sim N(\hat{\beta}_{Yi}, \sigma_{Yi}^2)$. The true causal effect is θ_0 , the estimated causal effect based on the observed data with cML-BIC is $\hat{\theta}$, and the estimated causal effect based on a perturbed dataset with cML-BIC is $\tilde{\theta}$. Let $\mathcal{D} = \{(\hat{\beta}_{Xi}, \hat{\beta}_{Yi}) | i = 1, \dots, m\}$ denote the observed data.

Assumption 1 for MR-cML. (*Plurality condition.*) Suppose that B_0 is the index set of the invalid IVs with non-zero direct effects, i.e. $r_i \neq 0$ if and only if $i \in B_0$, and $K_0 = |B_0|$. For any $B \subseteq \{1, \dots, m\}$ and $|B| = K_0$, if $B \neq B_0$, then there does not exist any constant S such that $r_i = S \cdot \beta_{Xi}$ for all $i \in B^c$.

Assumption 2 for MR-cML. (*Orders of the variances and sample sizes.*) There exist positive constants l_X, l_Y, l_N and u_X, u_Y, u_N such that we have $l_X/n_1 \leq \sigma_{Xi}^2 \leq u_X/n_1$, $l_Y/n_2 \leq \sigma_{Yi}^2 \leq u_Y/n_2$, and $l_N \cdot n_2 \leq n_1 \leq u_N \cdot n_2$ for $i = 1, \dots, m$.

Denote

$$V = \sum_{i \in B_0^c} \frac{\beta_{Xi}^2}{\sigma_{Xi}^2 \cdot \theta_0^2 + \sigma_{Yi}^2}.$$

Theorem 2 for MR-cML. Under Assumptions 1 for MR-cML and 2 for MR-cML, according to Definition 2.2 in [2], $\sqrt{V}(\tilde{\theta} - \hat{\theta})|\mathcal{D} \xrightarrow{w.P} N(0, 1)$ as $n_1, n_2 \rightarrow \infty$.

Proof. Denote $\tilde{B} = \{i : \tilde{r}_i \neq 0\}$ as the set of estimated invalid IVs with non-zero direct effects based on perturbed data. First we show that $P(\tilde{B} = B_0|\mathcal{D}) \xrightarrow{P} 1$, which is equivalent to for any $\varepsilon > 0, \delta > 0$, there exists n such that when $n_1 > n, n_2 > n$ we have $P(P(\tilde{B} = B_0|\mathcal{D}) < 1 - \varepsilon) < \delta$. Following similar argument in Theorem 1, we could get the unconditional probability $P(\tilde{B} = B_0) \rightarrow 1$. Suppose we could find a pair of $\varepsilon_0 > 0, \delta_0 > 0$ such that $P(P(\tilde{B} = B_0|\mathcal{D}) < 1 - \varepsilon_0) > \delta_0$ for arbitrarily large n_1, n_2 , then we can get

$$P(\tilde{B} = B_0) = \int_{\mathcal{D}} P(\tilde{B} = B_0|\mathcal{D}) dF(\mathcal{D}) < 1 - \varepsilon_0 \delta_0,$$

contradicts that $P(\tilde{B} = B_0) \rightarrow 1$, thus we have shown that $P(\tilde{B} = B_0 | \mathcal{D}) \xrightarrow{P} 1$. Now we could focus on the case that $\tilde{B} = \hat{B} = B_0$. Similar to [4], after profiling out b_{Xi} 's in the original log-likelihood function, we have

$$\tilde{\theta} = \arg \min_{\theta} \sum_{i \in B_0^c} \frac{(\tilde{\beta}_{Yi} - \theta \cdot \tilde{\beta}_{Xi})^2}{\sigma_{Xi}^2 \cdot \theta^2 + \sigma_{Yi}^2}, \quad \hat{\theta} = \arg \min_{\theta} \sum_{i \in B_0^c} \frac{(\hat{\beta}_{Yi} - \theta \cdot \hat{\beta}_{Xi})^2}{\sigma_{Xi}^2 \cdot \theta^2 + \sigma_{Yi}^2}. \quad (6)$$

Denote

$$f(\theta) = \sum_{i \in B_0^c} \frac{(\tilde{\beta}_{Yi} - \theta \cdot \tilde{\beta}_{Xi})^2}{\sigma_{Xi}^2 \cdot \theta^2 + \sigma_{Yi}^2},$$

and

$$\begin{aligned} \phi(\theta) &= \frac{\partial f(\theta)}{\partial \theta} = \sum_{i \in B_0^c} \frac{(\tilde{\beta}_{Yi} - \theta \tilde{\beta}_{Xi})(\theta \tilde{\beta}_{Yi} \sigma_{Xi}^2 + \tilde{\beta}_{Xi} \sigma_{Yi}^2)}{(\sigma_{Xi}^2 \theta^2 + \sigma_{Yi}^2)^2} \\ &= \sum_{i \in B_0^c} \frac{(\hat{\beta}_{Yi} - \theta \hat{\beta}_{Xi})(\theta \hat{\beta}_{Yi} \sigma_{Xi}^2 + \hat{\beta}_{Xi} \sigma_{Yi}^2) + (\hat{\beta}_{Yi} - \theta \hat{\beta}_{Xi})(\theta \xi_i \sigma_{Xi}^2 + \varepsilon_i \sigma_{Yi}^2) + (\xi_i - \theta \varepsilon_i)(\theta \hat{\beta}_{Yi} \sigma_{Xi}^2 + \hat{\beta}_{Xi} \sigma_{Yi}^2 + \theta \xi_i \sigma_{Xi}^2 + \varepsilon_i \sigma_{Yi}^2)}{(\sigma_{Xi}^2 \theta^2 + \sigma_{Yi}^2)^2}, \end{aligned}$$

here $\xi_i = \tilde{\beta}_{Yi} - \hat{\beta}_{Yi} \sim N(0, \sigma_{Yi}^2)$, $\varepsilon_i = \tilde{\beta}_{Xi} - \hat{\beta}_{Xi} \sim N(0, \sigma_{Xi}^2)$. We have

$$0 = \phi(\tilde{\theta}) = \phi(\hat{\theta}) + \phi'(\hat{\theta})(\tilde{\theta} - \hat{\theta}) + \frac{1}{2} \phi''(\theta^*)(\tilde{\theta} - \hat{\theta})^2,$$

with θ^* is between $\tilde{\theta}$ and $\hat{\theta}$, thus

$$\sqrt{V}(\tilde{\theta} - \hat{\theta}) = \frac{-\phi(\hat{\theta})/\sqrt{V}}{\phi'(\hat{\theta})/V + (1/2)(\tilde{\theta} - \hat{\theta})\phi''(\theta^*)/V}.$$

Next we show $\phi(\hat{\theta})/\sqrt{V} | \mathcal{D} \xrightarrow{w.P} N(0, 1)$. From equation (6), we can get

$$\phi(\hat{\theta}) = \sum_{i \in B_0^c} \frac{(\hat{\beta}_{Yi} - \hat{\theta} \hat{\beta}_{Xi})(\hat{\theta} \xi_i \sigma_{Xi}^2 + \varepsilon_i \sigma_{Yi}^2) + (\xi_i - \hat{\theta} \varepsilon_i)(\hat{\theta} \hat{\beta}_{Yi} \sigma_{Xi}^2 + \hat{\beta}_{Xi} \sigma_{Yi}^2 + \hat{\theta} \xi_i \sigma_{Xi}^2 + \varepsilon_i \sigma_{Yi}^2)}{(\sigma_{Xi}^2 \hat{\theta}^2 + \sigma_{Yi}^2)^2}.$$

Note that ξ_i 's and ε_i 's are $O_p(1/\sqrt{n})$, $n = \min(n_1, n_2)$, thus

$$\phi(\hat{\theta}) = \sum_{i \in B_0^c} \frac{\xi_i(\hat{\beta}_{Yi} \hat{\theta} \sigma_{Xi}^2 - \hat{\theta}^2 \hat{\beta}_{Xi} \sigma_{Xi}^2 + \hat{\theta} \hat{\beta}_{Yi} \sigma_{Xi}^2 + \hat{\beta}_{Xi} \sigma_{Yi}^2) + \varepsilon_i(\hat{\beta}_{Yi} \sigma_{Yi}^2 - \hat{\theta} \hat{\beta}_{Xi} \sigma_{Yi}^2 - \hat{\theta}^2 \hat{\beta}_{Yi} \sigma_{Xi}^2 - \hat{\theta} \hat{\beta}_{Xi} \sigma_{Yi}^2)}{(\sigma_{Xi}^2 \hat{\theta}^2 + \sigma_{Yi}^2)^2} + O_p(1), \quad (7)$$

thus $\phi(\hat{\theta})/\sqrt{V} | \mathcal{D} = N(0, V^*/V) | \mathcal{D} + O_p(1/\sqrt{n})$, with

$$V^* = \sum_{i \in B_0^c} \frac{\sigma_{Yi}^2(\hat{\beta}_{Yi} \hat{\theta} \sigma_{Xi}^2 - \hat{\theta}^2 \hat{\beta}_{Xi} \sigma_{Xi}^2 + \hat{\theta} \hat{\beta}_{Yi} \sigma_{Xi}^2 + \hat{\beta}_{Xi} \sigma_{Yi}^2)^2 + \sigma_{Xi}^2(\hat{\beta}_{Yi} \sigma_{Yi}^2 - \hat{\theta} \hat{\beta}_{Xi} \sigma_{Yi}^2 - \hat{\theta}^2 \hat{\beta}_{Yi} \sigma_{Xi}^2 - \hat{\theta} \hat{\beta}_{Xi} \sigma_{Yi}^2)^2}{(\sigma_{Xi}^2 \hat{\theta}^2 + \sigma_{Yi}^2)^4},$$

as $\hat{\beta}_{Xi} \xrightarrow{P} \beta_{Xi}$, $\hat{\beta}_{Yi} \xrightarrow{P} \beta_{Yi}$, $\hat{\theta} \xrightarrow{P} \theta_0$, we can get $V^*/V \xrightarrow{P} 1$, thus we get $\phi(\hat{\theta})/\sqrt{V} | \mathcal{D} \xrightarrow{w.P} N(0, 1)$.

Next we show $-\phi'(\hat{\theta})/V | \mathcal{D} \xrightarrow{w.P} 1$. After some calculation we get

$$\phi'(\theta) = \sum_{i \in B_0^c} \frac{2\sigma_{Xi}^4 \tilde{\beta}_{Xi} \tilde{\beta}_{Yi} \cdot \theta^3 + 3(\sigma_{Xi}^2 \sigma_{Yi}^2 \tilde{\beta}_{Xi}^2 - \sigma_{Xi}^4 \tilde{\beta}_{Yi}^2) \theta^2 - 6\sigma_{Xi}^2 \sigma_{Yi}^2 \tilde{\beta}_{Xi} \tilde{\beta}_{Yi} \theta + (\sigma_{Xi}^2 \sigma_{Yi}^2 \tilde{\beta}_{Yi}^2 - \tilde{\beta}_{Xi}^2 \sigma_{Yi}^4)}{(\sigma_{Xi}^2 \theta^2 + \sigma_{Yi}^2)^3}, \quad (8)$$

as $\tilde{\beta}_{Xi} \xrightarrow{P} \beta_{Xi}$, $\tilde{\beta}_{Yi} \xrightarrow{P} \beta_{Yi}$, $\hat{\theta} \xrightarrow{P} \theta_0$, we get $-\phi'(\hat{\theta})/V \xrightarrow{P} 1$, with Theorem 3.3 in [2], $-\phi'(\hat{\theta})/V|\mathcal{D} \xrightarrow{w.P} 1$.

Based on equation (8), we can see $\phi''(\theta)$ has its numerator of order n^5 and its denominator of order n^6 , thus $\phi''(\theta^*)/V = O_p(1)$. As $\tilde{\theta} \xrightarrow{P} \theta_0$, $\hat{\theta} \xrightarrow{P} \theta_0$, we have $\tilde{\theta} - \hat{\theta} \xrightarrow{P} 0$, again with Theorem 3.3 in [2] we get $\tilde{\theta} - \hat{\theta}|\mathcal{D} \xrightarrow{w.P} 0$. Thus we can get $\frac{1}{2}\phi''(\theta^*)(\tilde{\theta} - \hat{\theta})|\mathcal{D} \xrightarrow{w.P} 0$. Now with Theorem 3.2 in [2], we can get $\sqrt{V}(\tilde{\theta} - \hat{\theta})|\mathcal{D} \xrightarrow{w.P} N(0, 1)$, completeing the proof. \square

References

- [1] Lyon, M. S., Andrews, S. J., Elsworth, B., Gaunt, T. R., Hemani, G., & Marcora, E. (2021). The variant call format provides efficient and robust storage of GWAS summary statistics. *Genome Biology*, 22(1), 1-10.
- [2] Xiong, S., & Li, G. (2008). Some results on the convergence of conditional distributions. *Statistics & probability letters*, 78(18), 3249-3253.
- [3] Xue, H., Shen, X., & Pan, W. (2021). Constrained maximum likelihood-based Mendelian randomization robust to both correlated and uncorrelated pleiotropic effects. *The American Journal of Human Genetics*, 108(7), 1251-1269.
- [4] Zhao, Q., Wang, J., Hemani, G., Bowden, J., & Small, D. S. (2020). Statistical inference in two-sample summary-data Mendelian randomization using robust adjusted profile score. *The Annals of Statistics*, 48(3), 1742-1769.